



Molecular characterization of evolutionarily conserved signaling systems of *Echinococcus multilocularis* and their utilization for the development of novel drugs against Echinococcosis

Molekulare Charakterisierung evolutionsgeschichtlich konservierter Signalsysteme und deren Nutzung für die Entwicklung neuer Medikamente gegen Echinococcose

Doctoral thesis for a doctoral degree
at the Graduate School of Life Sciences,
Julius-Maximilians-Universität Würzburg

Section Infection and Immunity

submitted by

Sarah Hemer

from

Leutkirch

Würzburg 2012

Submitted on:
(Office stamp)

Members of the Promotionskomitee:

Chairperson: Prof. Dr. Paul Pauli

Primary Supervisor: Prof. Dr. Klaus Brehm

Supervisor (Second): Prof. Dr. Roland Benz

Supervisor (Third): Prof. Dr. Holger Barth

Date of Public Defense:

Date of receipt of Certificates:

Affidavit

I hereby confirm that my thesis entitled

Molecular characterization of evolutionarily conserved signaling systems of *Echinococcus multilocularis* and their utilization for the development of novel drugs against Echinococcosis

is the result of my own work. I did not receive any help or support from commercial consultants. All sources and / or materials applied are listed and specified in the thesis.

Furthermore, I confirm that this thesis has not yet been submitted as part of another examination process neither in identical nor in similar form.

Würzburg

Date

Signature

Acknowledgements- Danksagung

An dieser Stelle möchte ich die Gelegenheit nutzen, mich ganz herzlich bei denjenigen zu bedanken, die zum Gelingen dieser Arbeit beigetragen haben:

Prof. Dr. Klaus Brehm für die Möglichkeit, in seiner Arbeitsgruppe zu promovieren, die sehr gute Betreuung und die vielen interessanten und motivierenden Gespräche. Ich habe sehr viel gelernt.

Prof. Dr. Benz und Prof. Dr. Barth für die Übernahme der Gutachten, die regelmäßigen Gespräche und die Teilnahme an der Prüfungskommission.

Der Echinokokkenarbeitsgruppe Monika Bergmann, Dirk Radloff, Ferenc Kiss, Uriel Koziol, Justin Nono, Raphaël Duvoisin, Andreas Kalbflisch, und den Ehemaligen Echis, Kerstin Epping, Sabine Lorenz, Markus Spiliotis, Verena Gelmedin für die angenehme Arbeitsatmosphäre und viele schöne und motivierende Gespräche.

Den Azubis für die immer tatkräftige Unterstützung und die unentberhliche Hilfe im Laboralltag.

Den Mitarbeitern des Instituts für Hygiene und Mikrobiologie, vor allem Rainer Brandner, Michael Ullrich, Stefan Simon, Günther Troll, Matthias Brandt, Ida Paul und Edeltraud Rausch, den guten Seelen des Instituts für ihre unermüdliche Hilfsbereitschaft.

Meiner Familie, die mich jederzeit und in allen Bereichen meines Lebens unterstützt.

Meinem Freund Patrick für seine unerschöpfliche Geduld, Motivation und Hilfestellung.

Contents

1	Summary	9
2	Introduction	12
2.1	The small fox tapeworm <i>Echinococcus multilocularis</i>	12
2.1.1	Phylogeny and epidemiology of <i>E. multilocularis</i>	12
2.1.2	Biology and life cycle	13
2.1.3	Alveolar Echinococcosis, clinical manifestation and therapy .	15
2.2	The study of host-parasite interplay during Alveolar Echinococcosis .	16
2.2.1	Molecular and biochemical approaches	16
2.2.2	In vitro cultivation systems	17
2.2.3	Evolutionary conserved signalling in <i>E. multilocularis</i>	18
2.3	The insulin signalling cascade	19
2.3.1	The insulin and insulin/ IGF-I receptor family	19
2.3.2	The insulin signalling pathways	20
2.3.3	Insulin signalling in Platyhelminthes and nematodes	21
2.4	Abl tyrosine kinases	22
2.4.1	Abl kinases	22
2.4.2	Abl kinases in invertebrates	23
2.4.3	The Abl inhibitor Imatinib	23
2.5	Objectives	24
3	Material and Methods	26
3.1	Material	26
3.1.1	Equipment	26
3.1.2	Consumables	27
3.1.3	Chemicals, media, commercially available kits and enzymes .	27
3.2	Oligonucleotides	30
3.3	Antibodies	31
3.4	Working with RNA	32
3.4.1	Isolation of RNA	32
3.4.2	DNase treatment of isolated RNA	32

3.4.3	Determination of RNA concentration	33
3.4.4	Synthesis of cDNA	33
3.5	Working with DNA	34
3.5.1	Isolation of chromosomal DNA	34
3.5.2	Determination of DNA concentration	34
3.5.3	Polymerase-Chain Reaction (PCR)	34
3.5.4	Rapid amplification of cDNA ends (RACE)	35
3.5.5	Sequencing	36
3.5.6	Agarose gel-electrophoreses	36
3.5.7	TA-cloning	36
3.5.8	Addition of A-overhangs	36
3.5.9	Blunt-end ligation	37
3.5.10	Purification of DNA from agarose gels, PCR and enzyme reactions	37
3.5.11	Restriction digestion	37
3.5.12	Dephosphorylation of plasmid DNA	37
3.5.13	Ligation	37
3.6	Working with proteins	38
3.6.1	Preparation of protein samples	38
3.6.2	Quantification of protein concentration	38
3.6.3	SDS-PAGE	38
3.6.4	Coomassie	39
3.6.5	Western blot	39
3.6.6	Ponceau-red staining	40
3.6.7	Purification of polyclonal antibodies	40
3.6.8	IHC	41
3.6.9	Immuno precipitation	41
3.7	Working with bacteria	42
3.7.1	Chemically competent <i>E. coli</i>	42
3.7.2	Transformation of <i>E.coli</i>	42
3.7.3	Liquid culture of <i>E.coli</i>	42
3.7.4	Glycerin stocks	42
3.7.5	Recombinant expression of <i>E. multilocularis</i> proteins in <i>E. coli</i>	43
3.8	Working with <i>E. multilocularis</i>	44
3.8.1	Isolates and maintenance of parasite material	44
3.8.2	<i>In vitro</i> cultivation	45
3.8.3	Axenic culture	45

3.8.4	Isolation and cultivation of primary cells	45
3.8.5	Isolation of protoscoleces	46
3.8.6	<i>In vitro</i> activation of protoscoleces	46
3.8.7	Cultivation of protoscoleces	47
3.8.8	Life-dead staining of protoscoleces	47
3.8.9	<i>In vitro</i> stimulation of metacestode vesicles	47
3.8.10	BrdU incorporation	47
3.8.11	Glucose uptake	48
3.8.12	Resazurin assay in primary cells	49
3.8.13	Embedding of <i>E. multilocularis</i> material	49
3.9	Working with eukaryotic cell lines	49
3.9.1	Cultivation	49
3.9.2	Freezing stocks	50
3.9.3	Transfection of Hek293T cells with the PEI method	50
3.10	Working with yeast cells	50
3.10.1	Yeast strains and media	50
3.10.2	Liquid culture	51
3.10.3	Yeast two hybrid (Y2H)	52
3.11	Computer analysis and statistics	52
4	Results	53
4.1	The insulin signalling cascade as a possible target for anti-echinococcosis chemotherapy	53
4.1.1	Insulin affects the larval development of <i>E. multilocularis</i>	53
4.1.2	Effect of host insulin on glucose uptake	56
4.1.3	RT-PCR analysis of <i>emir1</i> and <i>emir2</i>	56
4.1.4	Production of an anti-EmIR2 immunoserum	57
4.1.5	Analysis of EmIR1 and EmIR2 expression on protein level	58
4.1.6	Immunohistochemical analysis of EmIR2 expression in <i>E. multilocularis</i> larval stages	60
4.1.7	The activation of EmIR2 by host insulin	61
4.1.8	Characterisation of the insulin receptor downstream signalling molecules PI3K, Akt and 4E-BP	63
4.1.9	Activation of the PI3K/ Akt pathway is involved in insulin signalling	67
4.1.10	Effect of HNMPA(AM) ₃ on <i>E. multilocularis</i> development	68

4.1.11	Effect of the PI3 kinase inhibitor LY294002 on <i>E. multilocularis</i> development	71
4.1.12	Insulin sensitivity in old and new isolates	72
4.1.13	Insulin-like peptides in <i>E. multilocularis</i>	73
4.2	The effect of the anti-cancer drug Imatinib and Imatinib responsive kinases in <i>E. multilocularis</i>	78
4.2.1	Characterisation of Abl kinases in <i>E. multilocularis</i>	78
4.2.2	Expression analysis of <i>emabl1</i> , <i>emabl2</i> and <i>emtk6</i>	81
4.2.3	The effect of Imatinib on <i>E. multilocularis</i> larval stages	82
4.3	K11777 a new inhibitor in anti-AE chemotherapy?	88
4.4	Targeting Jun kinase (JNK) with the inhibitor AS601245	91
4.5	The effect of Albendazole in the new <i>E. multilocularis in vitro</i> cultivation systems	92
4.6	The utilization of inhibitor combination treatment against <i>E. multilocularis</i> larvae	93
4.6.1	Comparison of inhibitors in single drug <i>in vitro</i> assays	94
4.6.2	Combination-treatment of parasite material	95
4.7	The effect of the <i>Clostridium botulinum</i> C2 toxin on <i>E. multilocularis</i>	98
5	Discussion	100
5.1	Insulin signalling in <i>E. multilocularis</i>	100
5.2	Abl kinases and Imatinib	107
5.3	The cystein protease inhibitor K11777	109
5.4	The JNK inhibitor AS601245	110
5.5	Albendazole	110
5.6	Combination therapy as a new approaches for anti-AE treatment	111
5.7	C2 toxin	112
	Bibliography	113
A	Supplementary	130
A.1	Analysis of ILP homologues	130
A.2	Sequences	130
B	List of Abbreviations	141
C	Publications	143

1 Summary

Summary

Alveolar echinococcosis (AE), a severe and life-threatening disease is caused by the small fox tapeworm *Echinococcus multilocularis*. Currently, the options of chemotherapeutic treatment are very limited and are based on benzimidazole compounds, which act merely parasitostatic *in vivo* and often display strong side effects. Therefore, new therapeutic drugs and targets are urgently needed.

Evolutionarily conserved signaling systems of *E. multilocularis* were suggested to be involved in host-parasite cross-communication and the development of the parasite larvae in the course of the disease. In the present work the role of two evolutionarily conserved signalling pathways in *E. multilocularis* has been studied in regard to host-parasite interaction and the possible use in anti-AE chemotherapy.

Previously, two insulin receptors, EmIR1 and EmIR2 were described in *E. multilocularis* and preliminary results indicated that host insulin plays a role in the larval development of this cestode. In this work the influence of host insulin on the parasite development was further studied. Host insulin significantly increased parasite metacestode vesicle formation from primary cell cultures and protoscoleces. Furthermore, DNA *de novo* synthesis and glucose uptake in metacestode vesicles were increased by insulin. Further study of the signalling processes revealed that EmIR2 is able to bind insulin, IGF-I and *Echinococcus* insulin-like peptides *in vitro* and is phosphorylated in the parasite *in vivo* upon stimulation with exogenous insulin. Additionally, I could show that insulin stimulation activates the parasite PI3K/ Akt signalling. Inhibition of the *Echinococcus* insulin receptors and PI3K led to a significant decrease in survival and development of parasite larvae and blocked signal transduction via the PI3K/Akt pathway.

Taken together, these results showed that host-parasite cross-communication via the *E. multilocularis* insulin signalling pathway is possible and that host insulin has an important influence on *Echinococcus* survival and development. Conse-

quently, insulin signalling pathway might be a promising target for anti-AE chemotherapy.

As additional possible drug targets, "extitEchinococcus Abl kinases were characterised for the first time in the present work. Two Abl kinase and one Src-Abl hybrid kinase are expressed in the *E. multilocularis* larval stages. The anti-cancer drug Imatinib, directed against human Abl-kinases, proved to be very effective also against *E. multilocularis* larvae. Imatinib drastically decreased the survival of *Echinococcus* larvae *in vitro* and had severe influence on parasite morphology after short term treatment.

To complement this work, further inhibitors were tested in the *E. multilocularis in vitro* cultivation systems. Among these was the JNK inhibitor AS601245, which showed highly synergistic effects in combination with Imatinib. Additionally, preliminary results indicated the cystein protease inhibitor K11777 as an effective compound in the culture system.

Taken together, this work yielded important insights into host-parasite communication during echinococcosis and several promising targets for future anti AE-chemotherapy development.

Zusammenfassung

Die alveoläre Echinokokkose ist eine ernste und lebensgefährliche Erkrankung, die durch den kleinen Fuchsbandwurm ausgelöst wird. Die gegenwärtigen chemotherapeutischen Behandlungsmöglichkeiten beschränken sich auf die Behandlung mit Benzimidazolen, die *in vivo* nur parasitostatische Wirkung besitzen und häufig sehr starke Nebenwirkungen aufweisen. Aus diesem Grund besteht ein dringendes Bedürfnis nach neuen Medikamenten und Angriffsziele für diese.

Es wird angenommen, dass evolutionsgeschichtlich konservierte Signalsysteme an der Wirt-Parasit Kreuzkommunikation und der Entwicklung des Parasiten im Verlauf der Erkrankung beteiligt sind. In der vorliegenden Arbeit wurde die Rolle zweier evolutionsgeschichtlich konservierter Signalsysteme in *E. multilocularis* in Hinblick auf die Wirt-Parasiten Interaktion und dem möglichen Nutzen in der AE Chemotherapie untersucht.

In früheren Arbeiten konnten zwei Insulin Rezeptoren in *E. multilocularis* beschrieben werde und vorläufige Ergebnisse deuten darauf hin, dass Wirtsinsulin eine Rolle in

der Larvenentwicklung dieses Cestoden spielt. In dieser Arbeit wurde der Einfluss von Wirtsinsulin auf die Parasiten Entwicklung weiter studiert. Wirtsinsulin stimulierte die Vesikelbildung aus Primärzellen und Protoscolizes signifikant. Weiterhin wurde die DNA *de novo* Synthese und die Glucose Aufnahme in Metacestoden Vesikeln verstärkt. Zusätzliche Untersuchungen der Signal-Prozesse ergaben, dass EmIR2 in der Lage ist, Insulin, IGF-I und die *Echinococcus* Insulin-ähnlichen Peptide zu binden und dass EmIR2 in Antwort auf die Stimulation mit Insulin phosphoryliert wird. Zusätzlich konnte ich zeigen, dass diese Stimulation die PI3K/Akt Kaskade des Parasiten aktiviert. Die Inhibition der *Echinococcus* Insulin Rezeptoren und der PI3K führte zu einer signifikanten Reduktion des Überlebens und der Entwicklung der Parasitenlarven und blockierte die Signaltransduktion über den PI3K/Akt Signalweg.

Zusammengefasst zeigen diese Ergebnisse, dass eine Wirt-Parasiten Kreuzkommunikation über den *E. multilocularis* Insulin Signalweg möglich ist und das Wirtsinsulin einen wichtigen Einfluss auf das Überleben und die Entwicklung des Parasiten hat. Folglich könnte der Insulin Signalweg ein vielversprechender Angriffspunkt für die anti-AE Chemotherapie sein.

In dieser Arbeit wurden zum ersten Mal Abl Kinasen in *E. multilocularis* beschrieben. Zwei Abl Kinasen und eine Src-Abl Hybridkinase werden in den *E. multilocularis* Larvenstadien exprimiert. Das Krebsmedikament Imatinib hat sich als sehr effektiv gegen *E. multilocularis* erwiesen. Imatinib verringerte das Überleben von *Echinococcus* Larven *in vitro* drastisch und hatte starken Einfluss auf die Morphologie des Parasiten nach kurzzeitiger Behandlung.

Um diese Arbeit zu vervollständigen wurden weitere Inhibitoren in den *E. multilocularis in vitro* Kultivierungssystemen getestet. Unter diesen war der JNK Inhibitor AS601245, der stark synergistische Effekte in Kombination mit Imatinib zeigte. Zusätzlich deuten vorläufige Ergebnisse darauf hin, dass der Cystein Protease Inhibitor K11777 eine effektive Substanz in den Kultursystemen darstellt.

Zusammengefasst brachte diese Arbeit wichtige Erkenntnisse über die Wirts-Parasiten Interaktion in *E. multilocularis* und einige vielversprechende Angriffspunkte für zukünftige anti-AE Chemotherapie konnten identifiziert werden.

2 Introduction

2.1 The small fox tapeworm *Echinococcus multilocularis*

2.1.1 Phylogeny and epidemiology of *E. multilocularis*

The small fox tape worm *Echinococcus multilocularis* belongs to the class Cestoda in the phylum of Platyhelminthes (flatworms). The Platyhelminthes is comprised of the classes cestoda, trematoda and turbellarians. All Platyhelminthes have a parasitic life-cycle with exception of turbellarians and can be allocated to the Bilaterata (Bilateria) and Protostoma. The protostomes can furthermore be divided into the Ecdysozoa, which include the Nematoda and Arthropoda and the Lophotrochozoa that consists of Platyhelminthes, Annelida and Mollusca and several other phyla [1]. Important model organisms from Ecdysozoa for genetics and developmental biology are the nematode *Caenorhabditis elegans* and the arthropod *Drosophila melanogaster*. The parasitic worms of the Nematoda and Platyhelminthes are combined in the historic term "helminths". In Fig. 2.1 a summary of the phylogenetic organization of the helminths is depicted.

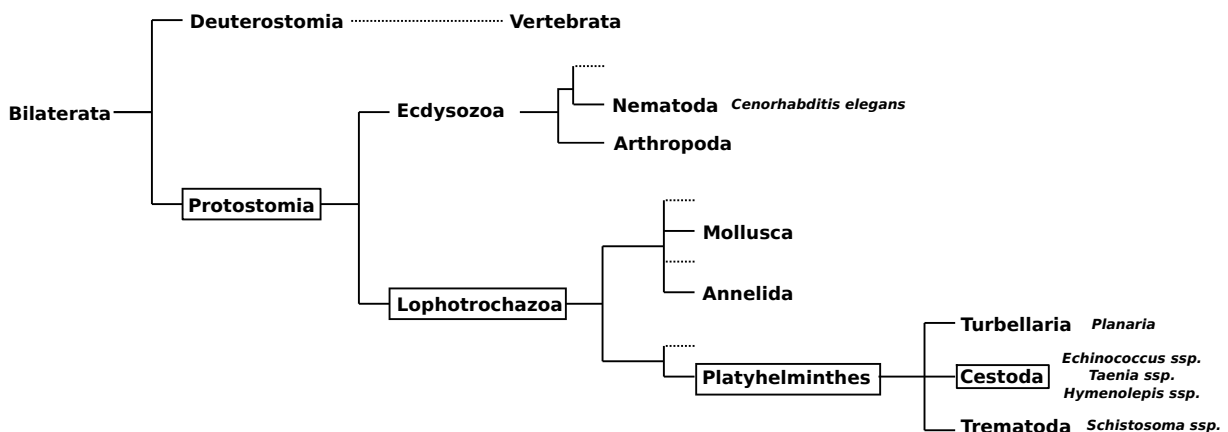


Fig. 2.1: Phylogenetic organisation of helminths within the Bilaterata [1]. The classification of cestoda is marked by boxes, example species are printed in italics

Echinococcus species are found in a variety of final and intermediate hosts and the genus *Echinococcus* contains at least eight species. The small fox tapeworm *E. multilocularis* and the dog tapeworm *E. granulosus* have the highest impact on human and animal health issues and cause severe diseases in humans, the alveolar (AE) and cystic echinococcosis (CE), respectively [2]. Further members of the genus are *E. oligarthus* [3], *E. vogeli* [3], *E. shiquicus* [4], *E. equinus* [5], *E. ortleppi* [5] and *E. felidis* [6], many of which were previously repositioned from *E. granulosus* strains [6, 7].

E. multilocularis is endemic worldwide in the Northern Hemisphere (Fig. 2.2) [2]. In recent years an increase in AE and a spread of *E. multilocularis* from south-central Europe to neighbouring countries like France, Italy and the Balkan states was observed [8, 9]. This expansion of endemic areas is most likely caused by an increase in the fox population due to rabies vaccination and urbanisation, resulting in a higher infestation rate with *E. multilocularis* [10, 11].

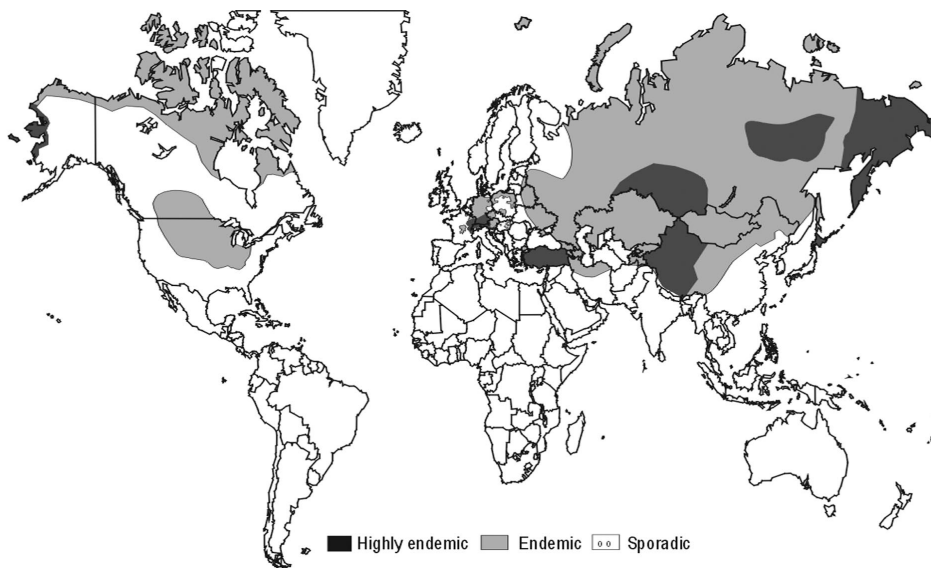


Fig. 2.2: Global distribution of *E. multilocularis* [2].

2.1.2 Biology and life cycle

The life cycle of *E. multilocularis* is characterised by two host changes, one adult stage and three larval stages, namely the metacestode stage, the protoscolex and the oncosphere (Fig. 2.3). The adult worm is found in the intestine of its final host, mostly the red-fox (*Vulpes vulpes*) and the polar fox (*Alopex lagopus*), but also other

carnivores can serve as definite host [2, 12]. Small rodents serve as intermediate hosts, however also primates and humans can be infected [8, 13]. When parasite material is ingested by the final host, the 2 to 4 mm long adult worm develops in a period of 28 to 35 days [8] and then starts to produce large amounts of eggs. The head region (scolex) of the adult worm is comprised of the rostellum and four suckers to attach itself to the intestine wall. The scolex is followed by the proliferative zone (strobila), which contains the proliferative segments (proglottids). In the terminal proglottid the eggs are formed. Each egg contains a multicellular oncosphere of 25 to 30 μm in diameter and are very resistant towards low temperatures and humidity [2]. With the feces, the oncospheres together with the gravid proglottid are shed to the environment from where they are then taken up by the intermediate host through their food source. During the stomach and the intestine passage the oncosphere hatches and becomes activated, most likely by the involvement of the acidic pH and bile salts. The oncosphere then penetrates the intestine wall and is transported to the liver via the blood stream, where it settles and forms the metacestode stage [8, 14, 15]. The metacestode stage is an infiltrative growing, tumour-like tissue consisting of mother and daughter vesicles. A single metacestode vesicle consists of a cellular and an acellular layer surrounding the hydatid fluid. The cellular layer of the metacestode vesicle is subdivided into the syncytial tegument and the underlying germinal layer, that contains several cell types, including the undifferentiated germinal cells that are responsible for asexual reproduction and metastasis formation [16]. The laminated layer (acellular) is highly glycosylated and has immune-evasive attributes [17]. Furthermore it gives the parasite tissue structural integrity and stability [18, 19]. In the further course of the infection the germinal layer forms brood capsules, in which the protoscoleces develop [5]. This larval stage already formed the scolex of the adult worm, but does not contain the proglottids. The infiltration of the liver with parasite tissue gradually weakens the intermediate host, which falls finally prey to the final host. By the stomach/intestine passage the protoscolex is activated, evaginates and develops into the adult stage [8, 19].

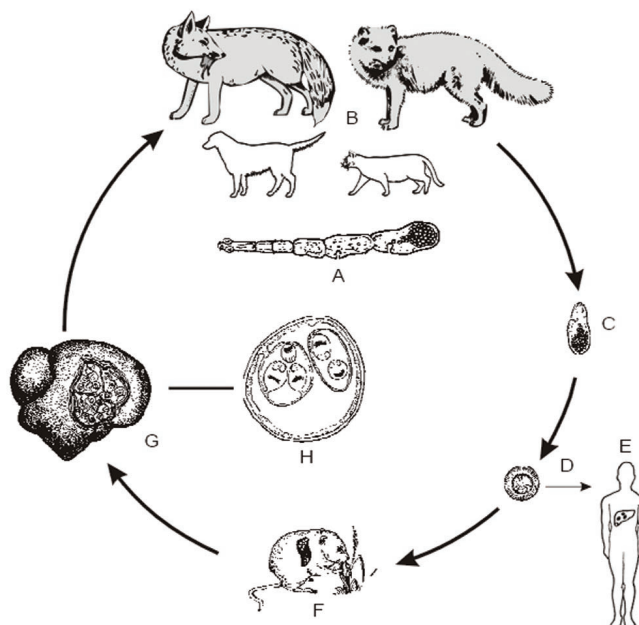


Fig. 2.3: The life cycle of *E. multilocularis* [2]. (A) Adult worm. (B) Final hosts: foxes, dogs, other canids and cats. (C) Proglottid with eggs. (D) Egg with oncosphere. (E) Infection of humans. (F) Intermediate host: Rodents. (G) Rodent liver with metacestodes. (H) Single metacestode cyst with developing protoscoleces.

2.1.3 Alveolar Echinococcosis, clinical manifestation and therapy

Infective eggs can be taken up by humans, in which case the natural passage between intermediate and final host is broken. However, as in the natural intermediate hosts the oncosphere is activated and transported to the liver, where the metacestode stage develops. The infiltrative, tumour-like growth of the parasite tissue in the liver impairs the liver function, the clinical manifestation accompanied by lesion formation is referred to as alveolar echinococcosis [20]. By metastasis formation the parasite can also spread to organs like lung, bones and the brain [8, 21]. Early symptoms are abdominal pain, jaundice, hepatomegaly, sometimes fever and anaemia, weight loss, and pleural pain and end in dysfunction of the affected organs resulting in the death of the patient [2]. Persons with high risk of infection are pet owners and in that regard especially those of dogs, but also farmers, hunters and gardeners [15, 22]. Exact AE rates are difficult to estimate due to a low prevalence and a large time span between infection and the first symptoms,

which can be up to 15 years [2]. In high endemic areas in central Europe between 2 and 40 cases per 100.000 inhabitants were reported [9].

For diagnosis of AE imaging techniques based on ultrasonography, computed tomography (CT), magnetic resonance tomography (MRT) and serology are used [23]. In serological tests a wide range of antigens are available which allow detection with a diagnostic sensitivity of 90–100 % and a specificity of 95–100 % [8,23].

Treatment options are currently very limited. Radical surgery is useful, when the lesions are detected in an early stage of infection. Due to the infiltrative growth of the parasite the complete removal is only possible in 20 to 40 % of the cases [2, 24]. Liver transplantation is not recommended, because the required immunosuppression can cause massive growth of residual and metastasize parasite material [8,25,26]. The current standard of therapy is chemotherapy, in somecases combined with surgery [8]. For therapy benzimidazoles, like Albendazole or Mebendazole are recommended [23]. These compounds bind to the parasitic β -tubulins and inhibit the formation of microtubuli [27, 28]. However, these drugs have severe side-effects, like fever, urticaria, neurological deficits, gastrointestinal disorders, decreased numbers of leukocytes and thrombocytes and bone marrow toxicity as they also bind the human protein [29]. Furthermore they act merely parasitostatic and therefore require lifelong treatment [29].

2.2 The study of host-parasite interplay during Alveolar Echinococcosis

2.2.1 Molecular and biochemical approaches

In the last decades studies of *E. multilocularis* were mostly aimed at the identification of antigens for diagnostic purposes [30] or the investigation of epidemiological and phylogenetic patterns [31, 32]. *Emelp* was the first chromosomal locus described for *E. multilocularis*, which encodes a errin-radixin-moesin (ERM)- like protein [33]. Trans-splicing was first reported in trypanosomes [34] and was subsequently studied in the cestodes *E. multilocularis* and *T. solium* [35, 36]. Trans-splicing involves the transfer of an exon derived from a small nucleolar pre-mRNA, the so called spliced leader (SL) to the 5' end exon of a different mRNA [37]. In *E. multilocularis* 30 % of transcripts seem to undergo this process [38]. The first

cDNA libraries of *E. multilocularis* were produced on the basis of trans-splicing. Primers against the 36 bp SL sequence and the poly-A tail were used to amplify the complete subset of trans-spliced cDNAs [35, 37]. After that further SL-independent cDNA libraries were produced [39], including a Y2H library [40]. In 2003 the whole genome sequence project for *E. multilocularis* by the Wellcome Trust Sanger Institute (Hinxton, Cambridge, UK) was started in cooperation with the groups of Klaus Brehm (Wuerzburg) and Cecilia Fernandez (Montevideo). The genomic sequence data is now available under <http://www.sanger.ac.uk/resources/downloads/helminths/echinococcus-multilocularis.html>. The publication of the annotated genome data is currently in preparation. Furthermore, the Sanger institute in cooperation Klaus Brehm (Wuerzburg) is presently working on a transcriptome project of distinct *E. multilocularis* larval stages. The access to genomic and transcriptomic data will considerably facilitate the work with *E. multilocularis* with respect to developmental and immunological questions of the parasite and will facilitate the identification of new possible drug targets.

2.2.2 In vitro cultivation systems

Elaborate cultivation systems have been developed in recent years that allow the investigation of *E. multilocularis* under defined, laboratory conditions. The influence of host factors as well as the effect of parasite factors on host systems can now be studied *in vitro*. The first long term cultivation systems for *E. multilocularis* were developed in the mid 90ties. 1995 Hemphill and Gottstein [41] introduced the tissue block system, in which tissue blocks from secondary infected rodents were incubated in serum containing medium. Metacestode vesicles emerged from the tissue block that were morphologically similar to the vesicles from the liver or peritoneum of infected mice. The system developed by Jura et al. [42] relied on the co-incubation of homogenised parasite tissue with primary rat hepatocytes embedded in a collagen layer. A disadvantage of both systems was the low amount of vesicles that could be gained. Therefore the large scale liquid culture systems was established [43]. Homogenised parasite material was incubated in the presence of actively dividing rat hepatoma feeder cells. Like in the other systems metacestode vesicles developed and subsequently produced protoscoleces. The removal of the feeder cells lead to a fast degeneration of the parasite material, indicating that the system relies on soluble factors secreted by the feeder cells. Large amounts of vesicles with comparable sizes and developmental stages were produced with this system. However, the investigation of the influence of host factors on the parasite

was hindered by the continuous presence of feeder cells in the cultivation system. It was not possible to distinguish between a direct effect on the parasite or an indirect effect mediated by the feeder cells. This led to the development of the axenic system [44]. In these systems anaerobic growth conditions and the presence of reducing agents were required for the larval development and survival, indicating that the larval material is sensitive to reactive oxygen species produced during culture. Medium containing serum was pre-conditioned with rat hepatoma cells, supplemented with reducing agents and then used for the cultivation of metacystode vesicles grown in the large scale liquid culture system. The next achievement in the cultivation of *E. multilocularis* was the development of primary cell isolation and cultivation [45]. Primary cells were isolated from metacystode vesicles and were cultivated in axenic or co-culture conditions. The isolated cells consisted of approximately 30 % undifferentiated cells. After a period of 3 to 6 weeks these cultures formed new metacystode vesicles, which were infected when injected into the peritoneum of rodents. Recently gene knock-down in primary cell cultures was successful [46]. The current cell culture methods make it possible to produce large amounts of metacystode vesicles. They are useful tools to investigate the development of the parasite in response to cytokines and culture conditions as well as the effect of novel, alternative chemotherapeutics.

2.2.3 Evolutionary conserved signalling in *E. multilocularis*

Cell-cell communication and signalling systems have arisen very early in the metazoan development. They are therefore well conserved between vertebrate and invertebrate organisms [47, 48] and are already present in the most basal phyla like sponges [49, 50]. It was demonstrated that due to the high conservation of the signalling molecules, mammalian insulin and BMP-like factors were able to stimulate the respective receptors of *D. melanogaster* and *C. elegans* [51, 52]. In *E. multilocularis* many factors of evolutionary conserved signalling pathways were already identified by our group. Among these are the epidermal growth factor receptor (EGFR), the insulin receptor family, the MAP kinase cascade, and receptors of the TGF- β and BMP family [16, 53–58]. Thanks to the *E. multilocularis* genome sequencing project many other factors were identified in the genome.

2.3 The insulin signalling cascade

2.3.1 The insulin and insulin/ IGF-I receptor family

The insulin superfamily in mammals contains insulin, IGF-I (insulin like growth factor) and IGF-II. Insulin regulates the glucose and fatty-acid metabolism [59,60], while IGF-I is involved in proliferation processes and has anti-apoptotic activity [61]. Additionally, it has also been reported that IGF-I is involved in cancer development [62, 63]. Insulin and IGF-I are expressed as pro-peptides. Insulin consist of a signal peptide followed by the B, C and A chains. During processing the B chain is cleaved out and the C and A peptides are connected by disulphide bonds [59,60]. IGF-I additionally contains the C-terminal D and E chains, but only the E chain is cleaved [59]. Therefore, although the structure between insulin and IGF-I is very similar the later is significantly larger. In mammals insulin is expressed in the pancreas within the β -cells of the islets of Langerhans [59,60], but reaches its highest concentration in the portal vein and the adjacent peripheral liver tissue [64,65]. IGF-I is synthesised primarily in the liver and to lesser extend in peripheral tissue [66].

The insulin receptor superfamily consists of the insulin receptor [67], the IGF-I receptor [61] and the orphan insulin-related receptor constitutive [68]. The mature receptor forms an constitutive heterotetramer on the cell surface [67, 69]. Insulin receptors are expressed as a pro-receptor with an N-terminal signal peptide, a ligand binding domain, a transmembrane domain and the intracellular tyrosine kinase domain. The pro-peptide is processed into an α chain containing the ligand binding site and a β chain with the transmembrane and kinase domains. The chains are connected by disulphide bonds, which also link two $\alpha\beta$ dimers to form the mature tetramer [70, 71]. Alternative splicing occurs in the ligand binding domain of the human insulin receptor, resulting in an A and B form, which have distinct ligand binding and signalling properties [72–74]. Furthermore the ligands show a high cross-reactivity with the insulin and IGF-I receptors, which can also hybrid-receptors in cells where they are expressed together [74–77].

2.3.2 The insulin signalling pathways

The binding of the ligand to the receptors activates the autophosphorylation activity of the receptor. Tyrosine residues in the kinase domain are phosphorylated, which activated the kinase and form binding sites for adaptor proteins [78–80]. Among the direct interactors with the receptors are the IRS proteins and SHC that get phosphorylated themselves and recruit other effector molecules to the receptor complex [81, 82]. The most important signalling cascades activated by insulin and IGF-I are the mitogen activated protein kinase (MAPK) cascade and the phosphatidylinositol 3-kinase (PI3K)/ Akt pathway [83] (see. Fig. 2.4).

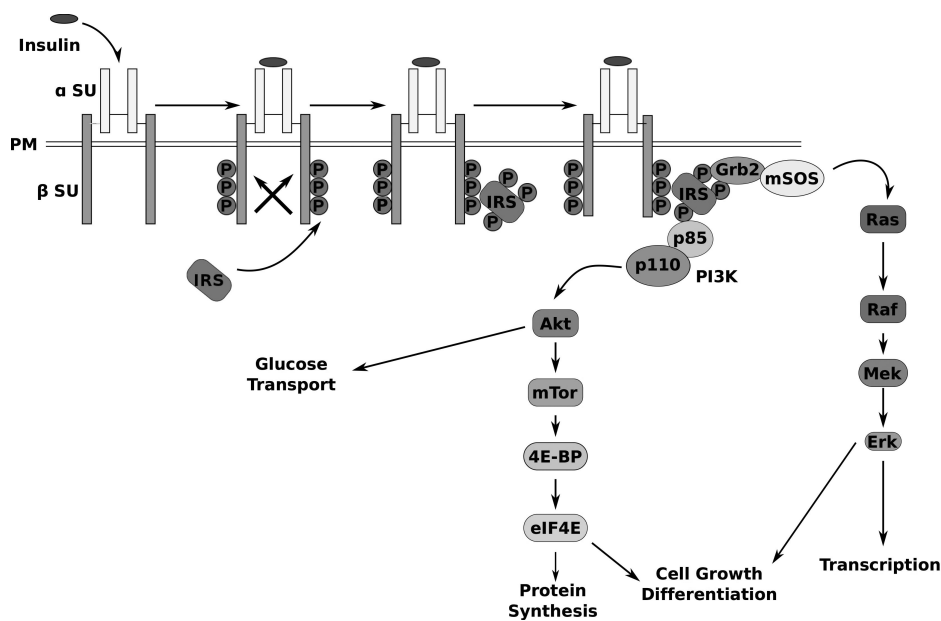


Fig. 2.4: *Insulin signalling pathways. Binding of the ligand induces the intrinsic kinase activity of the kinase domain, leading to auto-phosphorylation of the kinase at crucial tyrosine residues. that form the docking sites for downstream effectors. The MAPK cascade and the PI3K/ Akt pathways are the main mediators of insulin signals. Insulin signalling regulates the glucose and lipid metabolism, cell growth and differentiation, protein synthesis and gene expression [83].*

The MAPK cascade is activated by the recruitment of GrB2 to the receptor complex. GrB2 binds mSos, which catalyses the substitution of GDP to GTP of Ras [84, 85]. Subsequently Raf-1, MEK and Erk1/2 are activated. Erk1/2 dimerises and is transported to the nucleus, where it serves as a transcription factor. The protein synthesis is regulated by the subsequent activation of Mnk-1 and eIF-4G that phospho-

rylates eIF-4E [86]. The MAPK pathway in mammals is primarily associated with growth and differentiation processes [87].

The second pathway activated by insulin signalling is the PI3K/Akt pathway. The regulatory subunit of the PI3K binds to IRS-1 associated with the receptor, which activates the catalytic subunit. The PI3K catalyses the formation of phosphatidyl inositol triphosphate, which recruits the Akt kinase to the membrane [88, 89]. The glucose uptake is regulated by inducing the translocation of Glut4 to the cell surface [90]. Protein synthesis is regulated by the sequential activation of mTor, 4E-BP and eIF-4E [89, 91].

2.3.3 Insulin signalling in Platyhelminthes and nematodes

Several insulin-like (ILP) peptides were identified in invertebrates. *D. melanogaster* expresses seven ILPs (DILP 1 to 7) [92], while in *C. elegans* genome analysis revealed the presence of 37 distinct members of the insulin superfamily. Among these, Ins-1 and Ins-18 show the highest homologies to the human insulin [93]. Finally, in the *E. multilocularis* genome two genes coding for ILPs were identified. However, for all these peptides a processing similar to the human insulin is still unclear. Next to the ILPs insulin receptors and their intracellular signalling cascades were identified in invertebrates. The best characterised insulin receptor homologues are DIR from *D. melanogaster* and DAF-2 in *C. elegans* [94–96]. DIR is involved in the regulation of body and cell size, longevity, embryonal differentiation and lipid metabolism [59, 92, 97]. In *C. elegans* insulin signalling regulates entry and exit of the dauer larval stage [98].

Still very little is known about the role of insulin signalling in parasitic helminths. In *E. multilocularis*, *Schistosoma mansoni*, *Schistosoma japonicum* and *Mesocostoides vogae* insulin receptor orthologues have been identified [53, 99–101] and Yeast two hybrid studies on the *Echinococcus* and *Schistosoma* receptors homologues showed that they interacted with human pro-insulin. Additionally, it was shown that the *Schistosoma* receptors are involved in the insulin mediated glucose uptake [100, 102]. However, the maximum insulin concentration used by Ahier et al. [102] was unphysiologically high, while You et al. [100] only gave an indirect prove of insulin action by blocking the *S. japonicum* insulin receptors. For *M. vogae*, an influence of human insulin on glucose uptake, survival and asexual reproduction was shown [101] and Escobedo et al. [103] gave evidence that insulin promotes the budding of *Taenia crassiceps* significantly, indicating the presence

of an insulin receptor in this organism. A major drawback of this study was the high insulin concentration used to stimulate *Taenia* larvae. The concentrations ranged from 3.45 to 13.8 μM while the physiological systemic insulin concentration reaches a maximum of 100 pM [64]. Furthermore, budding in *T. crassiceps* measures asexual reproduction and is therefore not directly linked larvae development.

2.4 Abl tyrosine kinases

2.4.1 Abl kinases

The Abl kinases were first reported in form of the virally transduced oncogene of the Abelson murine lymphosarcoma virus (v-abl) [104] and the BCR-Abl fusion protein in chronic myeloid leukemia (CML) patients [105]. Abl genes are found in all metazoans [106]. In vertebrates two genes, Abl1 [107] and the closely related Abl2 [108] were identified, while in invertebrates normally only one *abl* gene is present [106]. Both, the oncogenic properties and the high conservation indicate an important role for endogenous Abl kinases. Among the various functions of endogenous Abl kinases are actin remodelling, cell adhesion and motility, DNA damage response, and microbial pathogen response [106]. Abl kinases have a modular structure. At the N-terminus SH3 and SH2 domains are located that are important for protein interaction and substrate specificity [106]. The SH domains are followed by the tyrosine kinase domain and at the C-terminal part of the protein, domains for the interaction with cytoskeletal components and DNA are found [106]. In the cytoplasm Abl localises with F-actin [109], where it is suggested to be involved in the signal transduction for the regulation of mitogenesis. The cytoplasmatic functions seem to be associated with the oncogenic properties of Abl kinases [109]. Nuclear Abl seems to be regulated in a cell-cycle dependent manner and is implicated to be involved in the regulation of transcription and the suppression of cell growth [110, 111]. Due to its role in cancer development the interactions and functions of Abl proteins were researched most thoroughly in BCR-Abl and are summarized in Fig. 2.5.

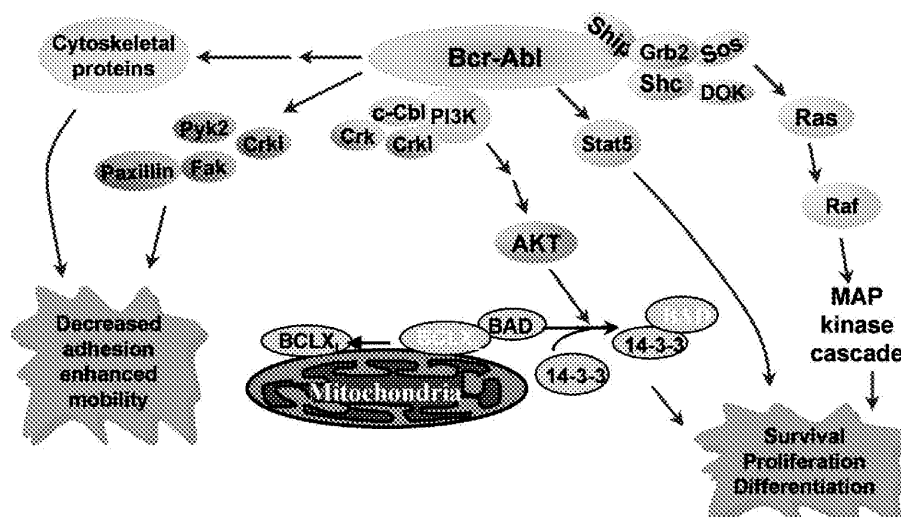


Fig. 2.5: Schematic representation of key pathways in the Bcr-Abl signalling cascade [112]. The oncogenic BCR-Abl is involved in proliferation, survival and cell mobility.

2.4.2 Abl kinases in invertebrates

D. melanogaster has a single Abl kinase (D-Abl) that is important for viability, the development of the central nervous system and dentritic morphogenesis [113–115]. Furthermore D-Abl was shown to have a critical role in the morphogenesis of epithelial tissues during early embryonic development [116]. In *C. elegans* Abl controls epithelial morphogenesis [117]. Furthermore, in eggs of the sea urchin *Strongylocentrotus purpuratus* an Abl kinase homologue was identified, which was suggested to play a role in fertilisation [118]. In the trematode *S. mansoni* two genes for Abl kinases and a unique Abl-Src hybrid kinase, SmTK6 were reported [119, 120]. Beckman and Grevelding [119] showed that that the Abl kinases are expressed in both genders in the reproductive system and weakly in some cells of the parenchyma and the gastrodermis, indicating a role in reproduction. Similarly, SmTK6 was mainly expressed within the testes of the male and the ovary of the female [121].

2.4.3 The Abl inhibitor Imatinib

Imatinib (Glevec, STI-571) is an ATP-competitive kinase inhibitor specifically designed against Abl kinases and other type III tyrosine kinases, like c-Kit and the platelet-derived growth factor receptor (PDGFR) [122]. Imatinib is currently used

in cancer therapy against CML, which is caused by the constitutively active BCR-Abl fusion protein [112, 123] and gastrointestinal stromal tumours (GIST) that are mostly caused by constitutive activation of the receptor tyrosine kinase c-Kit [112]. Recently the effect of Imatinib on the trematode *S. mansoni* was published, showing that Imatinib has a drastic effect on the survival and morphology of this parasite [119].

2.5 Objectives

In the past, studies of *E. multilocularis* were mostly focused on diagnostic, epidemiological and phylogenetic questions [30–32]. Only in recent years the investigation of conserved signalling systems and developmental processes was taken up [16, 48]. Therefore, the developmental mechanisms that *E. multilocularis* uses to thrive and to establish itself in the liver are poorly understood. Insulin reaches its highest concentration in the portal vein and IGF-I is expressed highly in the liver [64–66]. Previous works have shown the presence of insulin receptors that are expressed by *E. multilocularis* and preliminary investigations indicate an important role of insulin signalling in the development of this parasite [53, 124, 125]. The elucidation of the function of insulin signalling in *E. multilocularis* is an important step to understanding the development of AE and is therefore one major focus of this work.

Furthermore, current chemotherapeutic anti-AE treatment is based mostly on benzimidazoles (BZ) which target the parasite β -tubulin [20]. However, due to an affinity of the drugs to host β -tubulin, BZ treatment is often associated with severe side-effects and acts merely parasitostatic, which therefore makes life-long treatment necessary [126, 127]. Therefore new therapeutic drugs and targets are urgently needed. Four major pathways for the development of new anti-parasitic drugs are currently employed [29]: conventional drug screening, the testing of established anti cancer drugs, the study of similarities between parasite and mammalian cells for the identification of suitable drug targets and *in silico* analysis on genomic data.

Among these, targeting the cellular signalling components seems to be a promising approach, due to their important role in the development and survival of all metazoan organisms including parasitic helminths [56, 128]. Additionally, the biochemistry of these signalling components have been researched very thoroughly,

due to their important role in cancer chemotherapy and a broad range of molecules is therefore available to target these components [16].

Another useful approach for identification of new anti-parasitic therapies is the testing of compounds that showed promising effects in related parasites [129]. In the drug testing metacestodes are major targets of anti-parasitic chemotherapy due to their role as the disease causing stage [16, 29]. However, the newly developed primary cell cultivation system can give important insights on the effect of the tested compounds on stem cell viability and regeneration [45]. Therefore the second part of this work focuses on the identification of new possible drug targets and components and the characterisation of the involved *E. multilocularis* molecules.

3 Material and Methods

3.1 Material

3.1.1 Equipment

Developer for radiographic films (Agfa Graphics Germany, Duesseldorf)

ELISA reader Multiscan Ex Primary EIA V.2.1-0 (Thermo)

Gel documentation system: MidiDoc (Herolab, Wiesloch)

Gelelectrophoresis camber (Bio-Rad, Muenchen)

Heating block: DB-3 (Techne, Cambridge, UK), Heizblock (Liebisch, Bielefeld)

Heating stirrer: Typ RCT (Jahnke & Kunkel, Staufen i. Br.)

HERA safe (Heraeus, Thermo Electron, Langenselbold)

Incubator: Heraeus (Thermo Electron, Langenselbold)

Leica IRB (Leica Microsystems, Wetzlar)

Mikro 200 table centrifuge (Hettich, Tuttlingen)

Micro scales: R160P (Sartorius, Goettingen)

Microtom 2065 (Leica Microsystems, Wetzlar)

Mini-PROTEAN II System (BioRad, Muenchen)

MSC advantage laminar flow (Thermo Scientific, Braunschweig)

NanoDrop 1000 (PeqLab Biotechnologie, Erlangen)

Neubauer chamber (0.1 mm, 0.0025 mm²; (Hartenstein, Wuerzburg)

Nuaire laminar flow (Nuaire)

Power Pack P24 and P25 (Biometra, Goettingen)

Refrigerated Centrifuge 3K30 (Sigma-Aldrich, Muenchen)

Research Plus pipette set (Eppendorf, Hamburg)

Scale: 10-1000 g (Sartorius, Goettingen)

Selectomat S2000 autoclave (Muenchner Medizin Mechanik, Muenchen)

G24 shaking incubator(New Brunswick Scientific, Edison, N.J., USA)

Spectrophotometer U-2000 (Hitachi, NY, USA)

Tecan ELISA reader (Tecan Group, Crailsheim)

T-Gradient Thermocycler (Biometra, Goettingen)

TH30 shaking incubator (Hartensein, Wuerzburg)

Tricarb scintillation counter (Packard)

Trio-Thermoblock™ heated lid (Biometra, Goettingen)

Trio-Thermoblock™ oil(Biometra, Goettingen)

Vacuum pump (ILMVAC, Ilmenau)

Vortex mixer: L46 (Gesellschaft fuer Laborbedarf, Wuerzburg)

3.1.2 Consumables

96-well plates (Sarstedt, Nuembrecht)
12-well plates (Nunc, Roskilde, Denmark)
24-well plates (Nunc, Roskilde, Denmark)
96-well plates (Sarstedt, Nuembrecht)
25 cm² (Sarstedt, Nuembrecht)
75 cm² (Sarstedt, Nuembrecht)
175 cm² (Sarstedt, Nuembrecht)
Microtom sample adapter (Rudens Platinindusti, Hestra, Sweden)
Nitrocellulose membran (GE Healthcare, Muenchen)
PD-10 column (GE Healthcare, Muenchen)
Radiographic film (Fujifilm Europe, Duesseldorf)
Safe-Lock Tubes 0,5, 1,5 and 2 ml (Eppendorf, Hamburg)
Semi-micro cuvettes (Sarstedt, Nuembrecht)
Sterilfilter (Nalgene, New York, USA)
Sterile tubes, 15 and 50 ml (Greiner, Nuertingen)
Superfrost Plus slides (Thermo Scientific, Braunschweig)
Syringes and canula, sterile (Braun Melsungen AG, Melsungen)
Whatman blotting paper (GE Healthcare, Muenchen)
X-Ray film Hyperfilm™ -MP (Amersham, Braunschweig)

3.1.3 Chemicals, media, commercially available kits and enzymes

[14C]-D-Glucose (Hartmann Analytic, Braunschweig)
2',5'-Dideoxyadenosine (Sigma-Aldrich, Muenchen)
3,3 Diaminobenzidine 4 Hydrochloride (Serva, Heidelberg)
5-Bromo-2-Deoxyuridine (AppliChem, Darmstadt)
Adenine hemisulfate (Sigma-Aldrich, Muenchen)
Agarose (ROTH, Karlsruhe)
Aladin1 (By courtesy of ...)
Albumin fraction V (pH 7) Blotting grade (BSA) (AppliChem, Darmstadt)
Ammonium peroxodisulfate (APS), (Carl Roth, Karlsruhe)
Aqua demin. (VE-water)
Ampuwa (Fresenius, Bad Homburg)
Ampicillin (Sigma-Aldrich, Muenchen)
Antarctic Phosphatase (New England Biolabs Inc., Schwalbach)
AS601245 (Calbiochem, Merck, Darmstadt)
Bacto agar (Difco Laboratories, Augsburg)
Bathocuproine disulfonic acid (Sigma-Aldrich, Muenchen)
β -Mercaptoethanol (Sigma-Aldrich, Muenchen)
CIP (New England Biolabs Inc., Schwalbach)
Chloroform (Merck, Darmstadt)
CloneJET™ (Fermentas, St. Leon-Rot)

3 Material and Methods

Color Plus Prestained Protein Marker (10- 230 kDa) (NEB, Schwalbach)
Colorimetric Cell Proliferation ELISA BrdU (Roche, Grenzach)
Complete Mini phosphatase inhibitor Mix (Roche, Grenzach)
Dimethyl sulfoxide (DMSO) (Sigma-Aldrich, Muenchen)
dNTP lyophilised (ROTH, Heidelberg)
DMEM- glucose free (Biochrom, Berlin)
DMEM- GlutaMAX™ (DMEM) (Invitrogen, Darmstadt)
DMEM- no phenolred (Invitrogen, Darmstadt)
DO Supplement –Ade/–His/–Leu/–Trp (Clontech, Heidelberg)
DO Supplement –Leu/–Trp (Clontech, Heidelberg)
Entellan (Merck, Darmstadt)
Eosine (Roche, Mannheim)
Fetal Calf Serum (FCS) (Invitrogen, Darmstadt)
Haemalaun (Roche, Mannheim)
HNMPA(AM)₃ (Enzo Life Sciences, Loerrach)
Hystidine HCL mono-hydrate (Sigma Aldrich, Muenchen)
Imatinib- mesylate (Enzo Life Sciences, Loerrach)
Insulin, recombinant human (Sigma Aldrich, Muenchen)
K11777 (By courtesy of Caffrey Conor, UCSF, USA)
Luria-Broth (LB; Invitrogen, Darmstadt)
L-Cystein (Sigma Aldrich, Muenchen)
LY294002 (Biozol, Eching)
Matchmaker Two Hybrid System 3 (Clontech, Heidelberg)
NucleoSpin® Extract II (Macherey-Nagel, Dueren)
NucleoSpin® PC100 (Macherey-Nagel, Dueren)
NucleoSpin® Plasmid Kit (Macherey-Nagel, Dueren)
Oligonucleotides (Sigma, Muenchen)
Omniscrypt® RT Kit (Qiagen, Hilden)
pBAD/TOPO® ThioFusion™ Expression Kit (Invitrogen, Darmstadt)
PCR Cloning Kits (Qiagen, Hilden)
Penicillin/Streptomycin (Invitrogen, Darmstadt)
Pepsin (Sigma-Aldrich, Muenchen)
Pierce® BCA Protein Assay Kit (Thermo Scientific, Braunschweig)
Pierce® ECL westen blot substrate (Thermo Scientific, Braunschweig)
Pierce ReactBind® (Thermo Scientific, Braunschweig)
ProBond™ Nickel-Chelating Resin (Invitrogen, Darmstadt)
Proteinase K (AppliChem, Darmstadt)
RNase A (Roche, Grenzach)
RNaseOut (Invitrogen, Darmstadt)
Peptone (Difco Laboratories, Augsburg)
Phospho Detect™ Phosphoserine Detection kit (Calbiochem, Merck, Darmstadt)
PhosStop (Roche, Grenzach)
Polyethylene glycol (PEG 3350, Sigma-Aldrich, Muenchen)
PrimeScript RNA Polymerase (Takara, Verviers, Belgium)
Rapamycin (Cell Signalling, NEB, Schwalbach)
Resazurin (Sigma-Aldrich, Muenchen)
Restriction enzymes (New England Biolabs Inc., Schwalbach)

3 Material and Methods

Rotiphorese[®] Gel 30 (37,5:1) (Carl Roth, Karlsruhe)
Rotiphorese[®] Gel 40 (Carl Roth, Karlsruhe)
RQ1 RNase-Free DNase (Promega, Mannheim)
SmartLadder (Eurogentec, Koeln)
SMART[™] RACE cDNA Amplification kit (Clontech, Heidelberg)
SOC (Invitrogen, Darmstadt)
Sodium taurocholat (Sigma-Aldrich, Muenchen)
SuperSignal West Femto Chemiluminescent Substrate (Thermo Scientific, Braunschweig)
T4 DNA Ligase (New England Biolabs Inc., Schwalbach)
Taq-Polymerase (New England Biolabs Inc., Schwalbach)
Tavanic[®] (Tava, active component levofloxacin, 5mg/ml) (Aventis)
Technovit 8100 (Heraeus Kulzer, Wehrheim)
TEMED (N,N,N',N'-Tetramethylethyldiamin) (Merck, Darmstadt)
TNF α , recombinant human (Invitrogen, Darmstadt)
Triton[®] X-100 (Sigma-Aldrich, Muenchen)
Trizol[®] Reagent (Invitrogen, Darmstadt)
TOPO-TA Cloning[®] KIT (Invitrogen, Darmstadt)
Trypsin/EDTA (0,05%/0,02% (w/v)/ PBS w/o Ca²⁺, Mg²⁺) (Biochrom, Berlin)
Tween[®] 20 (Merck, Darmstadt)
UlitraGold[™] (Perkin Elmer, Rodgau)
Yeast extract (Difco Laboratories, Augsburg)
Yeast nitrogen base w/o amino acids (Difco Laboratories, Augsburg)

All buffers and solutions were made with distilled water, autoclaved and sterile filtrated. For RNA, either DEPC-treated or commercially available RNase-free water was used. For enzymatic reactions, double distilled and autoclaved water was used.

3.2 Oligonucleotides

cDNA, Race:

Name	Sequence
CD3RT	TCTCTTGAAAGGATCCTGCAGGT ₂₆ V; V= G, C, A
CD3	CTTGAAAGGATCCTGCAGGACT
CD3nested	ATCTCTTGAAAGGATCCTGCAGG
Em10 15	AATAAGGTCAGGGTGACTAC
Em1016	TTGCTGGTAATCAGTCGATC
pJG 4-5 5'	GCCTCCTACCCTTATGATGTG
pJG 4-5 SPR	CTTATGATGTGCCAGATTATG
pJG 4-3 up	TGGAGACTTGACCAAACCTCTG
pJG 4-3 nested	CTGGCGAAGAAGTCCAAAG
RandomOct	NNNNNNNN
SmartI	AAGCAGTGGTAACAACGCAGAGTACGCGGGGGGGG
SmartII	AAGCAGTGGTAACAACGCAGAGTACGCGGG
UPM long	CTAATACGACTCACTATAGGGCAAGC- AGTGGTATCAACGCAGAG
UPM short	CTAATACGACTCACTATAGGGC
NUP	AAGCAGTGGTATCAACGCAGAGT

Plasmids:

Plasmid	Name	Sequence
pDrive	T7	GTAATACGACTCACTATAG
	SP6	CATTTAGGTGACACTATAG
pBad/Thio-Topo [®]	pBad fw	GCTATGCCATAGCATTTCATCC
	pBad rev	GACTAAATTAGACATAGTCCG
pJet (Clonejet)	pJetfw	CGACTCACTATAGGGAGAGCGGC
	pJetrev	AAGAACATCGATTTTCATGGCA
pGADT7	Y2H T7	TAATACGACTCACTATAGGGC
	Y2H AD	AGATGGTGCACGATGCACAG
pGBTK7	Y2H T7	TAATACGACTCACTATAGGGC
	Y2H BD	TTTTCGTTTTAAAACCTAAGAGTC
pSec-Hygro	psecfw	CTAGTTATTGCTCAGCGGTGG
	psecrev	TAATACGACTCACTATAGGG
pcDNA3.1	pcDNA3.1rev	CTAGAAGGCACAGTCGAGGC
	T7	GTAATACGACTCACTATAG

Genespecific primers:

Name	Sequence
abl1dw1	CACCCCACCCATTCTCCTCTAC
abl1up1	CAGCCATGAGGACGTTGC
abl2dw	CCGGAGCTATGCAGAATATCTTC
abl2up-II	CACAGCCACAGTAACGTCATAGG
emil11 BamH1 up	GCGATGGATCCGCCTTTTGCACAGAAC
emilp1 EcoR1dw	GTCACGAATTCTTTGAGATGGATAAACG
emilp2 BamHI	GCGATGGATCCAACAACAGCATTGAG
emilp2 ecoRI	GTCACGAATTCTGATCACCTCTTCATG
emir2adw	CCCTCGAGTGATGCAGTGC
emir2bdw	GGAGCCTATGGATGCAGTGC
emir2cdw	CCCTCGAGTCCTCCTTGAGTTC
emir2ex EcoRI	GTCACGAATTCACAGACAATGAATGTGC
emir2ex SacI up	GTTGAGAGCTCCCATTCGTA AAAACCAC
emir2ex XhoI	GTTGACTCGAGGTCTTCACAGAAGC
emir2intra up	CTCAGAATTCATGTGAGAGTGGAAG
emirbdw3	GGACGAGTGGGAGGTGG
emirbdw5	GAGCCTATGCCTCCTTGAGTTCG
emirbF3dw	GCAACCACCTTCGCTAATG
emirbup3	GAAGTGTTCATGTGGGAGG
emirbup4	GGAAACTCAATTTTCGCCG
ilp1HindIII dw	GCATAAGCTTGTCGCCTCTGGCCCAAG
ilP1NotI Stop	GCATGCGGCCGCTCAGCCTTTTGCACA
ilp2HindIII dw	GCATAAGCTTGGTATCACCTCTTCAT
ilp2NotI Stop	GCATGCGGCCGCTAAACAACAGCATT
ins1dw3	GACCTTTTCACTAGTGAATTCC
ins2dw2	GCAATGTCTTCCCAAGTC
ins1 upnested	GGTGTAAGGCTCGTAGCG
ins2 upnested	GTACAGCCTAAACAACAGCATTG
RC19	GATGATTCCTTCGATTTGCA
RC21	TAAACGAGACGTTCCCAACATG
tk6dw	CTTCGAGCCGCCAACATCC
tk6up	GATGTAAGTACCCTCCGTCTGG

3.3 Antibodies

Primary antibodies:

3 Material and Methods

Antibody	Dilution		Source	Company
β -Actin	1: 1000	5 % BSA TBST	Rabbit	Cell Sig.
Elp	1: 1000	5 % skim milk TBST	Mouse	Cell Sig.
EmIR1 purified	1:300	5 % skim milk TBST	Rabbit	Immunoglobine
EmIR2 purified	1:300	5 % skim milk TBST	Rabbit	Immunoglobine
	1:30 (IP)			
	1:10 (IHC)			
P-Akt substrate	1: 1000	5 % BSA TBST	Rabbit	Cell Sig.
P-4E-BP	1: 1000	5 % BSA TBST	Rabbit	Cell Sig.

Secondary antibodies:

Antibody	Dilution		Company
anti-mouse IgG–HRP	1: 10.000	5 % skim milk TBST	Jackson, ImmunoResearch
anti–rabbit IgG–HRP	1: 5.000	5 % skim milk TBST	Jackson, ImmunoResearch

3.4 Working with RNA

3.4.1 Isolation of RNA

For the isolation of RNA, parasite material was resuspended in 1 ml Trizol and lysed for 5 min. Then 200 μ l Chloroform was added. The suspension was shaken vigorously for 15 s and subsequently centrifuged at 12000 g for 15 min at 4°C. The upper water-phase was transferred into a new Cap and the RNA was precipitated over night at -20°C by adding 0,25 Vol precipitation buffer (1.2 M NaCl, 0.8 M Sodium citrate) and 0,25 Vol isopropanol. The samples were then centrifuged at 12000 g for 30 min and 4°C and the pellet was washed with 70 % ethanol. The pellet was then air-dried and resuspended in 17 μ l DEPC-water.

3.4.2 DNase treatment of isolated RNA

For DNA digestion the RNA was heated for 15 min at 95°C, then the RNA was supplemented with DNase (2 U/ μ g RNA; RQ1 DNase, Promega) and 10 x DNase buffer and incubated at 37°C for 1 h. 1 μ l stop-solution was added and the DNase was inactivated at 65°C for 15 min.

3.4.3 Determination of RNA concentration

The RNA concentration was photometrically measured at a wavelength of 260 nm using the NanoDrop 1000. The purity of the nucleic acids was analysed on the basis of the ratios of 260 nm/ 280 nm (for protein impurity ≥ 2.0).

3.4.4 Synthesis of cDNA

Omniscript RT-PCR kit (Qiagen)

The reverse transcription of total RNA into the first strand of cDNA was done using the oligo-dT-primer CD3RT and the Reverse Transcriptase from the Omniscript RT-PCR kit (Qiagen) according to the manual instructions. 2 μ g RNA were incubated with CD3RT at a final concentration of 1 μ M at 65°C for 10 min to allow better annealing of the oligonucleotide. After cooling to RT, all remaining components, including 1 U RNaseOut (Invitrogen), were added. The reaction was incubated at 37°C for 90 min.

PrimeScript

Reverse transcription with the PrimeScript was carried out according to the product manual. 1- 2 μ g RNA was incubated with a random-octamer oligonucleotide for 5 min at 65°C. Subsequently, all remaining components were added, including 1 U RNaseOut (Invitrogen) and the reaction was incubated for 10 min at 30°C and then 90 min at 42°C. The reaction was terminated by incubating for 15 min at 70°C.

Smart cDNA synthesis

Synthesis of smart cDNA is based on the SMARTTM RACE cDNA Amplification kit (Clontech). Reverse transcription was carried out using the PrimeScript polymerase and the primers CD3RT, SmartI and SmartII. CD3RT was incorporated during first strand synthesis, while SmartI and SmartII bind to the 5' cystidine overhangs created by the polymerase. This approach allows amplification of unknown 5' and 3' ends via PCR.

3.5 Working with DNA

3.5.1 Isolation of chromosomal DNA

For the isolation of genomic DNA, *in vitro* cultivated metacestode vesicles were washed with 1x PBS, disrupted by pipetting and pelleted by a centrifugation step at 800 g for 3 min. The supernatant was removed and the pellet was dissolved in gDNA lysis buffer (100 mM NaCl, 10 mM Tris-HCl, pH8.0, 50 mM EDTA, pH8.0, 0.5 % SDS) supplemented with 20 µg/ml RNase A and 100 µg/ml Proteinase K. 1.2 ml buffer per 100 mg pellet was used. For total digestion of Echinococcus cells, the samples were incubated 4- 5 h at 50°C and agitated. The DNA extraction was carried out as follows. One volume of phenol-chloroform-isoamyl-alcohol (25:24:1) was added to the samples and centrifuged for 25 minutes at 2000 g and room temperature, the upper aqueous phase was transferred into a new tube and the extraction step was repeated one to two times. The DNA was precipitated by adding 0.1 Vol LiCl (stock 5 M; pH 4.5) and 2 Vol 96 % ethanol. The precipitation mix was incubated over night at -20°C. The samples were then centrifuged at 20,000 g for 30 min at 4°C and the pellet was washed with 70 % ethanol and air-dried. The pellet was resuspended in 1x TE buffer (10 mM Tris, 1 mM EDTA pH 8.0).

Isolation of plasmid DNA from E. coli

The isolation of plasmid DNA from *E. coli* strains was performed with the NucleoSpin® Plasmid Kit (Macherey-Nagel).

3.5.2 Determination of DNA concentration

DNA concentration was photometrically measured at a wavelength of 260 nm using the NanoDrop 1000. The purity of the nucleic acids was analysed on the basis of the ratios of 260 nm/ 280 nm (for protein impurity; 1.8- 2.0) and 260 nm/ 230 nm (for salt impurity, above 2.0). A method to measure DNA concentration of PCR products was the comparison of the band intensity with the defined SmartLadder (Eurogentec) DNA-standard.

3.5.3 Polymerase-Chain Reaction (PCR)

PCR reactions were carried out with custom-made oligonucleotides (Sigma-Aldrich). The annealing temperature was calculated with the equation $Ta[^{\circ}C] = 4x (G+C) + 2x (A+T)$.

The elongation time (t_e) was calculated with 1 min per 1000 nt for TaqPolymerase (NEB). The elongation temperature was 72°C. Therefore, the cycling parameters were generally as follows: an initial denaturation for 1 min at 94°C, 30- 35 cycles of a denaturation (30 s), primer annealing (30 s) and a elongation step (t_e) and with a final elongation for 10 min at 72°C. The PCR mix included 1- 5 μ l template, 2 μ l 10x buffer, 0.2 μ l of dNTPs (10 mM), oligonucleotides (50 μ M) and Taq DNA polymerase (2 U/ μ l) at a final volume of 20 μ l. Other polymerases were used according to the manufacturer's instructions.

Semi-quantitative RT-PCR

Total RNA was isolated from *in vitro* cultivated metacestode vesicles, primary cells, as well as activated or non-activated protoscolecis isolated from gerbil material. cDNA was produced using the Omniscript RT-PCR kit (Qiagen) and oligonucleotide CD3RT according to the manufacturer's instructions. The original cDNA was diluted 1:2 and ten-fold serial dilutions of the cDNA were used as template for PCR. Normalisation of the cDNA amount was carried out by comparison of the band intensity of the constitutively expressed emelp using the primer pair Em10 15 and Em10 16 at 35 cycles. For the studied genes, oligonucleotides were designed amplifying fragments of 300- 500 nt.

Colony-PCR

To test the successful integration of fragments into the target plasmids the colony PCR was used. Colonies were picked from the agar plate and transferred separately into 30 μ l sterile water. For PCR 3 μ l of this bacteria-suspension were used. The PCR reaction was carried out with the Taq-Polymerase under standard conditions.

3.5.4 Rapid amplification of cDNA ends (RACE)

The 5' and 3' RACE experiments were carried out on either smart cDNA or the Y2H cDNA library in the pJG4-5 plasmid [40]. For the first PCR a primer complementary to the 5 or 3' end of the template and a gene specific primer was chosen. For nested PCR primers within the amplified fragment close to the first primer binding sites were chosen.

3.5.5 Sequencing

DNA was sequenced in an ABI Prism™ Sequencer 377 (Perkin Elmer), according to the dideoxy method (Sanger, 1977). 300 ng plasmid or 1 µl PCR-product was mixed with 5 nM oligonucleotide and 5x sequencing buffer to a final volume of 9 µl. Polymerase was added directly before the PCR-reaction. From march 2012 onwards sequencing was carried out at GATC (Konstanz, Germany). The DNA (plasmid 400-500 ng and PCR-product 100- 200 ng) was mixed with the oligonucleotide at a final volume of 10 µl.

3.5.6 Agarose gel-electrophoreses

1- 2 % agarose gels were prepared according to the size of the DNA-fragments. The agarose was dissolved by heating in 1x TAE buffer (40 mM Tris, 1 mM EDTA, pH8.0, 0.11 % glacial acetic acid ad 1 l H₂O, pH8.5). At 50°C, the agarose-TAE solution was poured into a horizontal gel sleigh, where loading wells were left by inserting combs. The samples were mixed with 6x agarose buffer (0.25 % bromophenol blue, 0.25 % xylene cyanol, 40 % saccharose and 30 % glycerol) and the separation was carried out at a voltage of 100- 120 V for 20- 30 minutes. The separation was estimated by running of the two dyes included in the loading buffer. In a 1 % agarose gel, the bromophenol blue band and the xylene cyanol correspond to a 0.3 kb and 3 kb fragments, respectively. The DNA was visualised by staining with ethidium bromide (0.2 mg/ml in 1x TAE) and UV light. The SmartLadder (Eurogentec) was used as DNA standard.

3.5.7 TA-cloning

The Taq-Polymerase automatically adds A-overhangs to the 3' end of the synthesised fragments. These fragments can be ligated into plasmids supporting the TA cloning e.g. PCR-cloning kit (Qiagen) or the TOPO-TA Cloning®KIT (Invitrogen), which possesses corresponding 5'T overhangs. The reaction was carried out according to manufacturer's instructions. Selection of the positive colonies was done by blue-white selection and colony-PCR.

3.5.8 Addition of A-overhangs

PCR products without the 3' A-overhangs were incubated with Taq DNA polymerase and dATP for 10- 30 min at 72°C and subsequently ligated into pDrive or pBad.

3.5.9 Blunt-end ligation

For ligation of blunt-end fragments the CloneJET™ kit (Fermentas) was used according to the manual.

3.5.10 Purification of DNA from agarose gels, PCR and enzyme reactions

Purification of fragments was from agarose gels carried out by excising the band of interest and purification with the NucleoSpin® (Macherey-Nagel), according to the manual. PCR products and enzyme reactions were purified with the same kit, without the agarose melting step.

3.5.11 Restriction digestion

Restriction digestion was carried out with enzymes purchased from NEB. With the optimal buffer and temperature for every enzyme according to the instructions. The reaction was incubated for 15 min to 2 h depending on the enzyme.

3.5.12 Dephosphorylation of plasmid DNA

To avoid re-ligation, plasmids were dephosphorylated subsequently to restriction digestion. CIP or antarctic phosphatase (NEB) were added according to the manufacturer's specification and incubated for 30 min at 37°C.

3.5.13 Ligation

Inserts and plasmids resulting from restriction digestion were ligated with the T4 DNA ligase (NEB). The amount of insert DNA was calculated with the following formula. Ideally, a ratio between 3:1 and 5:1 was used.

$$ngInsert = \frac{ngVector * kbInsert}{kbVector} * Ratio$$

3.6 Working with proteins

3.6.1 Preparation of protein samples

Crude lysates were prepared by adding 5x sample buffer to a final concentration of 1x. The samples were boiled for 10 min and centrifuged for 1 min with 11.000 g. The supernatant was transferred to a fresh cap. For subsequent protein determination sample buffer without bromophenol blue was used. Membrane fractions were won by lysis of parasite material for 1-2 h in lysis buffer (20 mM Tris-HCl, pH 8.0; 150 mM NaCl; 1 mM EDTA pH 8, 0; 1 % TritonX-100 ; 2 % Sodiumdeoxycholate; 1 mM Na₃VO₄; 10 mM NaF) supplemented with 1x protease inhibitor (Complete Mini phosphatase inhibitor Mix, Roche). The lysis was carried out at 4°C on a rotor. The samples were centrifuged for 1 min at 11.000 g and the supernatant was transferred into a new cap. After determination of the protein concentration, the samples were diluted with 5x sample buffer and boiled for 10 min.

3.6.2 Quantification of protein concentration

The protein concentration was measured with the BCA protein assay (Pierce). The solution A and B were mixed with the ratio 50:1 and 200 µl were added to 10 µl protein solution in a 96 well plate. The following standard samples were prepared with BSA: Blank, 25 µg/ml, 125 µg/ml, 250 µg/ml, 500 µg/ml, 750 µg/ml, 1000 µg/ml, 1500 µg/ml. The reaction was incubated for 30 min at 37°C and measured at 540 nm.

3.6.3 SDS-PAGE

For the SDS-PAGE the Biorad Mini- Protean system was used. Separation gels were prepared in 8 10 or 15%, the stacking gel was 4%. Combs with 9, 10 or 15 pockets were inserted into the gel directly after filling the gel solution into the polymerisation chamber. The indicated amounts were calculated for 2 Mini-gels.

Solutions:

4 x Lower-Tris	1.5 M Tris-HCl pH 8.8; 0.4% SDS
4 x Upper- Tris	0.5 M Tris-HCl pH 6.8; 0.4% SDS
5x Sample buffer	15% Tris-HCl (250 mM pH6.8);50 % Glycerol; 10 % SDS, 25 % β-MerOH, bromophenol blue
TEMED (N, N, N', N'-Tetramethylethylenediamin)	

16% Ammonium-Persulfat (APS)

PAA

Running buffer 25 mM Tris pH 8.3; 192 mM Glycin, 0.1% SDS

Pipetting scheme for 2 gels:

	15 %	10 %	4 %
H ₂ O [ml]	3	5	3.2
Lower-Tris [ml]	3	3	-
Upper-Tris [ml]	-	-	1.6
PAA 30% [ml]	6	4	0.75
APS 16[μ l] %	60	60	35
TEMED [μ l] %	20	20	10

3.6.4 Coomassie

The protein gels were stained for 20- 30 min with staining solution on the seesaw. For destaining, the destaining buffer was changed several times until the desired band intensity was reached. Bands were visualised by destaining the unspecifically stained gel areas. To dry the gels cell glass was wetted in water with glycerol. The gel was completely covered with the foil and fixed in a dry-frame. The gels were dried for approximately 3 days.

Solutions:

Staining solution 1 g Coomassie Blue R-250, 450 ml Methanol,
450 ml H₂O, 100 ml acetic acid

Destaining solution 100 ml Methanol, 100 ml acetic acid, 800 ml H₂O

3.6.5 Western blot

For the transfer of the separated proteins onto a nitrocellulose membrane the Biorad Mini Trans-Blot Cell system was used. The transfer was carried out for 1 h at 350 mA. Subsequently, the membrane was blocked for 1 h at room temperature in blocking buffer. The corresponding antibody was incubated over night at 4°C on a seesaw. The membrane was washed 3x for 10 min at room temperature, after which the membrane was incubated

with the secondary antibody for 1 h at RT on the seesaw. The three washing steps were repeated and the proteins were visualised by chemiluminescence (ECL, Pierce) and exposing to X-ray-films. The films were developed with a Curix 60 automated developer (Agfa).

Solutions:

Running buffer	25 mM Tris pH 8.3; 192 mM Glycin; 5% Methanol
Blocking buffer	5 % skim milk in TBST 5 % BSA in TBST
TBST	20 mM Tris pH 7.5; 150 mM NaCl; 0.1 % Tween-20
Stripping buffer	20 mM Tris pH 6.8; 2 % SDS; 0.7 % β -Mercaptoethanol
ECL- Western Blot Substrate (Pierce)	

3.6.6 Ponceau-red staining

Nitrocellulose membranes were stained with Ponceau-red solution (2 % Ponceau-red in 30 % trichloroacetic acid) for 1- 2 min prior to blocking. The dye was washed out by rinsing with desalted water until the protein bands were visible.

3.6.7 Purification of polyclonal antibodies

To purify polyclonal antibodies the corresponding, heterologous expressed protein was separated on a 10 % SDS gel prepared with a 2- pocket comb. After western blot, the protein band was detected by Ponceau-staining and cut out. The nitrocellulose membrane was transferred to a 2 ml Eppendorf cap and blocked with 5 % BSA in PBS for 4 h at 4°C on a rotor. 2 ml immune-serum was added and incubated over night at 4°C on a rotor. The supernatant was transferred to a new cap for repeated use and the membrane was washed first with 0.15 M NaCl for 20 min at room temperature and then with 1x PBS. Subsequently, the membrane was incubated with 300 μ l elution buffer (0.2 M Glycin; 1 mM EGTA pH 2.5) for 20 min at room temperature. The supernatant was transferred into a fresh cap and neutralised with 0.01 M Tris pH 8. The membrane was washed with 1x PBS and stored at -20°C.

3.6.8 IHC

Samples embedded in Technovit 8100 were cut in 4 µm sections and taken up on a glass slide. The sections were dried for 2 h at 37°C and cauterised for 4 min with acetone. A decreasing ethanol series was used to rehydrate the sections (5 min 100 % ethanol; 5 min 96 % ethanol; 5 min 70 % ethanol; 5 min 1 x PBS). The samples were then permeabilised for 7 min with 1 % Triton in PBS and rinsed 3 x with PBS. To block endogenous peroxydases the slides were incubated for 10 min with 0.3 % H₂O₂ in methanol and washed 2x 5- 10 min with PBS. Blocking was carried out for 60 min with 2 % BSA in PBS. The first antibody was used at a dilution of 1:10 in blocking buffer and incubated over night at 4°C in a humid chamber. The samples were washed 3x for 5 min with PBS and the second antibody (POX-anti-rabbit 1:50 in blocking buffer) was incubated for 3 h at room temperature in a humid chamber. The samples were washed again and substrate solution (2 mg DAB; 2 ml PBS; 2 ml H₂O; 1.34 µl 30% H₂O₂) was added and incubated at room temperature until the desired intensity was reached. To stop the reaction the slides were rinsed with H₂O. Counterstaining with Haematoxylin was carried out by a 6 min incubation with Haemalaun (Roche) and rinsing in H₂O. The slides were then washed for 15 min in running tap water. The slides were then dehydrated by passing through an increasing ethanol series (5 min 70 % ethanol; 5 min 96 % ethanol; 5 min 100 % ethanol; 5 min xylol) and then mounted with Entellan (Merck).

3.6.9 Immuno precipitation

Metacestode vesicles were stimulated and prepared according to protocol. The vesicles were disrupted and 1 ml IP buffer (20 mM Tris-HCl, pH 8.0; 150 mM NaCl; 1 mM EDTA pH 8, 0; 1 % TritonX-100 ; 1 mM Na₃VO₄; 10 mM NaF) supplemented with 1x protease inhibitor was added. The samples were rotated for 2 h at 4°C and then centrifuged for 15 min at 13.000 g and 4°C. The supernatant was transferred to a fresh cap and supplemented with purified immune-serum in the dilution of 1:50. The samples were incubated over night at 4°C on a rotor. 60 µl Agarose-G beads were washed 3x with TBST (centrifugation at 2500 rpm for 1 min) and added to the protein-antibody solution. The samples were rotated for 4-5 h at 4°C and subsequently washed 3x with IP buffer (2500 rpm 1 min). 100 µl 2x sample buffer was added and the samples were boiled for 10 min. Technical controls were included to check for unspecific binding: First, protein samples without antibody and second, antibody without protein.

3.7 Working with bacteria

3.7.1 Chemically competent *E. coli*

E. coli strains Top10 or B121 were made chemically competent with the CaCl₂ method as follows. 1 ml LB- medium was inoculated with the *E. coli* strain and grown over night at 37 °C and 225 rpm. This culture was transferred into 50 ml of fresh LB and the bacteria were left to grow to an OD₆₀₀ of 0,5- 0.7 (app. 2- 3 h). The culture was centrifuged at 4000 rpm at 4°C for 10 min. The supernatant was discarded and the pellet was resuspended in 12 ml ice cold 100 mM CaCl₂ and again centrifuged. The pellet was carefully resuspended in 1 ml 100 mM CaCl₂ and incubated on ice for 30 to 60 min. Glycerol was added in a final concentration of 20 %. The bacteria were frozen on dry-ice in 50 µl aliquots and stored at -80°C.

3.7.2 Transformation of *E.coli*

Aliquots of competent *E. coli* aliquots were melted on ice and 2- 5 µl ligation reaction was added. The transformation reactions were incubated on ice for 30 to 60 min, followed by a heat-shock for 1 min at 42°C and additional 2 min on ice. 125 µl of Soc or LB medium were added and the reactions were incubated at 37°C and 225 rpm for 45 min to 1 h. Afterwards the bacteria were plated on LB- agar plates (LB, 15 % agar) supplemented with antibiotics (100 µg/ml ampicillin or 50 µg/ml kanamycin) and incubated at 37°C over night. Additionally, for blue-white selection of the pDrive plasmid (PCR cloning kit, Quia- gen) 40 µl X-Gal (40 mg/ml in DMSF) was plated before adding the transformation reaction.

3.7.3 Liquid culture of *E.coli*

4 ml to 1 l LB-medium supplemented with the corresponding antibiotics was inoculated with transformed *E. coli*. The culture was incubated over night at 37°C and 225 rpm.

3.7.4 Glycerin stocks

600 µl liquid solution were mixed with 400 µl 85 % glycerol and transferred to a cryo-cap. The glycerol stock was stored immediately at - 80°C. For inoculation of liquid cultures from the stocks small portions were scraped of the frozen culture and transferred to the LB-medium.

3.7.5 Recombinant expression of *E. multilocularis* proteins in *E. coli*

For expression of *E. multilocularis* proteins the pBAD/TOPO[®] ThioFusion[™] Expression Kit (Invitrogen) was chosen. The cloning of PCR products into the pBAD/thio plasmid is based on TA-cloning and was carried out according to manufacturer's instructions. The expression was tested in a pilot experiment for testing the expression conditions. Based on these experiment the expression was carried out using 1 l final volume of LB medium. Therefore 10 ml over night culture of *E. coli* transfected with the respective plasmid were transferred to 1 l LB-Amp. The culture was incubated at 37°C and 125 rpm until an OD₆₀₀ of 0.4- 0,5 was reached. The expression was induced by adding arabinose to a final concentration of 0.002 % and the culture was incubated for another 4 h. The cells were pelleted at 3000 rpm for 10 min at 4°C and the purification was carried out according to the ProBond[™] Purification System (Invitrogen) manual. The cell pellet was resuspended in 20 ml Guanidinium lysis buffer and incubated at room temperature for 10 min and gentle shaking. The samples were sonicated with 5 30 s pulses and centrifuged at 12.000 rpm for 20 min. The pellet was lysed a second time with 5 ml fresh lysis buffer and after centrifugation the supernatants were combined. The ProBond[™] Nickel-Chelating Beads (Invitrogen) were equilibrated by washing three times with guanidinium lysis buffer. 2 ml beads were added to the lysis supernatant and the samples were incubated over night at 4°C on a rotor. The mixture was then decanted into a PD-10 column (GE Healthcare) and the flow was set to 30- 40 drops/ min. The beads were washed with 150 ml Denaturing wash buffer. Elution was carried out two times for each buffer by incubation of the beads for 10 min with 1 ml elution buffer and collection of the elution fraction. Elution was done with Denaturing elution buffer, followed by Imidazole elution buffer and a third elution with 0.5 M EDTA. The beads were regenerated by washing with 15 ml of the following: 50 mM EDTA, 0.5 M NaOH, H₂O, 5 mg/ml Ni(II)Cl₂ and H₂O. The beads were stored at 4°C in 20 % EtOH.

Samples for SDS-PAGE were collected before and after induction, from the washing fraction and the elution fractions.

Buffers and solutions

Guanidinium Lysis buffer	6 M Guanidine-HCl, 20 mM Na ₃ PO ₄ , 0.5 M NaCl, pH 7.8
Denaturing wash buffer	8 M Urea, 20 mM NaH ₂ PO ₄ , 0.5 M NaCl, pH 5.8
Denaturing elution buffer	8 M Urea, 20 mM NaH ₂ PO ₄ , 0.5 M NaCl, pH 3.8
Imidazole elution buffer	250 mM Imidazole, 50 mM Na ₂ HPO ₄ , 300 mM NaCl, pH 8
0.5 M EDTA, pH8	
0.5 M NaOH	
5 mg/ml Ni(II)Cl ₂ and H ₂ O	
20 % EtOH	

3.8 Working with *E. multilocularis*

Media and solutions Preparation

MEM	DMEM without FCS and PST
Culture medium	DMEM, 10 % FCS, 1 % PST, 4 µl/ml Tavanic
Starvation medium	DMEM, 0.2 % FCS, 1 % PST, 4 µl/ml Tavanic
A4	pre-incubation of 100 ml culture medium for 7 d with 10 ⁶ Rh ⁻ , sterile filtration, storage at -20°C
B2	pre-incubation of 100 ml culture medium for 3 d with 2x 10 ⁷ Rh ⁻ , sterile filtration, storage at -20°C
cMEM	undefined conditioned medium (filtered supernatant of Rh ⁻ from co-culture)
Reducing agents	100 µM L-Cystein , 10 µM Bathocuproine disulfonic acid, 0.01 % β-mercaptoethanol

3.8.1 Isolates and maintenance of parasite material

The long-term maintenance of *E. multilocularis metacestodes* is ensured by passages in the peritoneum of Mongolian jirds (*Meriones unguiculatus*). The jirds were infected with homogenised larval material by intraperitoneal injection. The animals that developed a secondary alveolar echinococcosis (app after two months) were sacrificed with CO₂ and the larval material was isolated under sterile conditions. The isolated parasite tissue was cut into small pieces and passed through a metallic tea sieve. The sedimented material was washed with sterile PBS until the majority of red blood cells was removed. For reinfection of jirds the parasite material was treated with Tava (4 µl/ml parasite suspension) at 4°C over night. Then the material was washed again and the PBS was carefully decanted. Subsequently syringes with 0.3- 0.5 ml were prepared from the sediment and used for infection

of jirds. The Tava treated material was also used to set up metacestode *in vitro* cultures. For the isolation of protoscoleces the material was used without the antibiotic over night treatment [42,43].

Isolate	Source
H95	primary infection of <i>M. unguiculatus</i> by oncosphere uptake
Java, 7030, J31	Java monkey as intermediate host
GH09	Java monkey as intermediate host, 2009
G8065, GT10	Java monkey as intermediate host, 2010
Ingrid	Java monkey as intermediate host, 2011
MS10	dog as intermediate host, 2010

3.8.2 *In vitro* cultivation

For *in vitro* cultivation of *E. multilocularis* Tava- treated parasite material was used to set up co-cultures. The material was passed through a plastic tea sieve and transferred to a 50 ml greiner. Different fractions could be used to set up the culture: Crude material from the top of the sieve, liquid from the 20 ml mark after 10-30 s of sedimentation and the sediment in the greiner. 1 ml material was seeded into a 75 cm² bottle and 50 ml of 10 % FCS/ DMEM/ PST (100 U/ml penicillin G/ streptomycin) was added. Additionally 10⁷ trypsinised Rh⁻ cells were added. Medium change was carried out once a week and new Rh⁻ cells were added during each change. The parasite material was split after reaching 5, 10 and 20 ml of volume [42, 43].

3.8.3 Axenic culture

For axenic cultivation 15- 20 ml metacestode vesicles were washed with PBS. CMEM supplemented with L-Cystein (100 µM), Bathocuproine disulfonic acid (10 µM) and β- mercaptoethanol (0.01 %) was added to 50 ml. The culture was transferred to a 75 cm² sterile cell culture bottle and a nitrogen atmosphere was applied. The culture was incubated for 2- 3 d prior to experiments [43, 44].

3.8.4 Isolation and cultivation of primary cells

Axenic metacestode vesicles of a milky-white appearance with a thick laminar layer were washed with PBS until the supernatant was colourless. The vesicles were destroyed with a 10 ml pipette and washed again for two more times. Centrifugation for 3 min at 800 g could be included for better pelleting. The PBS was removed and 4 volumes of trypsin (0.05 %

trypsin, 0.02 % EDTA in PBS) was added and the vesicles were incubated for 15- 20 min at 37 °C. During the incubation the vesicles were shaken at regular intervals. The trypsinization was ready when the majority of vesicles were floating at the surface of the liquid. The suspension was then shaken vigorously for 2 min and filtered over a 150 µm gauze filter fixed to a glass beaker. The filter was rinsed with PBS and the flow-through was again filtered over a 30 µm gauze filter. this flow-through was decanted into a 50 ml greiner tube and centrifuged for 1 min at 100 g to remove calcium bodies. The supernatant was transferred to a fresh greiner and centrifugation to pellet the cells was carried out at 300- 500 g for 15 min [45]. The cells were resuspended in PBS corresponding to a volume of 1/2 of the original metacystode vesicle pellet. Subsequently the cell density was measured at OD₆₀₀. For that 12.5 µl of the cell suspension was mixed with 1 ml. An OD₆₀₀ of 0.02 corresponds to 1 Unit of cells in the cuvette (Markus Spiliotis personal communication). The following amounts of cells were used for ideal growing conditions:

Plate	Units
6 well	500
12 well	150-200
24 well	100- 150
96 well	50

3.8.5 Isolation of protoscoleces

To isolate parasite material from jirds PBS was added to a volume of 25 ml. The material was vigorously shaken for 10 min and the filtered first over a 150 µm gauze filter fixed to a glass beaker and then the flow-through with a 30 µm gauze filter. The protoscoleces were collected from the surface of the 30 µm gauze filter by pipetting and rinsing with PBS. The protoscoleces were transferred to a petri dish. Circular movement of the dish resulted in a concentration of pure protoscoleces in the middle of the dish, where they were collected with a pipette and transferred to a Eppendorf cap.

3.8.6 *In vitro* activation of protoscoleces

Isolated protoscoleces were activated by mimicking the gastrointestinal passage. They were incubated in 30 ml MEM supplemented 0.05 % pepsin pH2 (200 µl 25 % HCL) for 30 min at 37°C and 125 rpm. After washing with PBS until the supernatant was colourless the protoscoleces were transferred to 30 ml MEM supplemented with 0.2 % sodium

taurocholate and were incubated for another 3 h at 37°C and 125 rpm. The protoscoleces were washed again with PBS. Both activation media were sterile filtered prior to use [54].

3.8.7 Cultivation of protoscoleces

Non-activated or activated protoscoleces were ideally cultivated in A4 or B2 supplemented with reducing agents and a nitrogen phase. The amount of seeded protoscoleces was approximately 200- 400 protoscoleces per well of a 12 well plate [38].

3.8.8 Life-dead staining of protoscoleces

Protoscoleces were transferred to a Eppendorf cap washed 1x with PBS. The PBS was removed and 0.03 % methylene blue was added. After 1 min the samples were washed again. The protoscoleces were counted under a light microscope. Dead protoscoleces appeared blue, while healthy protoscoleces were not stained.

3.8.9 *In vitro* stimulation of metacestode vesicles

Metacestode vesicles were collected in a 50 ml Greiner tube and washed with PBS. Depending of the size of the vesicles 10 to 12 axenic vesicles of 3- 5 mm or 0.5 ml of smaller vesicles were used per sample. For starvation the vesicles were incubated with starvation medium (0.2 % FCS) and reducing agents for 16 h to 4 days. After starvation the medium was changed to pre-warmed fresh starvation medium and cytokines or inhibitors were added. For terminating the reaction, the samples were put on ice and washed 1x with cold PBS supplemented with 1 mM Na₃VO₄ and 10 mM NaF. The vesicles were destroyed by pipetting and centrifuged for 3 min at 800 g and 4°C. The PBS was removed and the samples prepared for SDS-PAGE (see section 3.6.3).

3.8.10 BrdU incorporation

Axenic metacestode vesicles were starved over night in starvation medium supplemented with reducing agents and nitrogen phase. The medium was removed and fresh medium was added. BrdU (final concentration: 1 mM) and insulin (1- 100 nM) were added and the samples were incubated for 2 d followed by isolation of chromosomal DNA (see section 3.5.1). A 96 well plate was coated with cDNA as follows. 0.5- 1 µg were mixed in a glass tube with the same volume of TE buffer. One volume of Reactibind (Pierce) was added. 96

well plates were loaded with 200 μ l of the coating solution and incubated over night at room temperature and gentle shaking. The plate was washed 3x with PBS and blocked with 2% skim milk in PBS for 1 h. After washing the BrdU incorporation was determined with the colorimetric cell proliferation BrdU ELISA kit (Roche), continuing with step 6 (Manual version: august 2007). The substrate reaction was stopped by adding 25 μ l of H₂SO₄ and the absorption was measured at 450 nm (reference wavelength 690 nm) on a Tecan ELISA reader.

For detection of BrdU incorporation in primary cell cultures, 10 U/ well of freshly isolated primary cells were seeded in a 96 well plate with 200 μ l of 2 % FCS/DMEM supplemented with reducing agents. Insulin was added and the cells were incubated for 24 h at 37°C and nitrogen phase. BrdU was added to a final concentration of 1 mM and incubated for another 4 h. The plate was centrifuged for 10 min at 4°C and 400 g followed by a washing step with PBS. Subsequently, the PBS was removed and the plate was dried for 1 h at 60°C, after which the plate could be stored at 4°C. The colorimetric cell proliferation BrdU ELISA kit (Roche) was used to measure the brdU incorporation. Lysis of the samples was carried out according to the manufacturer's instructions. After washing with PBS and a blocking step (2 % skim milk/ PBS 1h, RT) was included followed by washing 3 x with PBS. The protocol was continued at step 6.

3.8.11 Glucose uptake

Axenic metacystode vesicles were starved over night in 0.2 % FCS/ DMEM (glucose free) supplemented with 2.5 mM D-glucose. For the stimulation with insulin 5 vesicles (3- 4 mm) were transferred to a 15 ml Greiner tube, washed with PBS and 1.5 ml pre-warmed medium supplemented with 30 nM insulin or insulin and 30 nM Na₃VO₄ was added. All samples were prepared as triplets. The stimulation was carried out for 5 min and 0.1 μ Ci/ μ l (Hartmann Analytic) was added to each sample. The samples were carefully mixed and incubated for 1 h at 37°C. Subsequently, the vesicles were destroyed and washed 2x with PBS. The samples were centrifuged for 1 min at 2000 rpm and the supernatant was discarded. The pellet was lysed in 300 μ l 0.15 M NaOH for 5 min at room temperature. The samples were then centrifuged for 3 min at 10.000 rpm and 150 μ l of the sample was mixed with 1.5 ml UltimaGoldTM (Perkin Elmer). The C14 content was measured in a scintillation counter.

3.8.12 Resazurin assay in primary cells

Primary cells were isolated according to protocol (see section 3.8.4) and seeded with 10 U/ well to a 96 well plate. DMEM (10 % FCS, without phenol-red) was supplemented with the inhibitor in question and 100 µl medium were added to the cells. A dead-control was prepared with 1 % Triton. The plate was incubated for 2- 6 d at 37°C and nitrogen atmosphere. Subsequently, the resazurin stock solution (2 mg/ml in H₂O, stored at 4°C, Sigma) was diluted 1: 100 in PBS and 100 µl of the dilution was added to each well. The fluorescence was directly measured at 540 nm (reference wavelength 595 nm) with the Tecan reader to normalise the samples. The plate was then incubated for 3 h at culture conditions and the final fluorescence was measured (Markus Spiliotis personal communication).

3.8.13 Embedding of *E. multilocularis* material

Parasite larval stages were transferred from culture to 2 ml caps and washed with PBS. Metacystode vesicles were disrupted by pipetting or pricking with a needle. Subsequently, the samples were fixed for 1 h in 4 % PFA in PBS, followed by a over night with incubation acetone at -20°C. Technovit 8100 (Heraeus Kulzer) was used for embedding. First the samples were incubated with Technovit 8100 solution supplemented with hardener I for 6 h at 4°C, then the solution was changed to Technovit 8100 supplemented with hardener I and II. The samples were directly transferred to block forms and a Microtome plastic block was added on top. The hardening of the plastic was carried out at 4°C with a N₂ atmosphere.

3.9 Working with eukaryotic cell lines

3.9.1 Cultivation

In this work the cell lines Rh⁻ (Reuber hepatoma cells; ATCC No. CRL-1600) was maintained for the co-cultivation system. The cells were once a week trypsinized and approximately 10⁶ cells were seeded in a 75 cm² with 50 ml culture medium. Hek293T cells (ATCC No. CRL-11268) were seeded with 5x 10⁴ to 10⁵ and medium was changed accordingly.

3.9.2 Freezing stocks

Freezing stocks were prepared from all cell lines. For that the medium of a cell culture flask grown to 80 % density was transferred to a Greiner tube (conditioned medium) and the cells were trypsinized. The cells were also transferred to a greiner tube and centrifuged for 15 min at 400 g. The supernatant was discarded and the cells were resuspended in 2 ml conditioned medium, 1.2 ml fresh culture medium and 0.8 ml DMSO. The cell suspension was aliquoted at 1 ml per cryo-cap and immediately stored in the liquid nitrogen tank. For setting up new cultures from frozen stocks, the cell aliquots were melted on ice and transferred to a cell culture flask with 20 ml culture medium. The medium was changed to remove the DMSO as soon as the cells were adherent.

3.9.3 Transfection of Hek293T cells with the PEI method

Actively dividing Hek293T cells were seeded into wells of a 12 Ell plate with 0.3×10^6 cells per well and incubated over night in 10 % FCS/DMEM. For the transfection 100x PEI was diluted to 1x in MEM. 2 µg plasmid with 50 µl MEM and 2 µl 1x PEI with 50 µl MEM per transfection reaction were prepared separately. The suspensions were carefully mixed and incubated for 30 min at room temperature. The medium of the Hek cells was removed and 400 µl fresh medium was carefully added. The transfection mixture was added to the cells and incubated for 4-6 h, after which it was removed and 2 ml fresh 10 % FCS/DMEM was added. The expression was carried out for 24 h.

3.10 Working with yeast cells

3.10.1 Yeast strains and media

The *S. cerevisiae* strain AH109 (BD, Buosciences, Clontech), which was used for yeast two hybrid (Y2H) experiments has the following specifications:

MATa, trp1-901, leu2-3, 112, ura3-52, his3-200, gal4 Δ , gal80 Δ , LYS2::GAL1_{UAS}-GAL1_{TATA}-HIS3, GAL2_{UAS}-GAL2_{TATA}-ADE2, URA3::MEL1_{UAS}-MEL1_{TATA}-lacZ

Media:

YPDA:

20 g/l Difco Peptone

10 g/l yeast extract

20 g/l Bacto agar (for plates)

H₂O ad 950 ml

pH was adjusted to 6.5 by titration of 25 % HCl. After autoclavation 50 ml of 40 % glucose and 3 ml of 1 % adenine-hemisulfate solution were added. Both solution were sterile filtered.

SD:

6.5 g/l Difco™ Yeast Nitrogen Base, w/o Amino Acids

20 g/l Difco™ Bacto Agar

X g of the corresponding drop out supplement (DOS) (Clontech)

H₂O ad 950 ml

pH was adjusted to 6.5 by titration of 25 % HCl. After autoclavation 50 ml of 40 % glucose was added.

SD - Trp:

SD supplemented with 0.64 g/l Leu/- Trp DOS and 20 ml 50x Leu (5 mg/ml).

SD - Leu:

SD supplemented with 0.64 g/l Leu/- Trp DOS and 20 ml 50x Trp (1 mg/ml).

SD - Leu/- Trp:

SD supplemented with 0.64 g/l Leu/- Trp DOS

SD - Leu/- Trp/ -His:

0.6 g/l Ade/- His/- Leu/-Trp DOS and 0.64 mg/l histidine HCl mono-hydrate (Sigma-Aldrich).

SD - Leu/- Trp/ -His/-Ade:

0.6 g/l Ade/ - His/ - Leu/ - Trp DOS

3.10.2 Liquid culture

AH109 from freezing stocks or a YPDA plate were transferred into YPDA liquid medium and incubated over night at 30°C and 200 rpm.

3.10.3 Yeast two hybrid (Y2H)

Protein-protein interactions were analysed using the Gal4-based MATCHMAKER system (Clontech). The proteins of interest were expressed as fusion proteins either with the DNA-binding domain or the activation domain of the Gal4 transcription factor, that are encoded on the plasmids pGBKT7 and pGADT7, respectively. The plasmids containing the ORFs of the respective genes were co-transfected into AH109, grown over night in liquid culture. 10 ml of culture was needed for 10 reactions. The culture was centrifuged for 5 min at 750g and the pellet was resuspended in transformation buffer (40 % PEG 3350, 200 mM lithium acetate, 100 mM DTT). 500 ng of each plasmids were prepared in an Eppendorf cap and mixed with 100 µl of the transformation suspension. The samples were incubated for 30 min at 45°C. Then the transformation reactions were plated on -Leu/-Trp SD plates for double transformants. Controls included were the co-transfection of the large T- antigen (pGADT7: TAG-AD) with tumour suppressor p53 (pGBKT7; p53-BD) as positive control and the T-Antigen with lamin C (pGBKT7; LamC-BD) as negative control. Furthermore, the constructs of interest were co-transfected with the respective "empty" Gal4 plasmid. Expression of each construct was tested by western blot analysis. For that clones were picked and transferred to liquid culture with SD medium - Leu (pGADT7) or -Trp (pGBKT7). The cells were pelleted and prepared for SDS- PAGE. For the analysis of protein-interactions the double-transformants were transferred to selection plates. For high stringency selection, SD plates missing leucine, tryptophan, histidine and adenine were used. SD -Leu/ -Trp/ -His plates were used for medium stringency. The growth was assessed after 3 days of incubation.

3.11 Computer analysis and statistics

Amino acid comparisons were performed using the basic local alignment search tool (BLAST) available under <http://blast.genome.jp>. CLUSTAL W alignments were constructed employing the software BioEdit Sequence Alignment Editor (version 7.0.0) using the BLOSUM62 matrix. Alignments were manually modified as needed. Domain predictions were performed using the simple modular architecture research tool (SMART) available under <http://smart.emblheidelberg.de>. Genomic analyses and BLAST searches against the current assembly version of the *E. multilocularis* genome were done using the respective resources of the Sanger Institute (Hinxton, UK) available under <http://www.sanger.ac.uk/cgi-bin/blast/submitblast/Echinococcus> and the gene annotation available under <http://www.genedb.org/Homepage>.

4 Results

4.1 The insulin signalling cascade as a possible target for anti-echinococcosis chemotherapy

4.1.1 Insulin affects the larval development of *E. multilocularis*

It was recently shown, that insulin positively affects growth and survival of *E. multilocularis* metacestode vesicles *in vitro* [124, 130]. To study this further we employed the above described culture methods for primary cells, metacestode vesicles and protoscolices.

Development of primary stem cell cultures was shown to mimic oncosphere- metacestode transition *in vitro*, which is one of the earliest events during establishment of the disease [45]. Freshly isolated primary cells first form aggregates, which grow in size and develop internal cavities and then develop into new metacestode vesicles. In primary cell experiments morphological appearance, vesicle formation and proliferation of the cultures were investigated. In the primary cell system vesicle formation was significantly increased at host insulin concentrations of 10 and 100 nM (Fig.4.1A). Aggregates appeared larger and cavities were more pronounced (Fig. 4.1B). Furthermore, cell density and organisation of the cellular layer surrounding the cavities appeared healthier and more structured than in the samples without insulin. In a next experiment proliferation was measured by BrdU incorporation. Insulin stimulation with 10 nM lead to a significant increase of BrdU incorporation, whereas 1 nM only slightly increased proliferation (Fig. 4.1C).

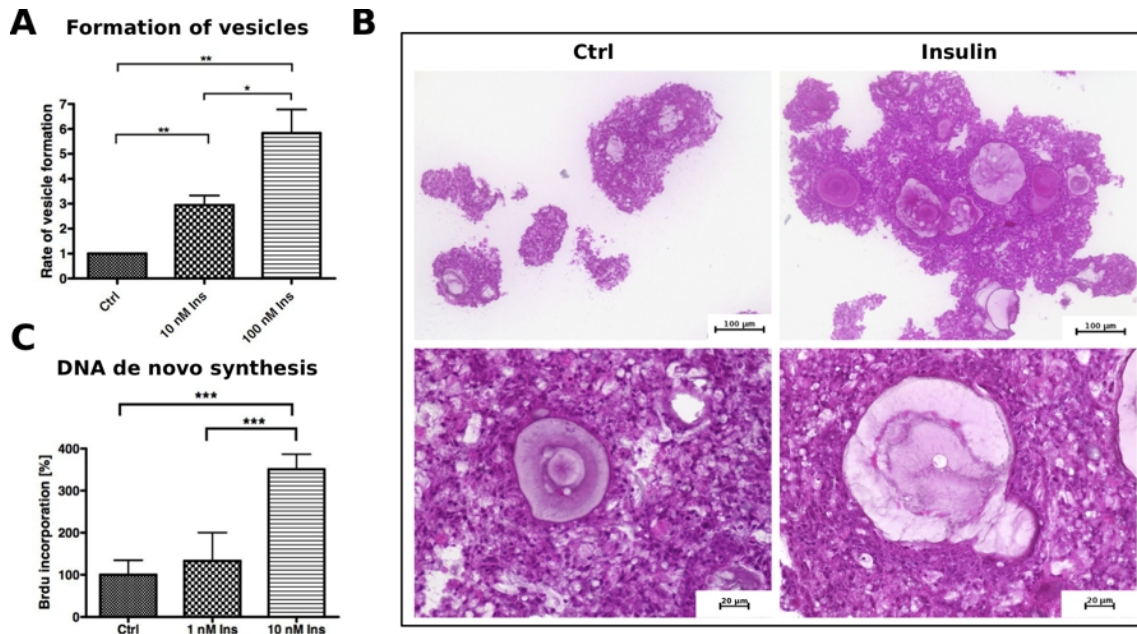


Fig. 4.1: Effects of recombinant host insulin on primary cell cultures. (A) Primary cells were cultivated in conditioned medium supplemented with human insulin for 3 weeks after which the formed vesicles were counted. Results were normalised against the control. (B) Primary cells were cultivated in 2 % FCS/DMEM with or without 10 nM human insulin for 1 week. Then the aggregates were fixed and embedded in Technovit 8100 and sections were stained with haematoxylin/eosin. (C) Primary cells were isolated from axenic vesicles and cultivated for 24 h with or without insulin. BrdU incorporation was measured with colorimetric BrdU ELISA kit (Roche). (*) *p* values below 0.05 (**) *p* between 0.001 and 0.01, (***) for *p* below 0.001

In metacestode vesicles a general increase in growth was observed when insulin was included in the culture [124], but due to a high variance no significance could be gained for these experiments. Therefore, DNA *de novo* synthesis was used as an indicator for insulin action. In these experiments the BrdU incorporation was significantly increased with 10 nM recombinant insulin, but 100 nM insulin led to a strong inhibition of proliferation even below the control value (Fig. 4.2).

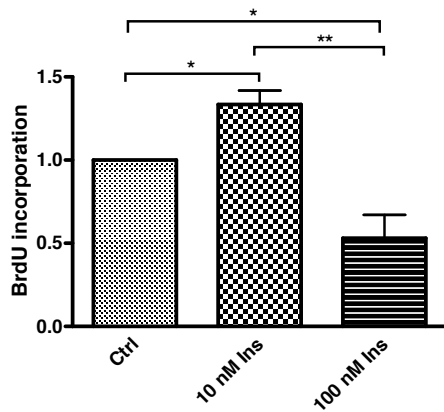


Fig. 4.2: Effects of insulin on BrdU incorporation in metacystode vesicles. Axenic metacystode vesicles were incubated for 2 days in the presence or absence of insulin in 0.2 % FCS/DMEM supplemented with BrdU. BrdU uptake was measured after chromosomal DNA isolation with colorimetric BrdU ELISA kit (Roche). (*) p below 0.05 and (**) p between 0.001 and 0.01

It was shown for protoscoleces of *E. granulosus* and *E. multilocularis* that they have the ability to develop into microcysts, that add to the pool of metacystode vesicles [131, 132]. We therefore studied the development of microcysts from protoscoleces in our cell culture system and showed that under axenic conditions microcysts form (Fig. 4.3A). Host insulin significantly increased the number of microcysts at concentrations of 1 and 10 nM human insulin (Fig. 4.3B). 100 nM insulin increased dedifferentiation, although no significance could be achieved. The amount of protoscoleces undergoing dedifferentiation was very low, between 2 and 4 % (data not shown).

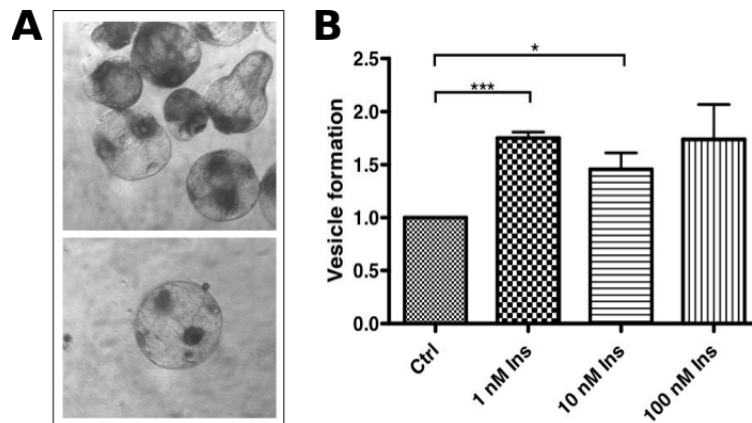


Fig. 4.3: Effect of insulin on dedifferentiation of protoscoleces. (A) Dedifferentiation of protoscoleces is characterised by a rounding up of the whole protoscolex. Suckers and hooks degenerate. The protoscolex appears transparent and vesicle-like. Muscle fibers, retained from the apical-basal organisation of the protoscolex are still visible in the microcyst (B) Protoscoleces were isolated from infected jird material and cultivated for three weeks in conditioned medium with or without insulin, after which dedifferentiated protoscoleces were counted (see A below). (*) p values below 0.05 (**) p between 0.001 and 0.01, (***) for p below 0.001.

Taken together these data showed that insulin clearly stimulated development of metacestode vesicles and promoted the development of *E. multilocularis* in vitro, where 10 nM insulin had the strongest effect on the parasite.

4.1.2 Effect of host insulin on glucose uptake

For EmIR1 a high expression in glycogen storage cells was detected [53], indicating an involvement of this receptor in glucose metabolism. Therefore, uptake of radioactively labelled glucose by metacestode vesicles in response to insulin was measured. At a concentration of 10 nM human insulin glucose uptake was stimulated significantly (Fig. 4.4). This effect was even more pronounced adding the phosphatase inhibitor Na_3VO_4 , which was previously used to stimulate insulin dependent glucose uptake [102]. These data suggest that host insulin, next to mitogenic effects, shown by proliferation and growth experiments also has metabolic effects on *E. multilocularis*.

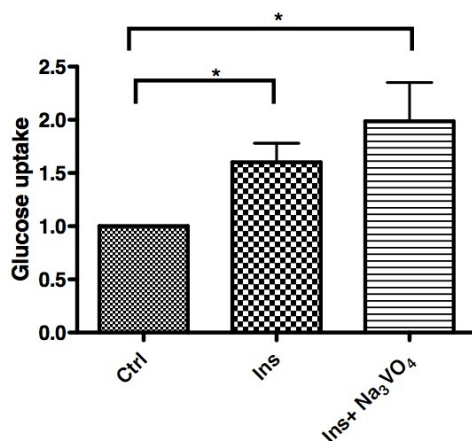


Fig. 4.4: Glucose uptake of metacestode vesicles. Axenic metacestode vesicles were incubated with ^{14}C -D-glucose with or without 10 nM insulin and 100 μM Na_3VO_4 . Control was set to 1 and results were normalised against the control. (*) p below 0.05

4.1.3 RT-PCR analysis of *emir1* and *emir2*

Previously two insulin receptor orthologues, EmIR1 [53] and EmIR2 [125] were identified, which are likely candidates to transmit insulin signals in *E. multilocularis*. EmIR2 is expressed in four isoforms that vary in the presence of two small alternative exons in the ligand binding domain [125].

New RT-PCR experiments for *emir1* and *emir2* were carried out to complete expression analysis with data from primary cell cultures. For these experiments protoscoleces were isolated from secondary infected jirds and part of the material was activated. Primary cells were isolated from axenic metacestode vesicles and harvested at day 3. Further, intact axenic metacestode vesicles of 3 to 5 mm were collected. RT-PCR experiments showed that *emir1* and *emir2* transcripts were present in all stages at nearly equal amounts (Fig. 4.5A).

Comparison of *emir2* isoforms [125] showed that *emir2a* and *b* are expressed equally in all stages, while *emir2c* was stronger expressed in non-activated protoscolecocytes and primary cell cultures (Fig. 4.5B). *Emir2d* could not be detected.

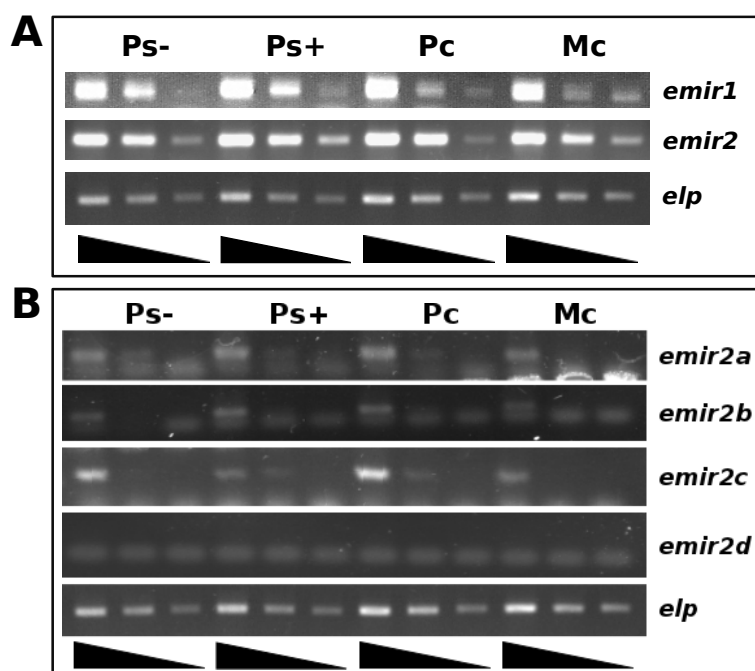


Fig. 4.5: Expression analysis of *emir1* and *emir2* in *Echinococcus multilocularis* larval stages by semi-quantitative RT-PCR. (A) *Emir1* was amplified with gene specific primers RC19 and RC21, *emir2* with *EmIRb dw3* and *EmIRb up3* was used. (B) Semi-quantitative RT-PCR of *emir2* isoforms. RT-PCR was carried out with the following primer combinations. *Emir2adw* and *emirbup4* for *emir2a*, *emir2bdw* and *emirbup4* for *emir2b*, *emir2cdw* and *emirbup4* for *emir2c* and primers *emirbdw5* and *emirbup4* to amplify *emir2d*. *Elp* was used as a cDNA control and amplified with *Em10 15* and *Em10 16*. Triangles indicate serial 10 times serial dilution of cDNA. PCR products were separated on a 1 % agarose gel and stained with ethidium bromide. (Ps-) non-activated protoscolecocytes, (Ps+) activated protoscolecocytes, (Pc) primary cells, (Mc) metacystode vesicles

4.1.4 Production of an anti-EmIR2 immunserum

The intracellular domain of EmIR2 was amplified via primers *emirbF3dw* and *emir2intra up* and cloned into pBAD/TOPO[®] ThioFusion[™] expression plasmid (Invitrogen). The EmIR2-Thio construct was expressed in *E. coli* analogous to the production of EmIR1 immunserum [124] and the protein was purified via the HIS-Tag. Elution fractions containing the protein were dialysed and used for immunisation of a rabbit (Fig. 4.6A). The immunserum was purified against EmIR2-GST by western blot. In subsequent western blot analy-

sis the purified immunserum detected only EmIR2-Thio and EmIR2-GST at 52 kDa and 75 kDa, respectively, but not EmIR1-GST (Fig. 4.6B). Expression of EmIR1 and EmIR2-GST constructs was proved using anti-GST antibody (Fig. 4.6C).

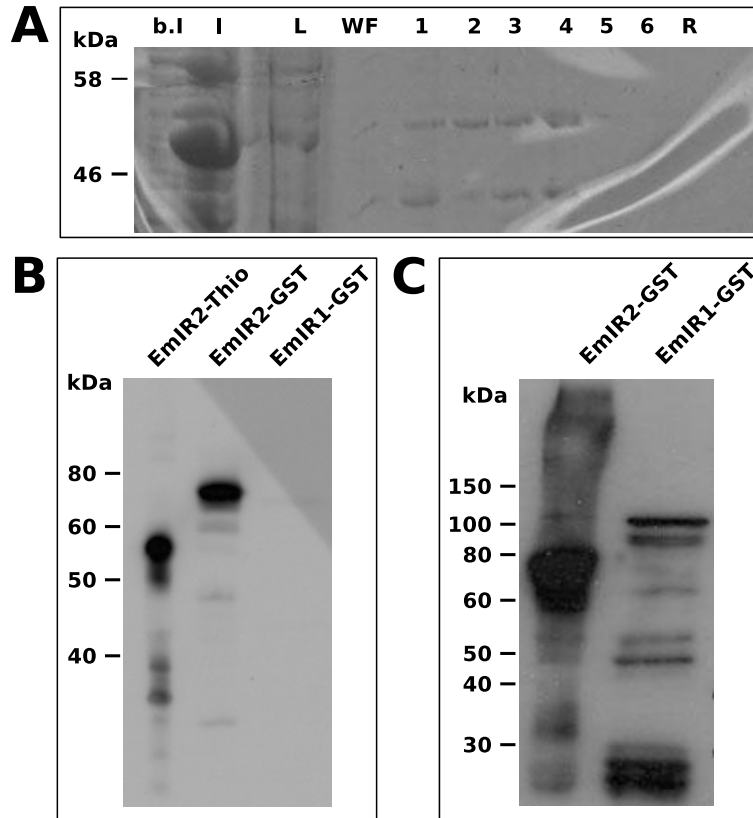


Fig. 4.6: Production of EmIR2 immunserum. (A) Purification of EmIR2-Thio expressed in *E. coli*. Protein samples were separated on a 10 % SDS gel and stained with Coomassie. EmIR2-Thio fusion protein was detected at 52 kDa. b.l.: before induction, I: after induction, L: lysate, WF: washing fraction, 1,2: Denaturing elution buffer, 3,4: Imidazole elution buffer, 5,6: 0.5 M EDTA, R: regeneration. (B) Test of the purified EmIR2 immunserum. Purified protein samples of EmIR2-Thio, EmIR2-GST and EmIR1-GST were separated on a 10 % SDS gel and a western blot was carried out with the purified EmIR2 immunserum. (C) Detection of EmIR2-GST and EmIR1-GST with anti-GST antibody.

4.1.5 Analysis of EmIR1 and EmIR2 expression on protein level

The purified immunserum of EmIR2 was used to analyse expression in different larval stages. Protein samples of axenic metacystode vesicles, primary cells and non-activated and activated protoscolecocytes were prepared. The EmIR2 serum detected a band at 87 kDa, corresponding to EmIR2 β subunit (Fig. 4.7A). A second band at 60 kDa was also

recognised by the serum most likely presented the IgG fraction or a degradation product of EmIR2. In contrast to RT-PCR analysis EmIR2 was highest expressed in primary cells and activated protoscolecetes and to a lower extent in non-activated protoscolecetes. No protein was detected in metacestode vesicles. To investigate expression of EmIR1 in primary cells the EmIR1 immunoserum was purified and used to analyse EmIR1 expression in protein samples. Corresponding to the analysis of Konrad [124] EmIR1 was detected in metacestode vesicles and protoscolecetes. New analysis revealed that EmIR1 is not present in primary cell cultures (Fig. 4.7B). The discrepancy in the results between protein and cDNA levels of EmIR1 and EmIR2 indicated a post-transcriptional expression regulation. In a next experiment the EmIR2 immunoserum was used to precipitate EmIR2 to analyse processing of the receptor. For human insulin- and IGF-receptor it is known that they form heterotetramers consisting of two α and β chains that are linked via disulphide bonds [67,69]. Therefore, EmIR2 immunoprecipitation samples were supplemented with 1 or 10 % β -Mercaptoethanol (β -ME) to allow incomplete and complete denaturation of the assembled receptor. With 10 % β -ME the β - subunit of EmIR2 was detected at 87 kDa and a fainter band at 211 kDa that could correspond to the $\alpha\beta$ dimer (Fig. 4.7C). Both bands were not present in samples containing 1 % β -ME. However a significantly larger band visible could indicate presence of assembled $\alpha_2\beta_2$ heterotetramer.

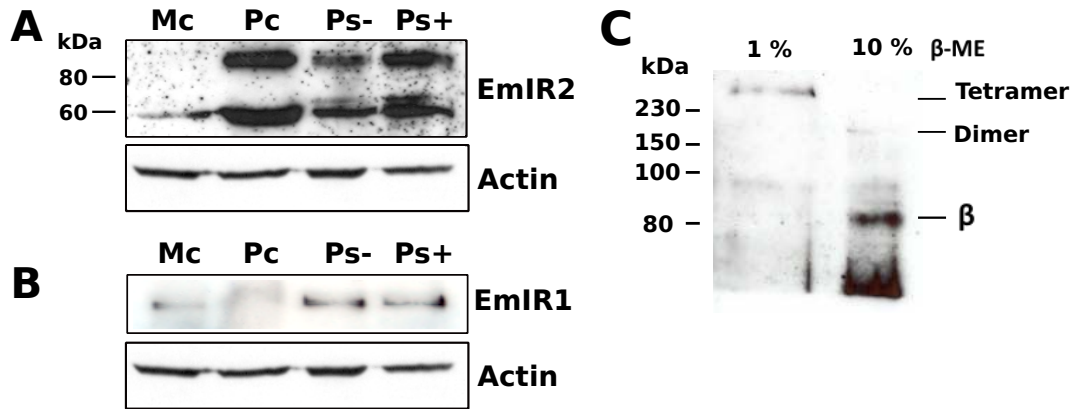


Fig. 4.7: Analysis of *EmIR2* and *EmIR1* protein expression. (A) Expression of *EmIR2* in larval stages. The purified immunoserum of *EmIR2* (1:300 in 5 % skim milk / TBS-T) recognised the *EmIR2* β subunit at 87 kDa and a second band at 60 kDa. Mc: metacestode vesicles, Pc: primary cell cultures, PS-: non-activated protoscoleces, PS+: activated protoscoleces. (B) The purified *EmIR1* serum (1:300 in 5 % skim milk / TBS-T) was used to detect *EmIR1* expression in metacestode vesicles, primary cells and nonactivated and activated protoscoleces. (C) Assembly of *EmIR2*. Immunoprecipitation of *EmIR2* from protoscoleces was carried out with the *EmIR2* immunoserum. Samples were supplemented with 1 or 10 % β -Mercaptoethanol (β -ME) and separated on a 10 % SDS gel. Western blot was carried out with the *EmIR2* serum (1:30 in 5 % skim milk / TBS-T). The antibody recognised the β subunit and bands corresponding to the $\alpha\beta$ dimer and $\alpha_2\beta_2$ heterotetramer.

4.1.6 Immunohistochemical analysis of *EmIR2* expression in *E. multilocularis* larval stages

The *EmIR2* immunoserum was employed to investigate the presence of *EmIR2* on sections of parasite material. In primary cells expression can be seen throughout the aggregate, with a denser stained layer at the cavity borders (Fig. 4.8A). In protoscoleces expression was found near the scolex and the tegumental layer (Fig. 4.8B). Interestingly, although no expression of *EmIR2* could be seen in western blot analysis of in vitro cultures, in infected liver material a specific staining of metacestode vesicles embedded in liver tissue was visible (Fig. 4.8D). The control without serum did not show any staining (Fig. 4.8C). Detection of *EmIR2* in liver material indicated a low expression level that could not be detected in western blot.

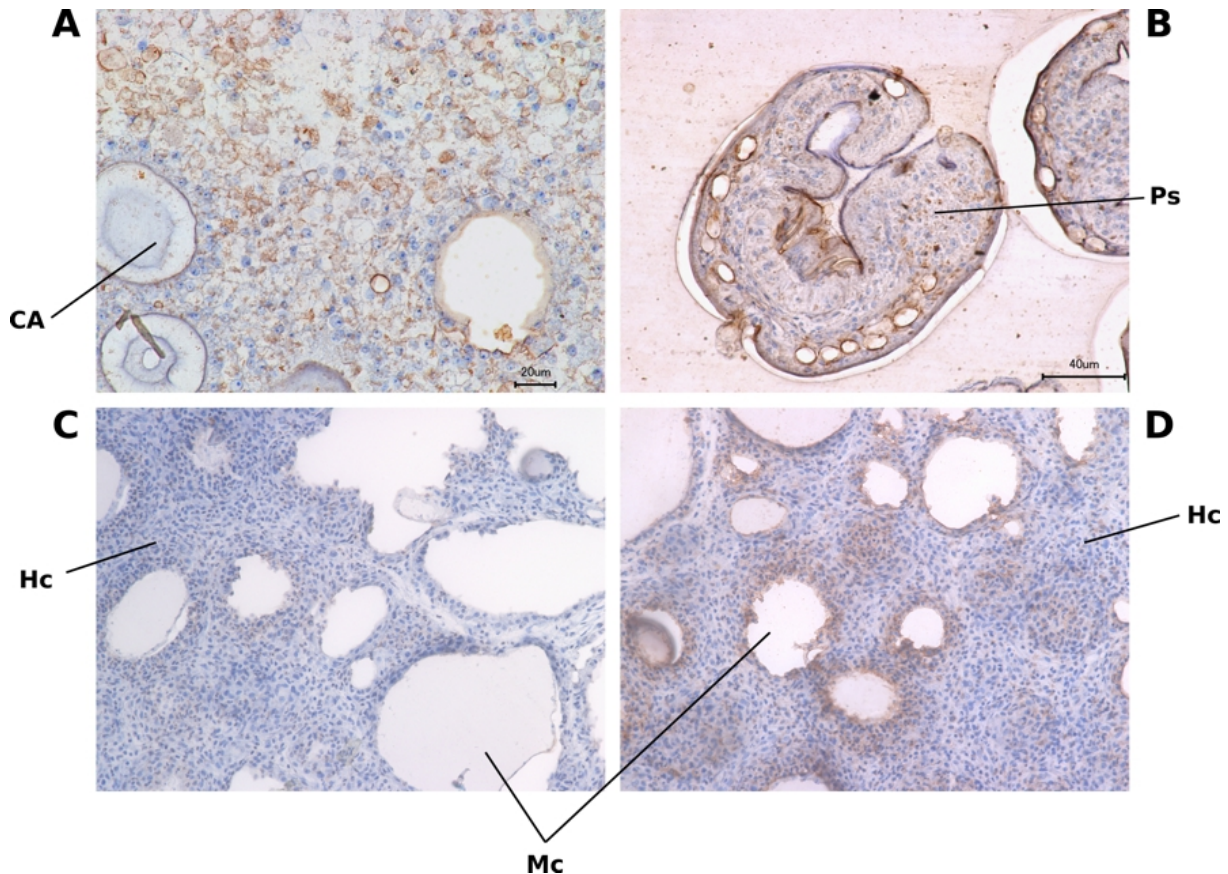


Fig. 4.8: Immunohistochemical expression analysis of *EmIR2*. (A) Primary cell aggregates were embedded in Technovit 8100 and sections were incubated with the *EmIR2* immunoserum (1:10 in 5 % skim milk / TBS-T) as first antibody. (B) Protoscoleces were embedded in Technovit 8100 and 4 µm sections were stained with the *EmIR2* immunoserum. The figure depicts an invaginated protoscolex. (C) Infected liver tissue of Mongolian jirds was used as a control by omitting incubation with the *EmIR2* immunoserum; (D) *EmIR2* expression in infected liver. CA: cavity; Ps: Protoscolex; HC: host cells; Mc: metacystode vesicle

4.1.7 The activation of EmIR2 by host insulin

Binding of insulin to the insulin receptor is the first step of the signalling process. Binding induces a conformational change in the receptor, which triggers autophosphorylation activity of the intracellular kinase domain [79]. The binding of insulin and IGF-I to *EmIR2* was studied in Yeast two Hybrid experiments (Y2H) analogous to analysis of *EmIR1* [53]. For *EmIR2* constructs the ligand binding domain (Thr23- Asp281) including leucine and cysteine rich regions (L1-CR-L2) was amplified with the primers *emir2ex* EcoRI and *emirex* XhoI and subsequently cloned into the vector pGADT7 (AD) via the restriction sites incorporated into the primer sequences. Furthermore constructs for *EmIR2* isoforms (a, b and c),

containing the full extracellular domain were produced (Thr23- Trp1141) using the primer combination emir2ex EcoRI and emirex SacI up. Due to a low expression the EmIR2d extracellular domain could not be amplified. Pro-insulin and pro-IGFI constructs were expressed as fusion proteins with the Gal4 binding domain (BD) [124]. All constructs were tested for expression by western blot prior to Y2H interaction experiments. For Y2H, yeast cells of the strain AH109 were co-transfected with the respective plasmids and double-transfectants were selected on leucine and tryptophan deficient agar plates (see section 3.10.3). The interaction assay was carried out on high and medium stringency plates. The plasmids pGADT7 and pBKT7 were used as negative controls control in combination with the respective fusion-proteins.

Y2H analysis showed that the N-terminal part of the ligand binding domain (EmIR2-LBD) interacted with pro-insulin as well as with pro-IGF-I (Tab. 4.1). In contrast, HIR and EmIR1 only bound to pro-insulin in Y2H experiments [124]. Binding of complete extracellular domains showed an overall weaker binding without differences between isoforms. The weaker binding is probably a consequence of the large size of the fusion-protein.

Tab. 4.1: Interaction studies of EmIR2 with insulin and IGF-I in Y2H assay. EmIR2 ligand binding domain (LBD) and full-length extracellular domain (ex) were expressed with the activation domain of Gal4 (pGADT7). Insulin and IGF-I were expressed as pro-peptides with the Gal4 binding domain (pBKT7). Co-transfection with pGADT7 or pBKT7 was used as negative control. (-) no growth, (+) weak growth, (++) moderate growth, (+++) strong growth

	pBKT7	pro-Insulin	pro-IGFI
pGADT7	-	-	-
EmIR2-LBD	-	++	+
EmIR2a-ex	-	+	-
EmIR2b-ex	-	+	-
EmIR2c-ex	-	+	-

Having shown binding of insulin to the receptor in the Y2H system, activation by autophosphorylation of the intracellular domain was investigated. For EmIR1 it was observed, that the TK domain is tyrosine phosphorylated upon stimulation with insulin indicating activation of the receptor [124]. Unfortunately, tyrosine phosphorylation could not be detected for EmIR2. However, serine phosphorylation was reported to occur subsequent to tyrosine phosphorylation in the mammalian receptor [133]. Therefore it served as an indirect proof of EmIR2 activation. For the experiments primary cell cultures were stimulated with host insulin and the β subunit of EmIR2 was immuno-precipitated using specific serum.

Stimulated samples showed a slightly increased serine phosphorylation compared to the unstimulated control (Fig. 4.9).

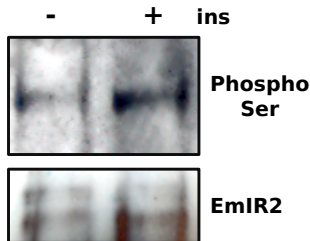


Fig. 4.9: Primary cells were grown for 5 days in conditioned medium under axenic conditions. Subsequently, cultures were starved for 5 h in 0,2 % FCS / DEMEM supplemented with reducing agents and stimulated with 10 nM insulin for 5 min. The EmIR2 β subunit was purified by immunoprecipitation with the EmIR2 immunoserum. Samples were normalised by the amount of EmIR2 and phosphorylation was detected with Phospho-serine sampler kit (Calbiochem).

4.1.8 Characterisation of the insulin receptor downstream signalling molecules PI3K, Akt and 4E-BP

With data from the whole genome sequencing project [134], molecules that are involved in insulin signal transmission in the mammalian signalling system were identified on genomic level (Tab. 4.2). Investigation of MAPK pathway involvement in insulin signalling only resulted in slight activation of EmMPK1 [124]. Therefore we investigated PI3K/Akt signalling in that respect. On the basis of genome data and BlastX analysis complete cDNAs of *empi3k*, *emakt* and *em4e-bp* were amplified and sequenced. RACE experiments were carried out to identify 5 and 3 prime ends of the cDNAs.

4 Results

Tab. 4.2: Homologues of PI3K pathway molecules were identified in the *E. multilocularis* genome.

Name	Systematic name	Location	Product
EmPI3K	EmW_000526100	supercontig pathogen.EMU_ scaffold.007636 : 1191161-1207682	phosphatidylinositol 3-kinase catalytic, alpha
EmAkt	EmW_000979200	supercontig pathogen.EMU_ scaffold.007780 : 4083862-4092994	akt-like serine/threonine protein kinase
Em4E-BP	EmW_000044600	contig pathogen.EMU_contig_ 60709 : 459698-462653	eukaryotic initiation factor 4e binding protein 1
EmIF-4E	EmW_000044600	contig pathogen.EMU_contig_ 60709 : 459698-462653	eukaryotic initiation factor 4E
EmIRS	EmW_000848300	supercontig pathogen.EMU_ scaffold.007768 : 10045618-10058030	insulin receptor substrate
EmmTor	EmW_000787900	supercontig pathogen.EMU_ scaffold.007768 : 5264722-5284913	target of rapamycin
EmFKBP12	EmW_000787900	supercontig pathogen.EMU_ scaffold.007768 : 5264722-5284913	rapamycin complex associated protein
EmPDK1	EmW_000723900	supercontig pathogen.EMU_ scaffold.007765 : 22476-24029	phosphoinositide-dependent protein kinase I
EmGSK3	EmW_000980300	supercontig pathogen.EMU_ scaffold.007780 : 4164112-4186701	glycogen synthase kinase 3
EmRps6	EmW_000877900	supercontig pathogen.EMU_ scaffold.007768 : 12109605-12110518	ribosomal protein S6 kinase
EmPKC	EmW_000455600	supercontig pathogen.EMU_ scaffold.007614 : 3119007-3125424	protein kinase c iota type

The *E. multilocularis* PI3 kinase orthologue

The cDNA of *empi3k* contained a single open reading frame (ORF) of 3582 bp coding for a protein of 1194 amino acids with a deduced weight of 134 kDa. In EmPI3K the characteristic domains were present [135]. The N-terminal p85 binding domain (30- 108), the ras binding domain (rbd, 183- 294), the C2 domain (411- 526), the PI3K accessory domain (PI3Ka, 611- 832) and the catalytic domain (PI3Kc, 923- 1193) were identified by Smart analysis (Fig. 4.10). Alignment with HsPI3Ka indicated the presence of three inserts of unknown function spanning amino acids 310- 369 in the rbd, 393- 423 in the C2 domain and 703- 732 in the PI3Ka domain. Homology between EmPI3Ka and HsPI3Ka was 32 % with the highest conservation in the catalytic domain and an overall 40 % with SmPI3K. The active center motives DRHNSN and DFG were conserved. The p85 binding domain mediates binding to the regulatory subunit [135]. Although no regulatory subunit was yet identified, the p85 binding domain shows an overall conservation, indicating presence of a binding partner, which could regulate PI3K activity. Before LY294002, an ATP-competitive PI3K inhibitor was tested in cell culture an analysis of the binding site

4 Results

conservation was carried out. Three out of four residues that were reported to mediate binding of LY294002 [136] were found in EmPI3K, therefore binding of the inhibitor was assumed.

```

1   MPPTTLESSDHMFQHCSSMKHDFLMPNGIVLTLKPPDISLADLKAHLWDLASAEPLYECLGPPNDYLFQGISSPKAEEE
81  EFYDEQCKFAGLQLFLPFMRLEKVSDDAQIIEQKRNAMIAKISTISQAHLKAAEGGNPELAWARQCLEEMSEANMRRLEA      p85B
161 GGPVMSMAHYLTAASLQPKLNTALQRRQLRPLPYLTISAVCVDCYSFPTQHLLKLNLPKISITVAAAIKEIIDEQRRLVQGDV
241 SCHDVPAPAOYLLKVVCCSQEYLFQEESALVHYAYVQECLEQRDDIPRLTPVLLKDVLECLGLPVPEVVNCEGCTPAYPSPA      rbd
321 VVSNAAAPLPSVIDLYGVKKEDEDEGDEAMFASVDLWDLRDYFSLITVRAAQKLTTLTQNPSTEQLDTGLFTGSSSFSDLT
401 TDVTSSSLGGSESSGSGGGGGAASATTPLSASSASSLDASSGSVVNYIVRVGLAHGGQLLAKYQNTRGAIIVMGGNSALQW      C2
481 NQSLNFRLLIYSNLPLATRVCVVLLQVRRPGRIMEFPVGNANMNLFDERGYLVTGRRSLPLWRSSFTSPETETTHQLNLA
561 GTVAENPDPEFTLVLFNCHPSNQKARIRFPISRFTTVRGASPNTPATIVPSLHSSSDIRVIRDLIHRDPFYELSEQD
641 KALLWRIRDSCRRLYPAESLPWLVOAVAWERRELVEEFYRLLAVWPRPLPVETCLQLLGVAGLAGSAAAFGTFGEGGGG      PI3Ka
721 SYVMAGGRRTTGVAADPLVRDIAVQGLQARLSNADLADYLLQLVQVVRTEAFLVNPLTCFLLQRALDCPTLIGVRLCWHLRS
801 QLDNPDARLRFGLILDALCRGFGPRLLLFVHEQVNALHRLTDLAI SVKRIAEDDEEQRARFKFELHRSEVRRDLEGILSPL
881 RFSIKLGPVVEQQCTVKRSKKRPLWIVWANPDNLGFHHHKIHQLLFKHGDDLRODMLTLQILKVMDSHIWKDEGLNLDLTT
961 YDCLATGDEMGLIEVVRNSOTIMSIQORVRSAMQIDSSQLHKWFLOKKAPPLGSEAYESAIRRFTNSCAGYCVATFVL
1041 GIRDRHNDNIMVDDSGRLFHIDFGHILNKKKKFGITRERVPFVLTSDFACVIARGEKPYRSKGFMDFTRLCEDAYRIL      PI3Kc
1121 RRHSNLLLTLLAMMVPSGLPELTCASDLEYVRKTLAVELRDEEALNYFNAKFNEAYNGAWTTKIDWFAHWVRR

```

Fig. 4.10: Deduced amino acid sequence of EmPI3K. Domains are underlined and indicated at the side. Insert regions are indicated by dotted lines and activation loop motifs are highlighted in bold. Asterics mark residues important for binding of the PI3K inhibitor LY294002.

The *E. multilocularis* Akt kinase

Only a single *akt* gene was identified using BlastX search on genome data. The *emakt* cDNA contained a single ORF of 2136 bp coding for a peptide of 712 amino acids with a deduced weight of 81 kDa. EmAkt displayed the characteristic structure of Akt kinases [88] with an N-terminal pleckstrin homology domain (PH, 124- 226), the serine/ threonin kinase domain (S/TKc, 262- 519) and an C-terminal regulatory domain (S/TKr, 520-587). The regulatory domain also contained a hydrophobic motif F-X-X-F/Y-S/T-Y/F specific for kinases of the AGC family. The homology between EmAkt and HsAkt1 lied at 39 % with very high conservation in the characteristic domains (Fig. 4.11). However EmAkt contained N- and C-terminal extensions, explaining the low overall conservation. In mammals Thr308 and Ser473 are phosphorylated in response to insulin or IGF-I [88]. Both residues were

present in EmAkt, corresponding to Thr419 and Ser584, which lied in the hydrophobic motif. In EmAkt the motif was not conserved, containing only the central residues F583 and S584.

```

1  MQVDESLNCSTPMGTLTPTSAPMAVDPLSSFVQFQASMSQIPCNTPQFNSNPSTVSSSLVPGAGTPCAGLSQEHFVPHAPV
81  SMPHLTGGLPGSTDLLGHQQALAINPTSMLQYFRIRTLPLTRKVIREGWLMKRGEHIKTWRRRYFILREDGTFYGYKNIP      PH
161 RDNLEQPLNFTVRDCQIICLNKPKPYTILMRGLQWTTVVERLFFVEHEVERDEWISAIQMVANRLRSENEAPTSVFKVD
241 FAEDVVIDFPQRPPKRYSTDDFELLLKVLGKGTFGKVVLCKEKESGCFYAMKILKKTVLIEKEEVGHTQTEHRVLQLNHHP
321 FMTQLKYSFTTRDHIFVMEYCNNGELFYHLSREHVFSERTQFYAAEITSALGYLHSONIVYRDLKLENLLLDKDGHIK      S/TKc
401 ITDFGLCKEDIGFGSTTKTFCGTPEYLAPELLLLDNDYGLSVDWWSLGVVYEMMCGRLPFYSNEHEILFELILQESVKVP
      *
481 DNLSPVARDILIRLLMKDPAERLGGGKADAIEVMVHPFFESISWDKLIKRDIIIPWKPVDVNGMDTKYIPEEFORENAV
561 TPPEKSVASAIMAADRVSVVKVFSASETMALYLKAPFPDTSPTLSSAKAQLTVYIRGTFGGSPVDVITVRRIQPNSPS      S/TKr
      *
641 LRRIFGHAYFSPRGQLFDSCLRVSFVEIMVISHCVSLCLFISLSIPATWHFSCTIADAVRPLLSSSLPLWDV

```

Fig. 4.11: Deduced amino acid sequence of EmAkt. Domains are underlined and indicated at the side. The activation loop motifs are highlighted in bold. Asterics mark phosphorylation sites and the hydrophobic motif is indicated by a box.

The *E. multilocularis* 4E binding protein

The cDNA of *em4e-bp* was identified by BlastX analysis and fully sequenced. The ORF was 351 bp in length, with only one exon. The deduced peptide was 117 aa in length and had a calculated molecular weight of 12.6 kDa. The Em4E-Bp was well conserved with 39.5 % identity to the human protein. In the mammalian homologue the residues Thr37, Thr46, Ser65 and Thr70 are phosphorylated after stimulation [137]. These residues were found to be conserved in Em4E-BP and correspond to the residues Thr30, Thr39, Ser58 and Ser63 in Em4E-BP (Fig. 4.12). For further analysis of the protein, a phospho specific antibody was used directed against the phosphorylated peptide surrounding the residues Thr37/46.

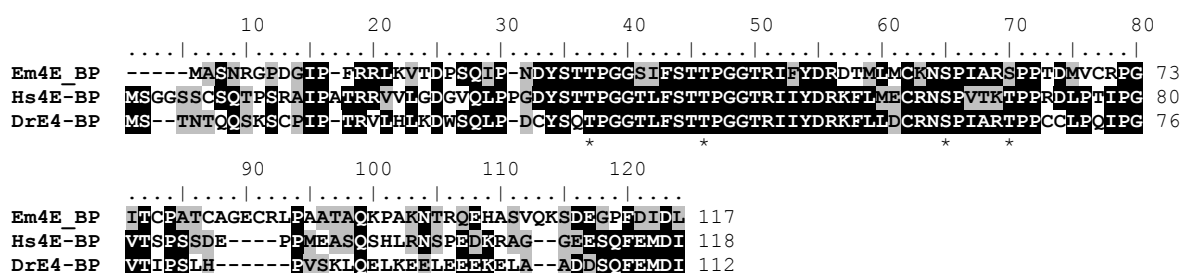


Fig. 4.12: Alignment of *Em4E-BP* with the *Homo sapiens* and *Danio rerio* homologues. Identical residues are highlighted in black, similar in grey. Asterisks mark phosphorylated serine and threonine residues.

4.1.9 Activation of the PI3K/ Akt pathway is involved in insulin signalling

To investigate activation of the PI3K/ Akt pathway, anti-phospho antibodies specific for phosphorylated Akt substrate motif RXXRXXS/T [88] and phosphorylated 4E-BP (Thr37/ 46) were selected. Metacestode vesicles were stimulated with 10 nM insulin for 5 min to 1 h. The strongest increase in phosphorylation was observed after 5 min of stimulation for Akt substrate and 4E-BP (Fig. 4.13). At 30 and 60 min no significantly higher phosphorylation was observed, indicating a fast activation of the pathway followed by termination of the signalling.

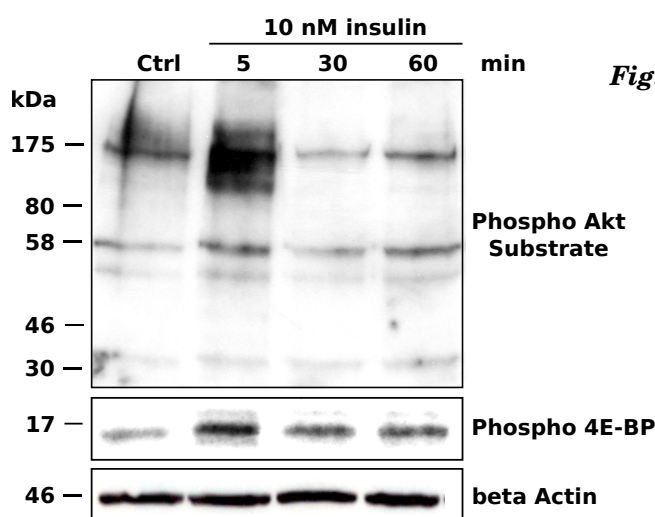


Fig. 4.13: Insulin triggers phosphorylation of PI3K/ Akt pathway molecules. Metacestode vesicles were starved in 0.2 % FCS/DMEM for 16 hours, followed by stimulation with 10 nM insulin for the indicated time. Detection of phosphorylated proteins was carried out using antibodies against phosphorylated Akt substrate motif and 4E-BP. Actin was used as loading control.

To verify direct activation of the PI3K/ Akt pathway by *Echinococcus* insulin receptor and PI3K, specific inhibitors were used to block insulin induced signalling. HNMPA(AM)₃ is an ATP-competitive insulin inhibitor designed against the human insulin receptor [138].

Due to high conservation of the ATP binding domain in helminthic insulin receptors, the inhibitor was used previously to block *Schistosoma* insulin receptors [100]. LY294002 was used to block EmPI3K [139]. Both inhibitors were added in concentrations of 100 μ M 2 h prior to insulin stimulation to ensure uptake into the cells. Insulin stimulation was carried out for 5 min with 10 nM recombinant human insulin and activation of the signalling cascade was tested using the phospho-E4-BP antibody. In this experiment insulin only slightly increased phosphorylation of 4E-BP, which is probably a consequence of short activation of the signalling as seen in Fig. 4.13. However, the inhibitor HNMPA(AM)₃ completely abolished phosphorylation, while LY294002 was less effective, but still reducing phosphorylation below the level of the control (Fig. 4.14)

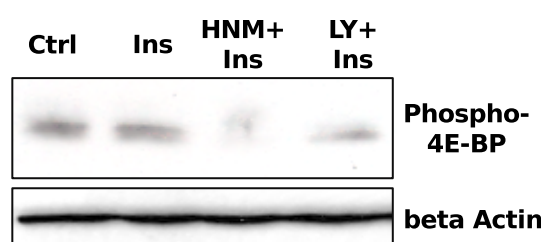


Fig. 4.14: The inhibitors HNMPA(AM)₃ and LY294002 blocked phosphorylation of 4E-BP. *Metacostode vesicles* were starved in 0.2 % FCS / DMEM for 16 hours. The inhibitors were added 2 h prior to insulin stimulation. Ten nM insulin were added and samples were incubated for 5 min. Protein samples were separated on a 15 % SDS PAGE and a western blot was carried out. Detection of phosphorylated proteins was carried out using the phospho-4E-BP antibody. Actin was used as loading control.

4.1.10 Effect of HNMPA(AM)₃ on *E. multilocularis* development

HNMPA(AM)₃ showed promising results in blocking insulin signalling. Therefore it was tested in the cell culture system on primary cells, metacostode vesicles and protoscoleces to investigate the importance of insulin signalling on survival and development of parasite material.

In the Resazurin cell health assay, 25 μ M and 50 μ M HNMPA(AM)₃ reduced viability of primary cell cultures to 75 and 50 %, respectively (Fig. 4.15).

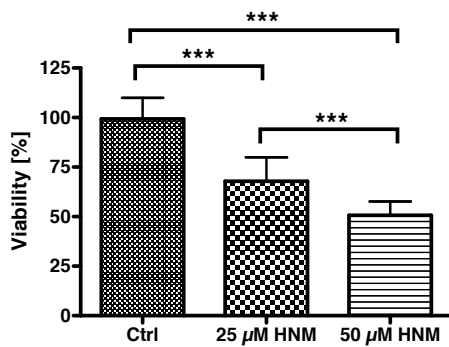


Fig. 4.15: Cell viability assay of HNMPA(AM)₃ treated primary cell cultures. Freshly isolated primary cells were incubated for 2 d with the indicated concentration of HNMPA(AM)₃ or DMSO. Resazurin was added for 3 h after which the fluorescence was measured. (***) *p* below 0.001

To analyse morphological changes induced by HNMPA(AM)₃, primary cells were incubated with the inhibitor for 7 days, followed by staining of aggregate sections with haematoxylin/eosin. Aggregates treated with 25 μM showed a loss of tissue integrity, while aggregates treated with 50 μM were completely dead (Fig. 4.16). Untreated aggregates appeared healthy, with large cavities and a good organization with a clear cavity border.

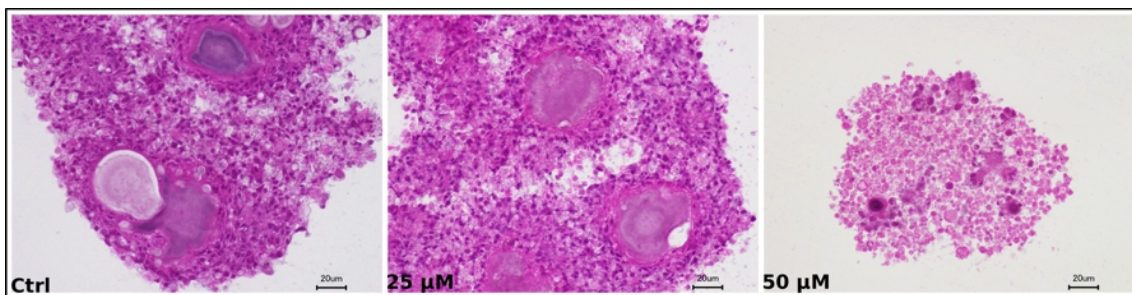


Fig. 4.16: HNMPA(AM)₃ induced morphological changes in primary cell aggregates. Primary cells were cultivated in conditioned medium supplemented with DMSO or HNMPA(AM)₃ for 7 days. Samples were embedded in Technovit 8100 and sections of 4 μm were stained with haematoxylin / eosin.

The effect of HNMPA(AM)₃ was more pronounced on vesicle formation of primary cell aggregates (Fig. 4.17A). Vesicle formation was increased two fold when insulin was included in the culture medium. In samples treated with 25 μM and 50 μM HNMPA(AM)₃ no significant vesicle formation took place. This finding corresponded with the observed growth of the cultures (Fig. 4.17B). Both the control and the insulin treated samples showed strong aggregation and regeneration, while in 25 μM inhibitor treated samples aggregation was strongly impaired and no aggregation was observed in cultures treated with 50 μM HNMPA(AM)₃ (see also [140]).

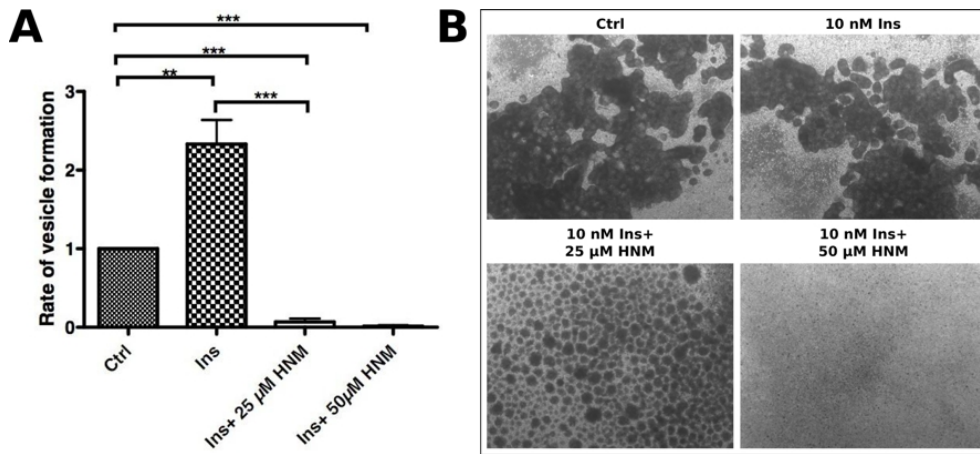


Fig. 4.17: HNMPA(AM)₃ impaired vesicle regeneration in primary cell cultures. (A) Freshly isolated primary cells were incubated with conditioned medium supplemented with insulin and HNMPA(AM)₃ or DMSO for one week. (B) Aggregation in 7 day old primary cell cultures treated with or without HNMPA(AM)₃ and host insulin. (*) *p* values below 0.05 (**) *p* between 0.001 and 0.01, (***) for *p* below 0.001

HNMPA(AM)₃ at a concentration of 100 μM HNMPA(AM)₃ severely decreased survival in metacystode vesicles (Fig. 4.18A). In protoscoleces 50 μM inhibitor reduced survival significantly, while 25 μM HNMPA(AM)₃ only had a slight effect (Fig. 4.18B). Furthermore, HNMPA(AM)₃ had an even more pronounced effect on dedifferentiation of protoscoleces *in vitro* cultures. 25 μM reduced the number of microcysts by more than 50% and only few microcysts formed in samples treated with 50 μM HNMPA(AM)₃ (Fig. 4.18C).

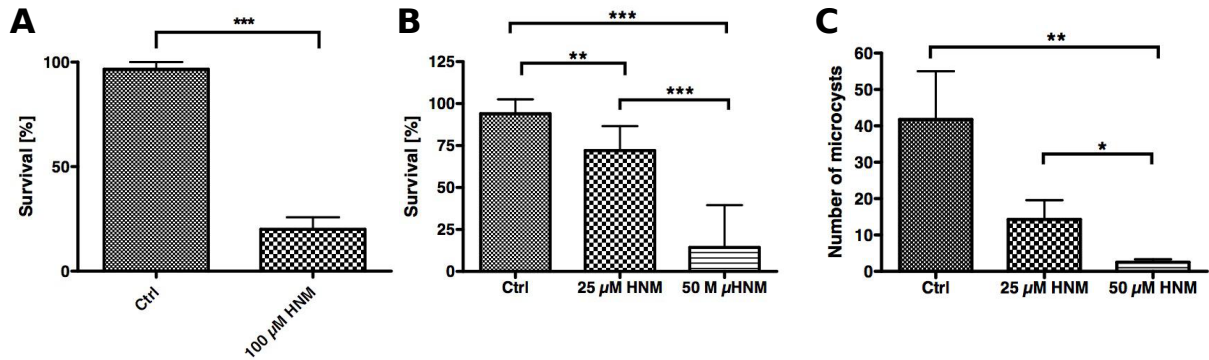


Fig. 4.18: Effect of HNMPA(AM)₃ on metacystode vesicles and protoscolecids. (A) Metacystode vesicles were cultured in conditioned medium supplemented with DMSO or HNMPA(AM)₃ for 7 days. (B) Protoscolecids were isolated from infected jird material and cultured under axenic conditions with DMSO or HNMPA(AM)₃ for three weeks, after which living and dead protoscolecids were counted. (C) After three weeks of incubation in conditioned medium supplemented with inhibitor round, transparent microcysts were counted. (*) *p* values below 0.05 (**) *p* between 0.001 and 0.01, (***) for *p* below 0.001.

4.1.11 Effect of the PI3 kinase inhibitor LY294002 on *E. multilocularis* development

LY294002 was tested in cell culture on metacystode vesicles and primary cells. Metacystode vesicles were susceptible to LY294002 treatment at a concentration of 50 and 100 μM (Fig.4.19A). After 14 days nearly all of the vesicles appeared to be dead. At day 7 only 50 % of the vesicles were killed. The inhibitor therefore exhibits a weaker effect than HNMPA(AM)₃. Primary cell cultures, measured with the Resazurin health assay 100 μM showed a 50 % reduced viability (Fig.4.19B). In the Resazurin assay, the weak effect is probably caused by the short treatment period and would be more pronounced at a longer treatment. Therefore, primary cells were treated for two weeks with LY294002 (Fig.4.19C). Cultures treated with 50 μM LY294002 showed reduced aggregation compared to the control. However, the aggregates had an overall healthy appearance with well formed cavities. In cultures incubated with 100 μM LY294002 initially aggregates formed (data not shown), but disintegrated after two weeks of incubation with the inhibitor (Fig.4.19C).

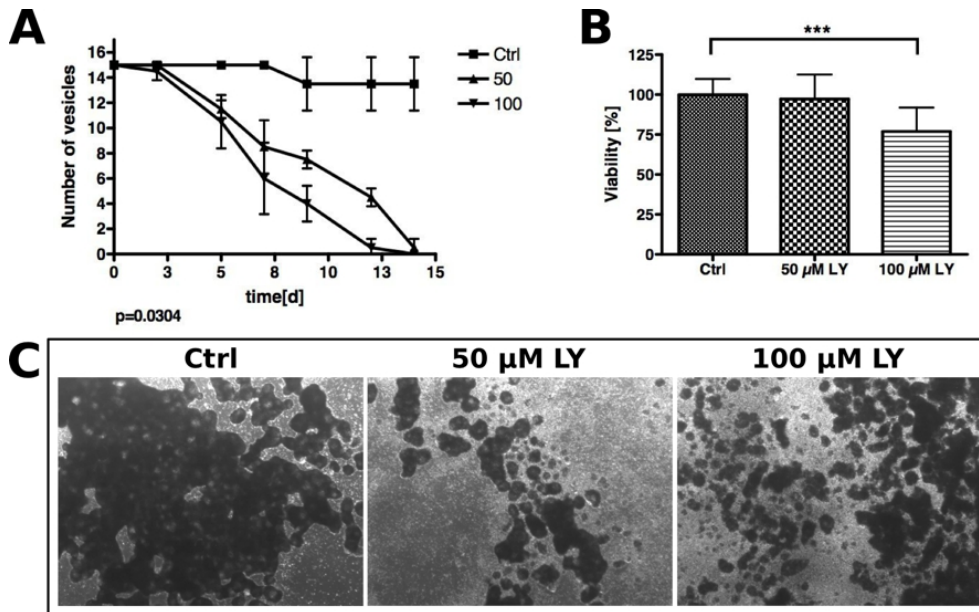


Fig. 4.19: Effect of LY294002 on *in vitro* cultivated metacestode vesicles and primary cell cultures. (A) Metacestode vesicles were cultured in conditioned medium supplemented with DMSO or LY294002 for 14 days. Survival was measured by counting damaged vesicles. p below 0.001. (B) Primary cells were cultivated with DMSO or LY294002 for 2 days and the Resazurin assay was performed. ***: p below 0.001. (C) Freshly isolated primary cells were cultivated in the presence or absence of LY294002 for 14 days in conditioned medium.

4.1.12 Insulin sensitivity in old and new isolates

Larval cestode material is routinely kept in peritoneal culture [43]. In the course of the experiments, isolates that were kept in culture for several years lost their ability to respond to insulin. In regeneration experiments old isolates still aggregated and regenerated normally (data not shown). To investigate insulin responsiveness further, the isolates H95 and Ingrid, that represent an old and new isolate, respectively, were tested in phosphorylation and BrdU incorporation experiments. In Ingrid, 4E-BP was phosphorylated in response to insulin, although basal phosphorylation in the control was very high in these experiments. H95 did not show any insulin stimulated phosphorylation (Fig. 4.20A). Incorporation of BrdU in primary cell cultures showed that basal proliferation rate is approximately the same between H95 and Ingrid. However, 10 nM of insulin strongly stimulated DNA de novo synthesis in Ingrid, while H95 did not react to insulin stimulation (Fig. 4.20B). The range of 1 nM to 100 nM of insulin also excluded the possibility, that H95 differs only in its ligand concentration optimum from Ingrid. A similar low reaction to insulin in different experiments was also observed for J31 and Java (data not shown). Taken together these

data indicated that the capacity to react to insulin is lost during prolonged passages in peritoneal culture, while isolates freshly isolated from natural hosts still reacted in the investigated manner. Insulin insensitivity was observed for old isolates (H95, J31, Java), while the isolates GH09, GT10, G8065 and Ingrid that were recently isolated from primates, were still responsive to host insulin.

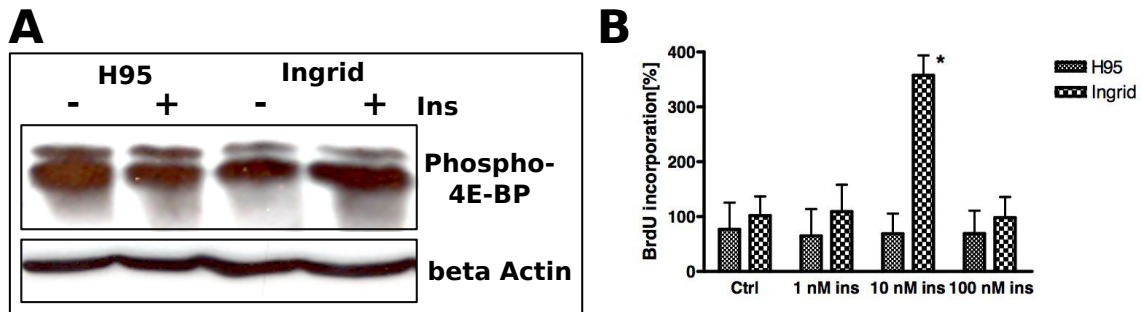


Fig. 4.20: Comparison of insulin responsiveness in old and new isolates. (A) Metacestode vesicles of H95 (old isolate) and Ingrid (new isolate) were starved in 0.2 % FCS/DMEM for 16 hour, followed by stimulation with 10 nM insulin for 10 min. Detection of phosphorylated proteins was carried out using the anti-phospho 4E-BP antibody. Actin was used as loading control. (B) Primary cells were incubated for 24 h with the indicated amount of insulin and subsequently incubated with BrdU for 4h. BrdU uptake was measured with the colorimetric BrdU ELISA kit (Roche).

4.1.13 Insulin-like peptides in *E. multilocularis*

Previously, two insulin like peptides (ILP) were identified that were termed EmIns1 and EmIns2 [125]. According to current terminology these genes were renamed *ilp1a* and *ilp2a*. Additionally for each gene an alternative splice variant was detected (Fig. 4.21). In the *emilp1* gene two ORFs of 366 bp and 510 bp, respectively, which differ in their 5' ends. EmIlp1a is composed of 122 amino acids, while the newly described EmIlp1b is 170 amino acids in length. Only EmIlp1b is expressed with an N-terminal signal peptide and is therefore expected to be the active, secreted form of EmIlp1. The previously described EmIlp2a and the newly identified EmIlp2b have the same N-terminus containing a signal peptide, but differ in their C-terminus. Both are likely to be secreted, active peptides. The *emilp2b* ORF is comprised of 465 bp, coding for a peptide of 155 aa.

4 Results

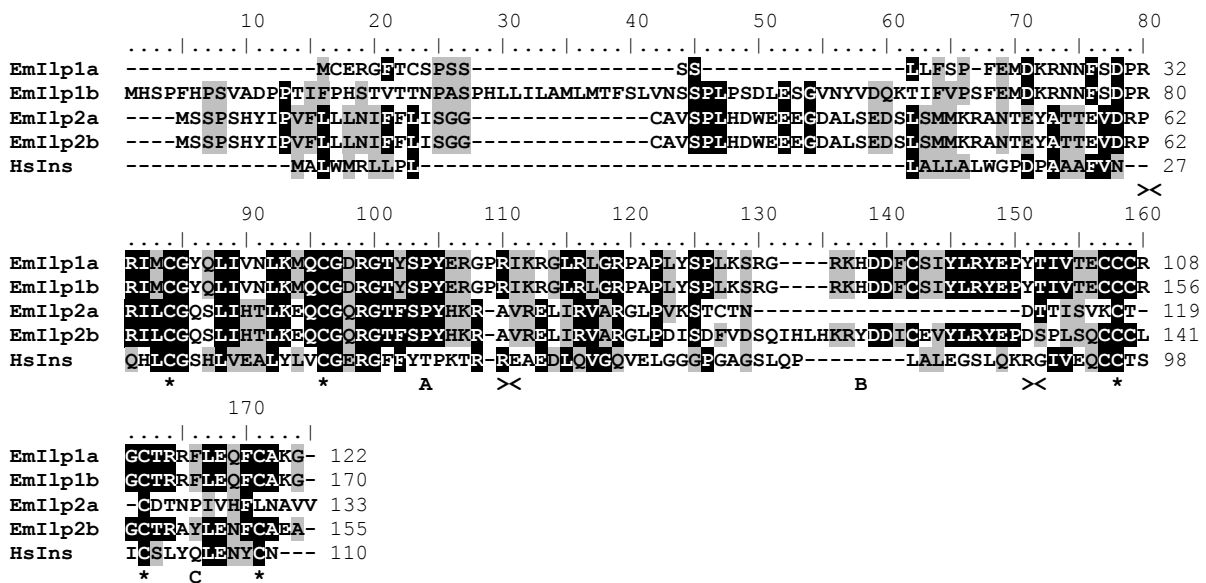


Fig. 4.21: Alignment of *EmIlp1* and *EmIlp2* orthologues with human insulin. Identical residues are highlighted in black, similar in grey. Beginning and end of A, B and C chains are marked by brackets and cysteine residues important for folding are indicated by asterisks.

A genome wide search was performed on *S. mansoni*, *Hymenolepis microstoma* (available under GeneDB.org), *E. granulosus* (<http://www.sanger.ac.uk/resources/downloads/helminths/echinococcus-granulosus.html>) and *Taenia solium* (labintern data) genomic data with EmILP1 and EmILP2 sequences to identify insulin like peptides in these helminth (Fig. 4.22 and Tab A.1). In *E. granulosus* homologues of both sequences were identified, which are fully identical to *E. multilocularis* sequences. Each two ILPs were found in *H. microstoma* and *T. solium* genome which are over 70 % identical to EmILP1 and EmILP2. No sequence homologies to ILPs were found in *S. mansoni*. However, an insulin homologue seems to be present in *S. japonicum*, although no distinct homologues could be found in *S. mansoni* genome.

4 Results

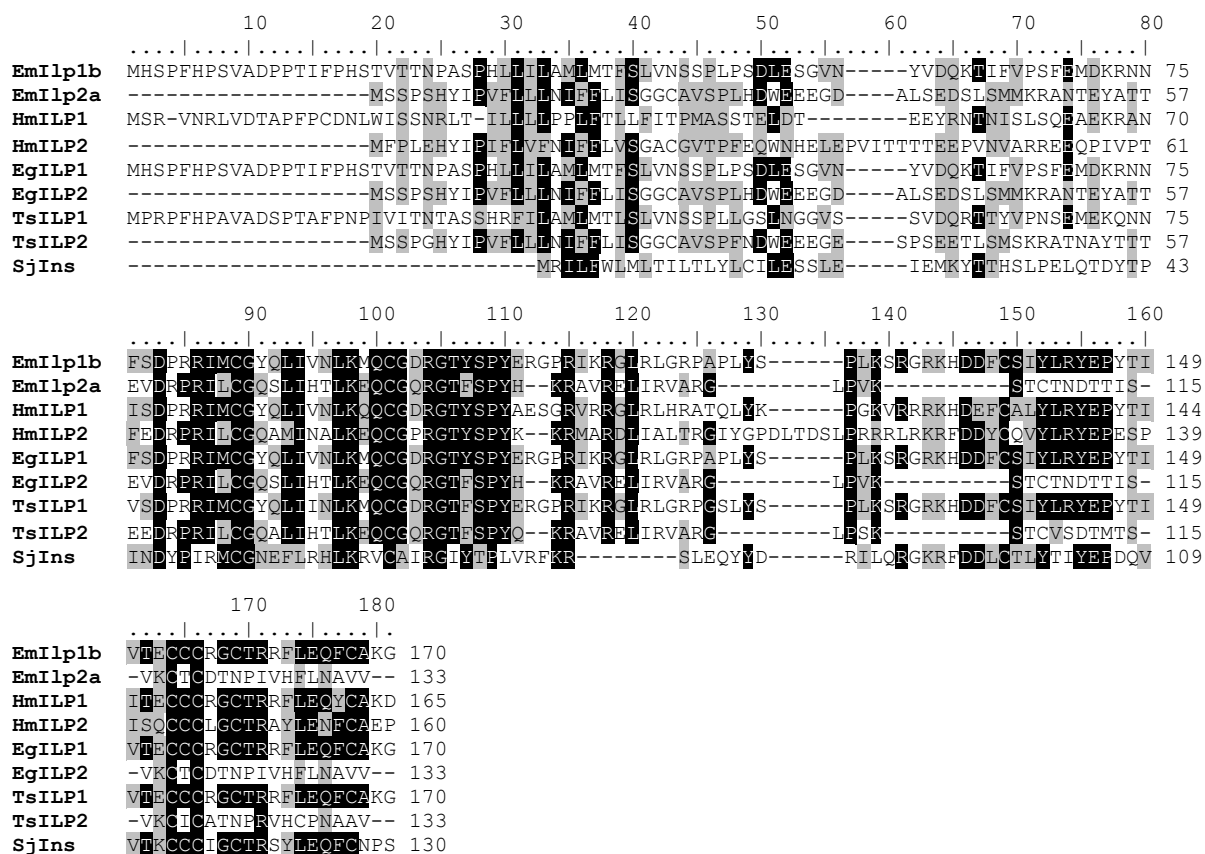


Fig. 4.22: Alignment of *EmIlp1* and *EmIlp2* with members of the *Ins/ILP* family of other helminths. Identical residues are highlighted in black, similar in grey.

To confirm *ilp* expression analysis [125] semi-quantitative RT PCR was repeated to include primary cell samples from the same origin as the metacestode vesicles and protoscoleces. In contrast to previous results expression was now observed in all stages, but still with the highest expression in protoscoleces (Fig. 4.23).

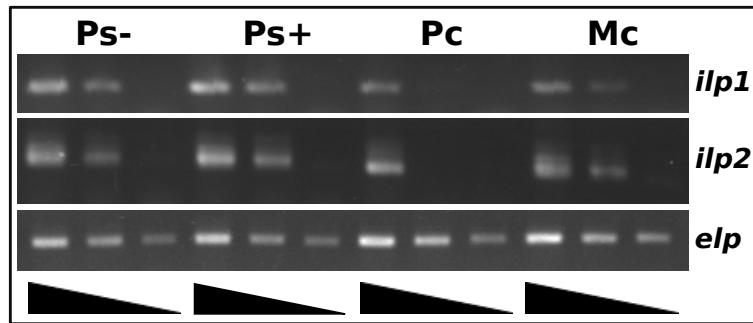


Fig. 4.23: Expression analysis of *emilp1* and *emilp2* by semiquantitative RT-PCR. *Emilp1* was amplified with the primers *ins1dw3* and *ins1 upnested*, and the primer combination *ins2dw2* with *ins2 upnested* was used to amplify *emilp2*. *Emelp* was used as *cDNA* control and amplified with the primers *Em10 15* and *Em10 16*. Triangles indicate serial 10 times serial dilution of the *cDNA*. Samples were separated on a 1 % agarose gels and subsequently stained with ethidium bromide. (*Ps-*) non-activated protoscolecocytes, (*Ps+*) activated protoscolecocytes, (*Pc*) primary cells, (*Mc*) metacystode vesicles

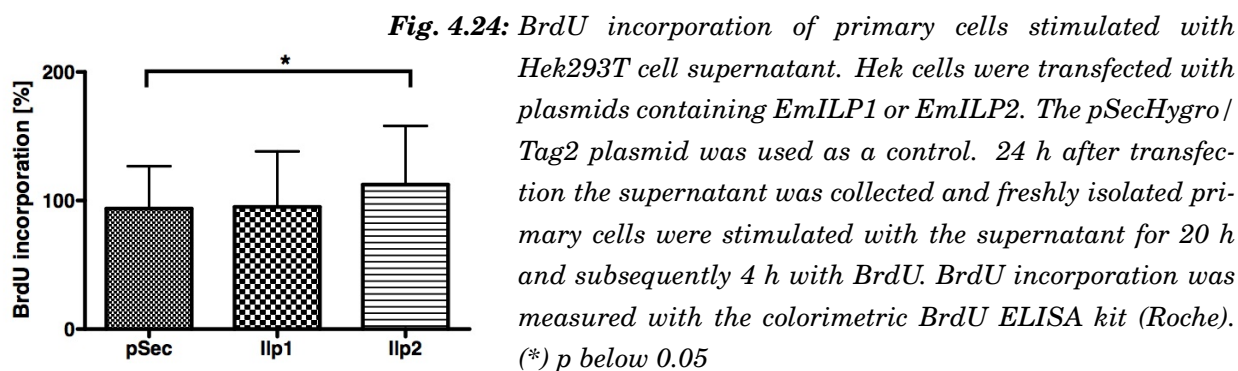
Y2H analysis was carried out to study binding of EmILP1 and EmILP2 to the human and *Echinococcus* insulin receptors. Constructs amplified from *ilp1b* and *ilp2a* were used for the experiments. The fragments were amplified with the primers *emilp1EcoRI* and *imilp1BamHI* for *Ilp1A* and *emilp2EcoRI* and *imilp2BamHI* for *Ilp2A* and cloned into the pBKT7 plasmid. Constructs for HIR and EmIR1 containing the ligand binding domain were cloned by Christian Konrad [53] and the EmIR2-LBD was already used in section 4.1.7. All constructs were tested for expression with western blot analysis. Co-transfection of the plasmids pGADT7 and pBKT7 with the corresponding constructs was used as negative controls.

In the Y2H experiments only EmIR2 interacted with the ILPs, whereas HIR and EmIR1 did not show any interaction with EmILP1 and EmILP2.

Tab. 4.3: Interaction studies of HIR, EmIR1 and EmIR2 with EmILP1 and EmILP2. The ligand binding domains (LBD) of HIR, EmIR1 and EmIR2 were expressed with the activation domain of Gal4 (pGADT7). Insulin, EmIlp1 and Emilp2 were expressed as pro-peptides with the Gal4 binding domain (pBKT7). Co-transfection with pGADT7 or pBKT7 was used as negative control. (-) no growth, (+) weak growth, (++) moderate growth, (+++) strong growth

	pBKT7	pro-Insulin	ILP1	ILP2
pGADT7	-	-	-	-
HIR-LBD	-	+++	-	-
EmIR1-LBD	-	+++	-	-
EmIR2-LBD	-	+++	++	++

The finding that EmILP1 and EmILP2 bind EmIR2 and not EmIR1 and HIR lead to the assumption that the peptides could have proliferative effects in primary stem cell cultures. Therefore, the EmILPs were expressed by transient transfection of mammalian cells, an approach that was previously used for expression of active IGF-I, IGF-II and insulin peptides [141–143]. To this end, *emilp1* and *emilp2* were amplified with the primer pairs *ilp1HindIII dw* and *ilp1NotI Stop* for *emilp1* and *ilp2HindIII dw* with *ilp2NotI Stop* for *emilp2*. The fragments were cloned into the pSecHygro/Tag2 plasmid for heterologous expression in eukaryotic cell lines. As the 3' end primers contained a stop codon, the peptides were expressed without the C-terminal Tag of the plasmids. Therefore, no analysis on expression of these two peptides were available. Hek293T cells were transfected with the constructs with the PEI method. The experiments showed that primary cells stimulated with EmIlp2 containing supernatant incorporated more BrdU than samples stimulated with pSec or EmILP1 (Fig. 4.24). However it is not clear, if EmILP1 has no effect or is not expressed in a similar manner as EmILP2.



4.2 The effect of the anti-cancer drug Imatinib and Imatinib responsive kinases in *E. multilocularis*

4.2.1 Characterisation of Abl kinases in *E. multilocularis*

BlastX search on genome data of *E. multilocularis* revealed the presence of three kinases with high homologies to *Schistosoma* Abl1, Abl2 and TK6. Based on the genome data complete cDNA sequences were amplified and sequenced using the yeast two hybrid library [40] as template.

Characterisation of EmAbl1

The cDNA of *emabl1* was 3558 bp in length coding for a protein with 1186 aa and a deduced weight of 127.9 kDa. Domain analysis indicated the presence of a SH3 (63- 136), SH (169-252) and tyrosine kinase (TK, 306-559) domains with the classical arrangement for Abl kinases. A low conserved F-actin binding domain (FABD, 1012- 1151) could be present, although the C-terminus is not strongly conserved and no other Abl typical domains were identified. Two small inserts were found in the SH3 domain (106- 121; 137-164) and one (268- 286) between the SH3 and SH2 domain. In the kinase domain important motifs for kinase activity were found including the activation loop Tyr412, which corresponds to Tyr459 in EmAbl1 [106]. Several other tyrosine residues are reported to be phosphorylated in Abl kinases including residues at the positions 70, 214, 225, 253 and 257 (HsAbl1) [106]. The residues correspond to Tyr69, Tyr259, Tyr316, Tyr320, Ser625 and Thr792. The phosphorylation sites 225 and 618 are not preserved. The human Abl1b form was shown to be myristoylated [144]. In EmAbl1 the sequence MGGSIG was found, which corresponds closely to the myristoylation motif MGNCFT (MGXXX(S/T)), missing only the Ser/Thr residue, which is not obligate for myristoylation [145]. Proline rich sequences with the motif PXXP [106] were found at the positions 112, 645, 818, 946, 956-967, 1167. Furthermore two arginine rich stretches R798RR and R898RMR were found that could serve as NLS [106]. Alignment with human Abl1 and SmAbl1 revealed 33/ 44 % (identities/ similarities) homology between EmAbl1 and SmAbl1 and 33/ 46 % with HsAbl1. The highest conservation was calculated for the TK domain with 82/ 91 % for SmAbl1 and 63 / 78% for HsAbl1. The sequence of EmAbl1 with the identified characteristics is depicted in Fig. 4.25.

4 Results

```

1  MGGSIGKPASSKEGSEKVDLSLSFNQQPDEISTGGECEKSAPVKKQILSVTQNFETSGLVEQCIMIVLYDFSATLDSOLT
   m
81  VKRGEIVRLLSYSYPAGDWSEVEAPSHLPNRTPRVPWAGAGGWVRGWVPTSYLTHEVRRVGGIGSGTNGWRRVGDDEEA SH3
161 GAAAAATMAYPWYHGAVSRQAAEQLLRSGITGSYLVRESESAFGQLSVTVRNLGRVYHYRISRDCGWYFITETHRFPTVV SH2
241 QLIHHSQAADGLICPLLYPAARREQPSVMRGAATNSGAVEGCADSKGGGGYVGFDDWEIDRSEIMMRNKLGWGQYGDVY
   *
321 EALWKRYNSIVAVKTLKQVDLNLNDFLAEASIMKNLOHKNLVRFLGVCTREPPYYIVA EYMPHGNNLLNYLRQRSPGELT
   *
401 PPILLYMAVQIASGMAYLEANNFIHRDLAARNCLVGDQYTIKVADEFLARYMQLHEDTYTARNGAKFPIKWTAPEGLAYF TK
   *
481 RFSSKSDVWAFGVVLWELATYGLSPYPGVELHGVIQLLEKGYRMQRPHGCPESVYSIMLRCSWEAADRPTFLSIKAELE
561 EMWRTIDMTEAVAQELATPPAAQTTDHMQFITATSTATTITAVGVGPGINGGGEAMLSSVPVSMIVRMPYSQQDDDE
   *
641 AAEDPSSFSQSTTSCTSSSSAAVSSSSAAETDQGDGDEGEEDLCLKSLVDKALSSSTANWITTRTSDSLYQGDYIVSGG
721 GGGGGGVVRATPASDLPFATHKSTTCDSQVSAPASLPPLHHLQQFQHRNRANNHSHHYHRHYQHQLQHSETGRSMPPRRR
   *
801 SGPNHLAGQFEEGSLRCPMRPKEKNITPAESGVGESIVSADSPGGNSNAMQQE EGVVMAPQRSNHKAAAVVAVAVEANN
881 CCVTPTRDMI SEVAPDERRMRLDVESVTQFTTLP AQDRITRYLES LGELGDASEERTPKAKGGAHPPHPELLSHFPPPPP
961 VPPPPQPAQH LRNSRMLPTEHRRNAVGRSASCYQTVSSVQLLLPSTTTTNGSVETQESLPTTSTPSPAVGETITPTDDV
1041 YQAPTLAQDSSIGNGGVKAAPTAEVSSEVEQAE L TACLNTLSLEATELSTACPQLAAELSALSQLSACRGKVEARLRA
1121 SANGVGGTAEENLCLAGVAQALRH IQQALAE MRARVEEAQTPTPSLEAPSATAPAAATNANATTVST

```

Fig. 4.25: Deduced amino acid sequence of *EmAbl1*. Domains are underlined with the inserts depicted as dotted lines. Activation loop motifs are highlighted by bold letters. Asterisks mark phosphorylation sites and boxes indicate proline rich motifs. Putative NLS are highlighted grey and the myristoylation motif is marked by an (m).

Characterisation of *EmAbl2*

The ORF of *emabl2* consisted of 3297 bp with a deduced amino acid sequence of 1099 aa and 119,9 kDa. Fig. 4.26 displays the amino acid sequence with the structural characteristics of *EmAbl2*. A putative myristoylation site was found at the N-terminus. A Smart domain search revealed the presence of a SH3 domain (50- 111), a SH2 domain (140- 223) and the tyrosine kinase domain (257- 509). A low conserved FABD was indicated in the C-terminal part (932- 1069). A small inserts was present in the SH3 domain (112- 135) that corresponds to the second insert in *EmAbl1*. The phosphorylation sites 214, 253, 257, 412 and 569 of *HsAbl1* were found at the positions, 230, 268, 272, 409 and 566. Furthermore eight prolin rich stretches (534- 543, 634, 664, 706, 748, 821, 861, 1072) and 2 putative NLS motifs (695, 873) were identified. At the N-terminus the sequence MGSQHA closely resembled the myristoylation motif MGXXXS/T. The highest homology of *EmAbl1* was calculated for *SmAbl2* with 37/ 51 % (identities/ similarities) for the full length sequence and 76/ 85 % for the TK domain.

4 Results

```

1  MGSQHAKPKKAASESVDRNFTFRINKGKSKCGDDGTSVSSSLDVMSVPDGDLTALYDYDPPVNAHGSAIVVRKGDLSLWLY      SH3
   m
81  GRSSTGDWLDVLCRRGTGERGWVPVSCLEFDFTSSKPLIASGAATASSAPSAHVSCPSLIGERWYHGAIHRSYAEYLLNSGI      SH2
161 TGSFLVRESESSFGKLTLSLRSDGRIFHYRISTDENNQFYVNEVSRFATVSELVQHHEKVADGLACPLLYGVSKRDQNNH
241 GGFDSYDAWEIDRTDVIMKHKLGSGQYGVVYEAIFKPYDVTVAVKTLKEDITLRDEFLOEARLMKSLRHPNLVRLLGVC
   *
321 TOEPPYYIITEFMCNGNLLDYLRIQPRDVLSPVLLQMAIHVCCAMTYLEEHNFIHRDLAARNCLVGEAMTVKVADDFGLA      TK
401 RYMERDVTYRAREGAKFPIKWTAPEGLVYNCFSIKSDVWAFGVLLEWELIATYGAAPYPGVELQDVYVLLQRGTRMEAPQGC
   *
481 PDAVYQLMLDCWSWNSDRPSFKEVYTRLETIRTSSDISEAVEHELQRHRIRMPPPPLPPSPTTVAaftPRRSSCDRI
561 DESNLSPTAEMGRRGHAESFTVQDAVSRVLVDSGGSGSDLHQQQQFSAYPCCQQCMVPGNRFSEVFPSSLLPPPLHT
   *
641 NADFAVVGAEIGGAGSLGRRKAAPPAPLRTTTLRADEPCEKVPVSLQVSTDDRQTFSQPGEERLPSPENAVLCGVNWPS
721 SRSQSSPPLNSDVAVSVTASVPRRTPIEVPPQRTSTRSQDSEVAEGVPKSSPKMGLPSTTQSPSNGLATASSGSTNSEL
801 SSRLKRQLDNRSTDSPTRSEVPPGAAVTVAEMIQASKSKLKATTTTTPATITAIETQPAPSVFAWRELVVQRRLKNAEP
881 PAGKRMSWTPMSNSCSSSALKQQQSSNVEVFPEVVEVEEEEGGEEREGALPAIMSQSVTYTSSSTVMPPSSLVSRSSYE
961 HLLRQVTDLCADLNLAQVNLVNEHNSTLVDRIEGLKQACLGADMDCSAHAKFRFRDECARLQAAADTLRSICGVGAKA
1041 AVGAEELGGRKTYQAVYTTVEAIHQSLRLTPAVESSDAVEESTAPSTRSAFVSTGVIS

```

Fig. 4.26: Deduced amino acid sequence of *EmAbl2*. Domains are underlined with the inserts depicted as dotted lines. Activation loop motifs are highlighted by bold letters. Asterics mark phosphorylation sites and boxes indicate proline rich motifs. Putative NLS are highlighted grey and the myristoylation motif is marked by (m).

Characterisation EmTK6, a Src-Abl hybrid kinase of *E. multilocularis*

Besides the previously identified Abl kinase *EmAbl1* and *EmAbl2*, a Src-Abl hybrid kinase was identified in *E. multilocularis* (Fig. 4.27). BlastX analysis was carried out on available genome data using the sequence of SmTK6 [120]. The *emtk6* cDNA comprised 1710 bp coding for a protein with 570 aa and a deduced weight of 64 kDa. A SH3 (115-172), SH2 (179-267) and tyrosine kinase domain (296-551) were identified, which is the classical structure for a src and abl kinases. At the N-terminus a myristoylation motif MGNCFT (MGXXX(S/T)) was identified. In the kinase domain the important motifs for kinase activity were found. However, at position 446, which corresponds to the Tyr412 in the HsAbl1 an exchange to valine occurred. In EmTK6 tyrosines at position 121 and 311, corresponding to 70 and 257 were conserved, the later being specific for Abl kinases. Two tyrosine residues Tyr527 and Tyr416 in src kinase are reported to have regulatory function [146]. Tyr527 is found in EmTK6 at position 562 whereas tyrosine 416 is not conserved. Proline rich motifs were found at the positions 196, 515 and 518. The highest homology of EmTK6

4 Results

was found for SmTK6 and was 53/ 68 % (identities/ similarities) for the full length sequence and 67/ 81 % for the TK domain.

```
1  MGNCFTCHDHKENLQCHGDNGMTPMGANSQGGGQGLGQAPFGRHYGPSGDAASVGANQSAIVPASRGAHQPSQQYSVNL  
   m  
81  GMQNGPQQSASYAYSLSAQPPATLDQQLAEQSPRVVRVAHALYTYVAQNADDLSFQKGDVMLVESGLSEAWWLARHLRTGQO  
   * SH3  
161 GYIPSNYVTVENGLSTQMEAWYDITRKDAERMLLMPGLPOGTYILRPCSDRSYALSIRFEIERNMYAIKHYKIRTRDNG  
   SH2  
241 AGFYITNRTNFASVADLISHYQSTSDGLCCRLSQPCPRKYTPPVQFRDIEANRRSLEFICELGNGSFGMVYRARWNKTFD  
   *  
321 VAVKKRLATTDRALFIEEAKVMHKLHHRRIVRLLGVCTEPADEPVFIITELLEKGALNRNLSSEEGROLFLSDLIDMIAQ  
401 IAEGMAYLEEMNFVHRDLRAANILVDRDNSVKVADFGLAKMLDSDVQNDGVIKFPIKWTAPEAAALPDHHFSIKSDVWSFG  
   TK  
481 VLMYEIVTYGGTPYPRFTNRETVQQVERGYRMPNPNTPTQPCPDDLIDIMQCWSARPEDRPTFHNLYDIFENWAVQTEG  
561 QYISDGAQNT  
   *
```

Fig. 4.27: Deduced amino acid sequence of *EmAbl2*. Domains are underlined with the inserts depicted as dotted lines. Activation loop motifs are highlighted by bold letters. Asterisks mark phosphorylation sites and boxes indicate proline rich motifs.

4.2.2 Expression analysis of *emabl1*, *emabl2* and *emtk6*

A semi-quantitative RT-PCR approach was used to investigate expression of *emabl1*, *emabl2* and *emtk6* [147]. All three transcripts are present in non-activated and activated protozoa, primary cell cultures and metacystode vesicles at nearly equal amounts (Fig. 4.28), indicating an important role of the protein throughout parasite development.

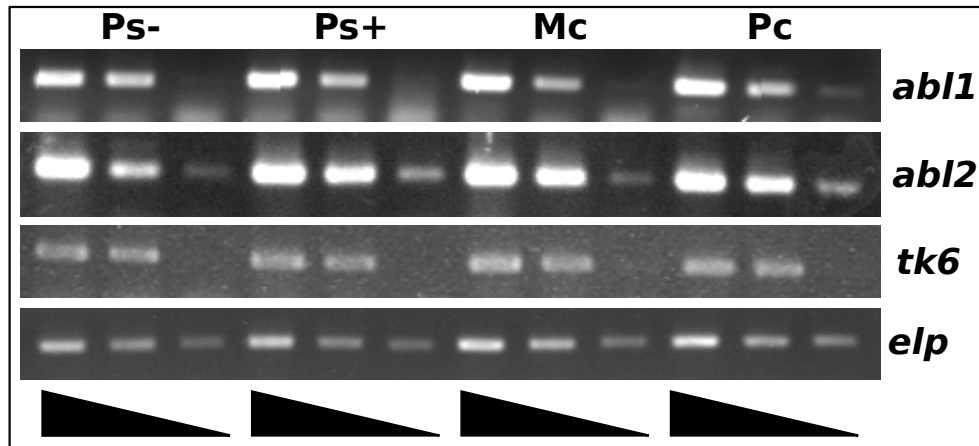


Fig. 4.28: Expression analysis of *emabl1*, *emabl2* and *emtk6* by semiquantitative RT-PCR. *Emabl1* was amplified with the primers *abl1dw1* and *abl1up1*, *emabl2* with *abl2dw* and *abl2up-II* and the primer combination *tk6 dw* and *tk6up* was used to amplify *emtk6*. *Emelp* was used as cDNA control and amplified with the primers *Em10 15* and *Em10 16*. Triangles indicate serial 10 times serial dilution of the cDNA. The PCR products were separated on a 1 % agarose gel and stained with ethidium bromide. (Ps-) non-activated protoscolexes, (Ps+) activated protoscolexes, (Pc) primary cells, (Mc) metacystode vesicles.

4.2.3 The effect of Imatinib on *E. multilocularis* larval stages

Imatinib (Gleevec) is used in cancer therapy against chronic myelogenous leukemia (CML), which is caused by constitutively active BCR-Abl fusion protein [112]. The compound targets the ATP binding pocket, where 21 amino acids were identified that mediate binding [148]. Alignment of the kinase domains of *Echinococcus* Abl1, Abl2 and TK6 sequences with those of *Schistosoma* and the human Abl kinase revealed conservation of binding-mediating residues (Fig. 4.29). Of the 21 amino acids important for Imatinib binding 18 are conserved in EmAbl1, 20 in EmAbl2 and 18 in EmTK6 (SmAbl1: 18/21; SmAbl2: 19/21; SmTK6: 15/21). The high conservation in the Imatinib binding site suggested a likely binding of Imatinib to *Echinococcus* homologues.

4 Results

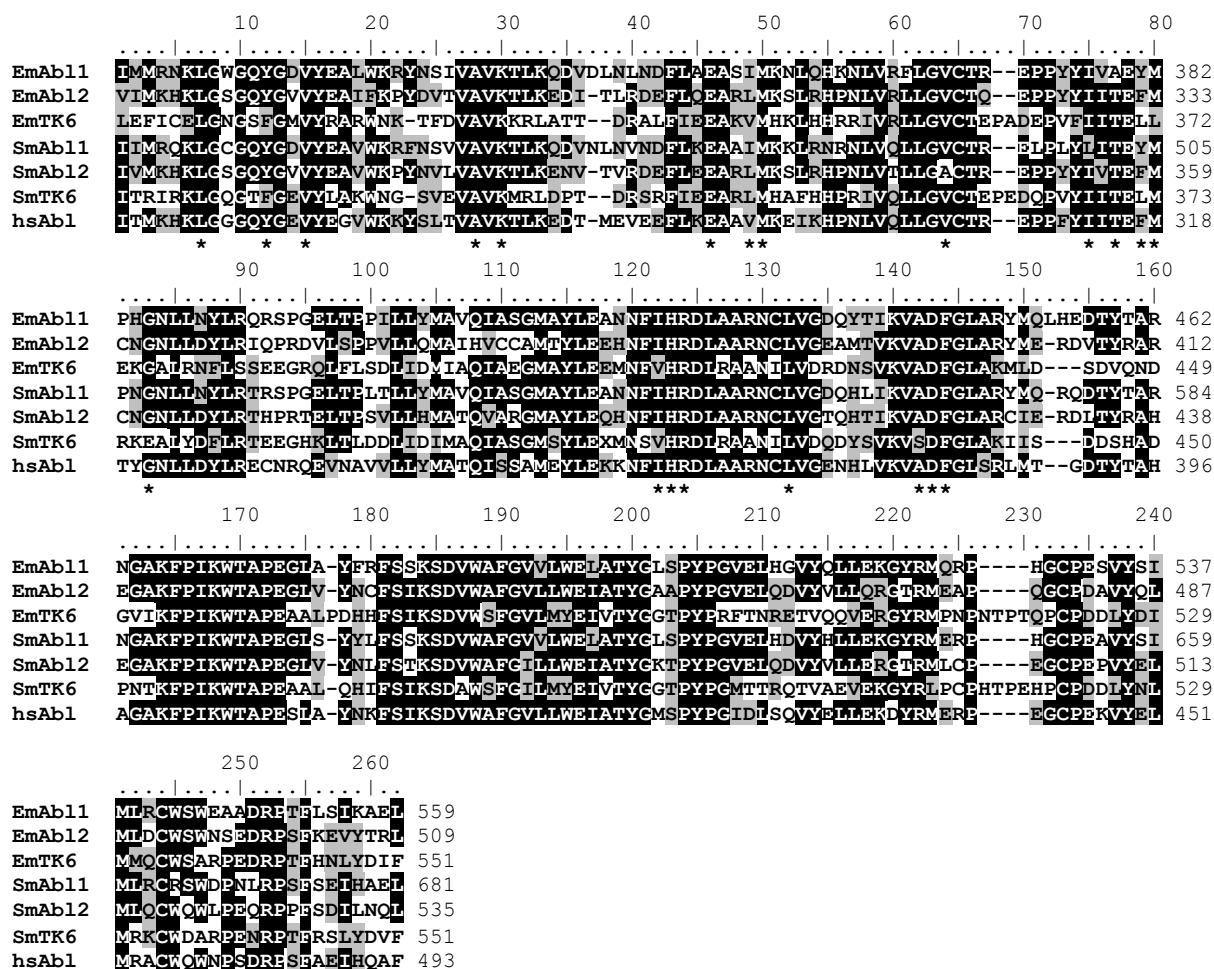


Fig. 4.29: Alignment of Abl and TK6 kinase domains [147]. Em: *E. multilocularis*; Sm: *S. mansoni*, Hs: *H. sapiens*. Identical residues are highlighted in black, similar in grey. Asterisks indicate residues important for Imatinib binding.

The high conservation of the Imatinib binding site and the presence of transcripts in all larval stages suggested that Imatinib could block parasite development *in vitro*. Therefore, Imatinib was tested on Metacystode vesicles, primary cell cultures and protoscoleces [147].

Metacystode vesicles were treated with 10, 25 and 50 μM Imatinib for up to 7 days (Fig. 4.30). At day 5 a significant decrease in survival was observed in samples treated with 25 and 50 μM Imatinib. At that time point no difference was observed in samples treated with 10 μM inhibitor. At day 7 nearly all vesicles in the 25 and 50 μM groups were dead and survival of vesicles in 10 μM treated samples was reduced to 50%. In cultures treated with 100 μM all vesicles were dead at day 2 (data not shown).

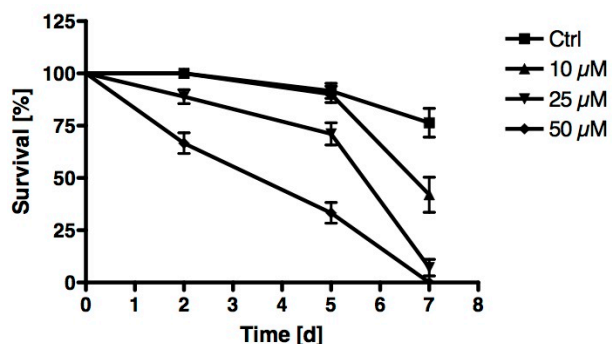


Fig. 4.30: Survival of metacestode vesicles treated with Imatinib [147]. Metacestode vesicles were cultivated for 7 days in 0.2 % FCS/DMEM supplemented with reducing agents and the indicated concentration of Imatinib. p below 0.0001 (χ^2)

Because 10 μM lead only to a slight decrease of survival to about 50 % in 0.2 % FCS/DMEM, viability and regenerative ability of primary cells from these cultures was investigated. Metacestode vesicles were pre-treated for 9 days in 2 % FCS/DMEM to ensure a better viability of the primary cells. Subsequently, primary cell were isolated and cultivated under axenic conditions. Although nearly all vesicles treated with 10 μM Imatinib were intact in this experiments, no regeneration occurred in the corresponding primary cell culture at day 7 (Fig. 4.31). As was expected no regeneration was observed in the 25 μM pre-treated samples.

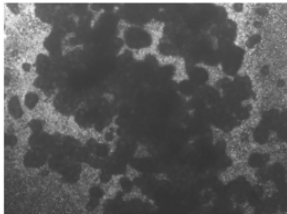
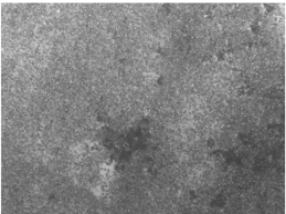
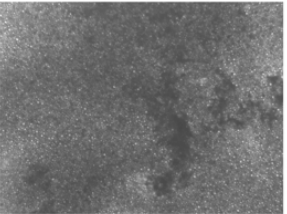
Pre-treatment	Ctrl	10 μM	25 μM
Intact Mc	100 %	96,9 %	11,4 %
Pc			

Fig. 4.31: Regeneration of primary cell cultures from Imatinib pre-treated metacestode vesicles. Vesicles were cultivated for 9 day with or without Imatinib in 2 % FCS/DMEM. Primary cells were isolated from these vesicles and cultivated in conditioned medium. After 7 days, regeneration was documented.

Protoscoleces were treated with Imatinib for 7 days in 2 % FCS/DMEM. Subsequently, protoscoleces were stained with methylen blue and dead parasites were counted. 50 μM Imatinib had a drastic effect, killing all protoscoleces in the samples (Fig. 4.32). Treatment with 25 μM Imatinib showed a 50 % reduced survival, while 10 μM had no significant effect. The low effect for 10 μM is comparable to metacestode vesicles in 2 % FCS/DMEM (Fig. 4.31) and is therefore probably caused by the FCS in the culture.

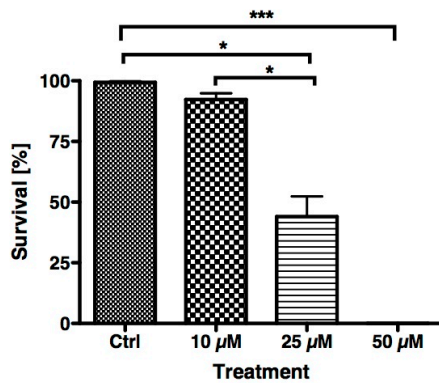


Fig. 4.32: Survival of protoscoleces treated with Imatinib [147]. Protoscoleces were isolated from infected jird material and cultivated for 7 days in 2 % FCS/DMEM supplemented with reducing agents and the indicated concentration of Imatinib. After the indicated time protoscoleces were stained with 0.03 % methylen blue and dead protoscoleces were counted. (*) p values below 0.05 (**) p between 0.001 and 0.01, (***) for p below 0.001

In a next set of experiments Imatinib was tested on primary cells to investigate the effect of Imatinib on stem cell rich cultures. Imatinib significantly decreased viability of primary cell cultures treated with 25 μM and 50 μM to 50 and 25 %, respectively (Fig. 4.33A). 10 μM only had a slight effect on viability. However, when primary cell cultures were treated with Imatinib for a period of 3 weeks, vesicle formation was drastically decreased (Fig. 4.33B) [147]. Samples treated with 10 μM or 25 μM Imatinib still showed aggregation, although it was severely impaired in the 25 μM samples (Fig. 4.33C). No regeneration and therefore also no vesicle formation was observed in cultures incubated with 50 μM Imatinib.

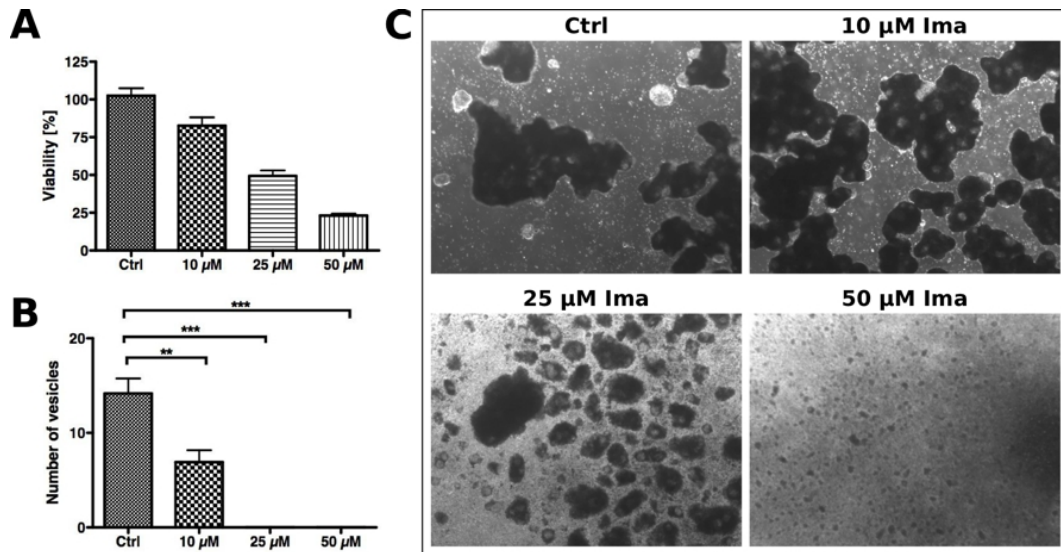


Fig. 4.33: Treatment of primary cells with Imatinib. (A) Freshly isolated primary cells were incubated with or without Imatinib for 2 days in 10 % FCS/DMEM without phenol red. Viability was measured using the Resazurin assay. p below 0.0001 for all samples compared to the control. (B) Primary cells were cultivated in conditioned medium supplemented with Imatinib in the indicated concentrations. After 3 weeks the formed vesicles were counted. (*) p values below 0.05 (**) p between 0.001 and 0.01, (***) for p below 0.001. (C) Aggregation of primary cells treated with Imatinib for 3 weeks in conditioned medium.

Next, morphological changes after short term treatment with Imatinib were investigated. Samples from metacystode vesicles [147], primary cells and protoscoleces were treated for 24 h with Imatinib and subsequently embedded for haematoxylin/eosin staining (HE). In metacystode vesicles, non-treated vesicles showed a strong staining in the tegument (Teg) and an intact and healthy germinal layer (GL) (Fig. 4.34Mc). Treatment with 10 µM Imatinib already induced morphological changes in the tegument, reflected by a loss of staining. In 25 and 50 µM treated samples the germinal layer was detached from the laminated layer (LL), organisation of the germinal layer is lost and the cells appear to die. Treatment of 50 µM Imatinib lead to complete killing of parasitic cells. Non-treated primary cells looked healthy, the cavities (CA) and the cells surrounding them were well structured (Fig. 4.34Pc). Treatment with 10 µM Imatinib already lead to a loss of structure surrounding the cavities. In 25 and 50 µM treated samples the cavities were disrupted and the cells appeared to be dead. In untreated protoscoleces the apical basal structure was clearly visible. Muscle fibers (Mf) were running longitudinal through the protoscolex body (Fig. 4.34Ps). These fibers already vanished in samples treated with 10 µM Imatinib. 50 and 100 µM Imatinib lead to dying of the cells and complete loss of structural integrity. It is interesting to note that in samples treated with 10 µM or DMSO still invaginated

protoscoleces were found, with a higher number in the control, while in 50 and 100 μM all protoscoleces were evaginated (data not shown).

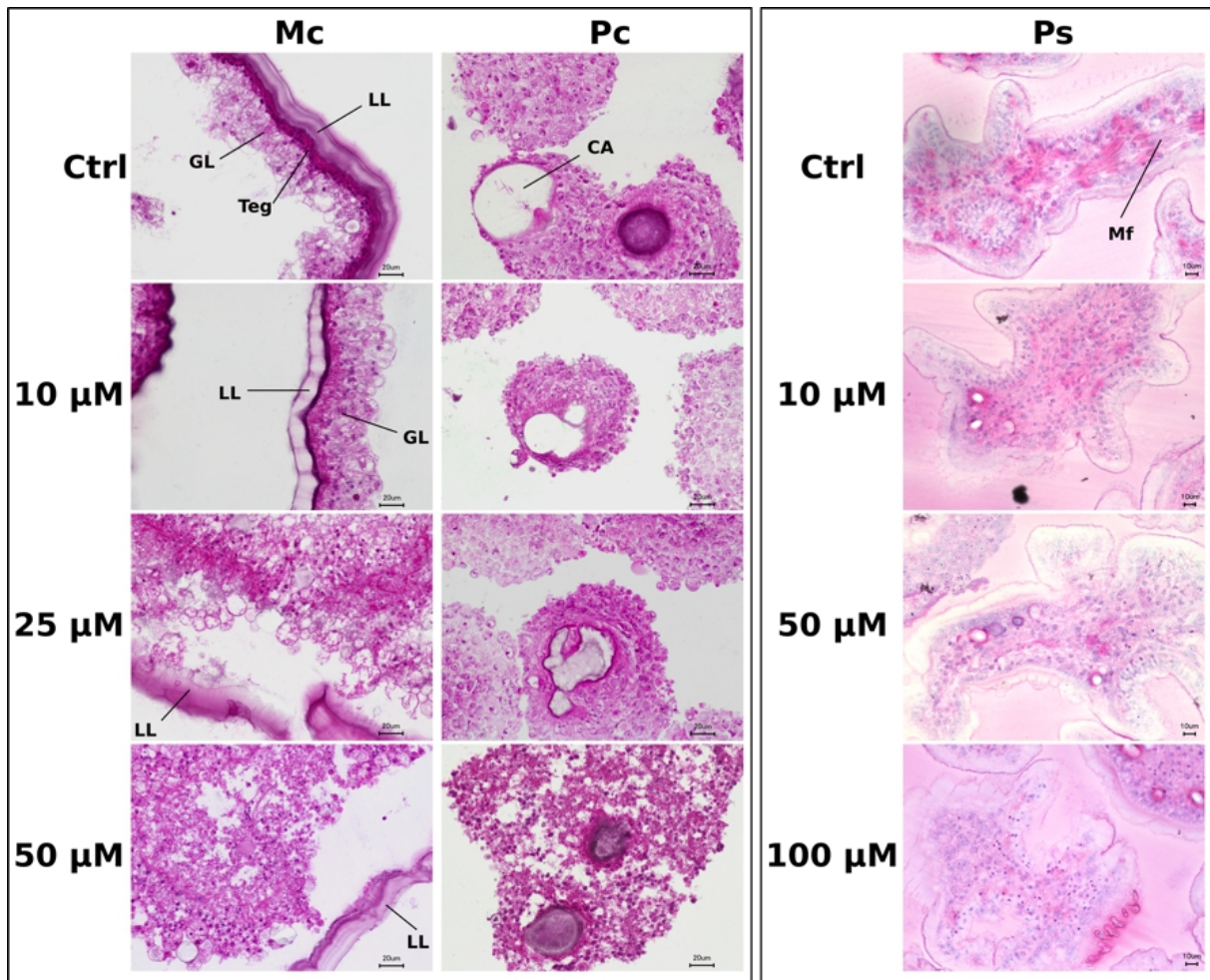


Fig. 4.34: (Mc) Axenic metacystode vesicles were cultivated for 24 h in 2 % FCS/DMEM supplemented with the indicated concentrations of Imatinib, after which they were embedded in Technovit 8100 and 4 μm sections were stained with haematoxylin/ eosin. (Pc) Primary cell cultures were grown for 5 days in conditioned medium and subsequently transferred to 2 % FCS/DMEM supplemented with Imatinib for 24 h. Aggregates were embedded in Technovit 8100 and 4 μm sections were stained with HE. (Ps) Protoscoleces, isolated from infected jirds were cultivated in conditioned medium for 3 days. The medium was changed to 2 % FCS/DMEM and Imatinib was added for 24 h. The samples were embedded in Technovit 8110, 4 μm were prepared and stained with HE. Mc: metacystode vesicles; GL: germinal layer; LL: laminated layer; Teg: tegument; Pc: primary cells; CA: cavity; Ps; protoscolex; Mf: muscle fibers; the larval stage is indicated above the pictures and on the left site of the pictures the concentration of Imatinib is indicated.

4.3 K11777 a new inhibitor in anti-AE chemotherapy?

Cysteine proteases of the papain superfamily are involved in numerous cellular processes and play an important role in the pathogenesis of parasitic infections [149]. K11777 (N-methyl-piperazine-Phe-homoPhe-vinylsulfone-phenyl), a new inhibitor of the vinyl sulfone group emerged as an effective inhibitor of papain proteases and already showed high efficacy in reducing egg burden and organ pathology in mice infected with *Schistosoma mansoni* [129]. To identify possible targets for K11777 a genome wide Pfam search with the papain family cysteine protease domain (PF00112) was carried out on the *E. multilocularis* genome. Ten genes coding for *Echinococcus* cathepsin-like proteases were identified (Tab. 4.4), among them were two cathepsin B-like and 7 cathepsin L-like proteins. EmW_000654500 and EmW_000654600 sequences were identical and characterised by Sako et al. [150] as EmCLP1. Interestingly, the two genes were found directly next to each other in the genome. The five genes on scaffold_7728 were highly homologous, sharing over 92 % identical amino acids and most probably are the result of gene multiplications. K11777 forms irreversible, covalent complexes with the cysteine of the catalytic triad characteristic for the papain superfamily enzymes [151]. Further bindings involve Gln19, Gly66, Asp161, His162, Trp184 (TcCruzain, Papain family cysteine protease domain). Alignment of the papain family cysteine protease domains of the *Echinococcus* cathepsins with Sm-CathepsinB1 and TcCruzain revealed conservation of the papain specific catalytic triad and the presence of the Gln19, Gly66, Trp184 corresponding residues (Fig. 4.35). Asp161 is only conserved in EmW_000654100, EmW_000654500 and EmW_000654600 and is exchanged to a Gly in the cathepsin B-like proteins and to Asn in the other cathepsin L-like homologues.

Tab. 4.4: Identification of cysteine proteases in *E. multilocularis*. Pfam search on sequence data available under <http://www.genedb.org>. EmCLP1 (Acc. No: BAF02516) and EmCLP2 (Acc. No: BAF02517) were characterised by Sako et al. [150], EmCBP1 (Acc. No: BAJ83490) and EmCBP2 (Acc. No: BAJ83491) were identified by Sako et al. [152].

Systematic Name	Location	Product	Name
EmW_000654100	scaffold_007728 : 8608026-8610326	cathepsin L-like	
EmW_000654500	scaffold_007728 : 8635659-8637959	cathepsin L-like	EmCLP1
EmW_000654600	scaffold_007728 : 8641231-8643531	cathepsin L-like	EmCLP1
EmW_000654200	scaffold_007728 : 8617974-8620387	cathepsin L-like	
EmW_000654800	scaffold_007728 : 8656821-8659233	cathepsin L-like	
EmW_000790300	scaffold_007768 : 5441376-5443678	cathepsin B-like	EmCBP2
EmW_000790200	scaffold_007768 : 5437741-5440037	cathepsin B-like	EmCBP1
EmW_000967900	scaffold_007780 : 3105356-3111019	cathepsin L-like	
EmW_000989200	scaffold_007780 : 5012240-5015594	cathepsin L-like	EmCLP2
EmW_000477200	scaffold_007614 : 4912844-4914073	cathepsin L-like	

4 Results

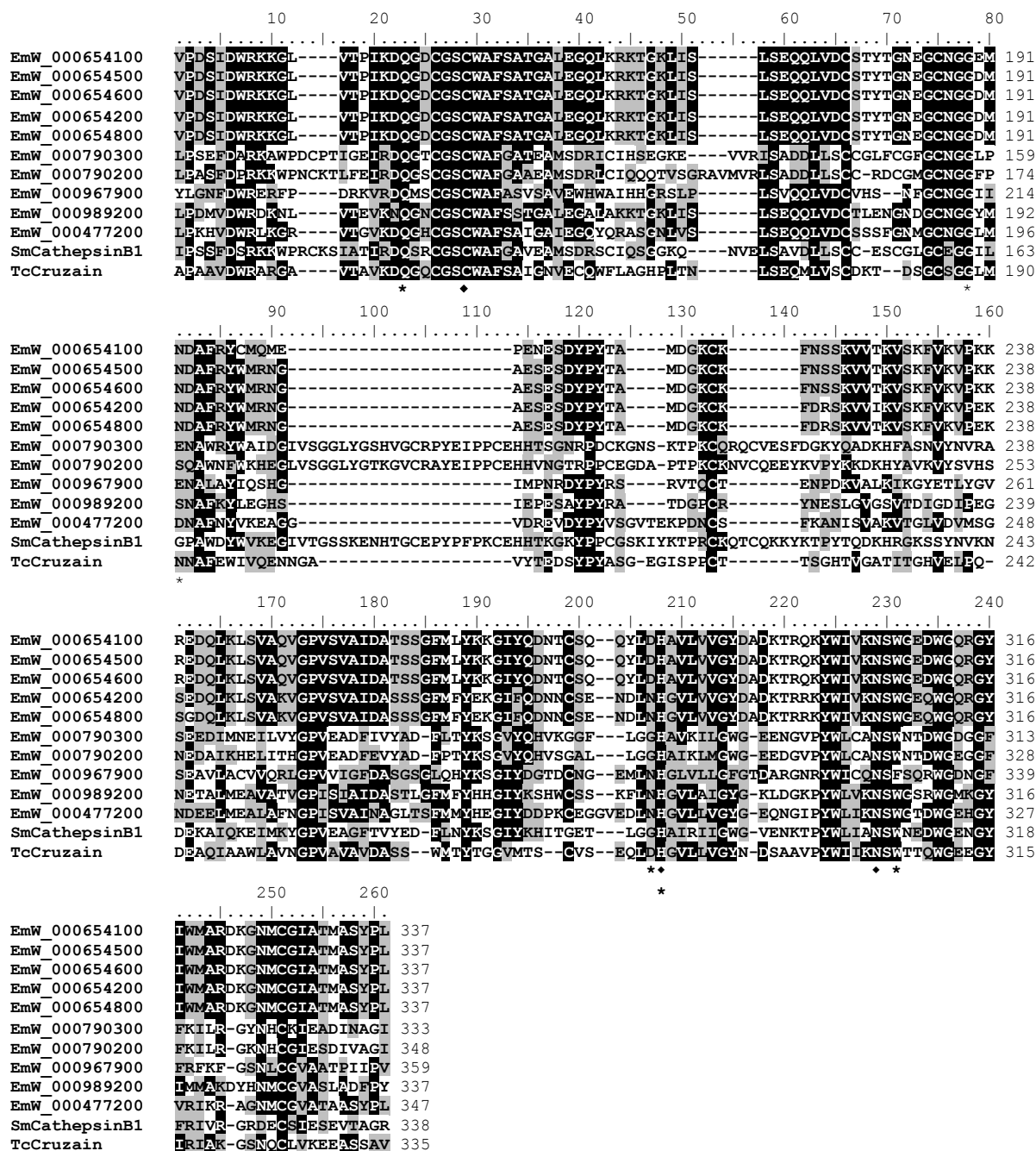


Fig. 4.35: Alignment of the papain family cysteine protease domains of *Echinococcus* cysteine proteases with *SmCathepsinB1* (Genebank accession number: AJ506157), *TcCruzain* (Acc. No: M84342). Identical residues are highlighted in black, similar in grey. Squares indicate residues of the catalytic triad, asterisks mark residues that are involved in polar interactions with K11777.

In a first experiment the inhibitor K11777 was tested on metacestode vesicles (Fig. 4.36A). After 7 days treatment with 25 μ M and 50 μ M K11777 had severe effects on survival of

4 Results

metacestode vesicles. Nearly all vesicles were dead after that time. At day 4 a difference in the concentration dependent effect was visible with a 25 % higher effect of 50 μM than with 25 μM K11777. 10 μM had no effect on survival of metacestode vesicles. Therefore, a pre-treatment experiment was carried out, which clearly showed that regeneration of primary cells pre-treated with 10 μM K11777 was severely impaired in comparison to the control (Fig. 4.36B). Regeneration in the control was very low due to a low amount of starting material. Further experiments on the influence of K11777 on viability of primary cells showed that the inhibitor has a devastating effect on this culture system (Fig. 4.36C). Concentrations as low as 10 μM reduced viability to 50 % of the control. Viability in samples treated with 25 μM and 50 μM was decreased to 25 and 10 %, respectively. Taken together these results show, that the inhibitor K11777 has a severe effect on both, metacestode vesicles and primary cell cultures.

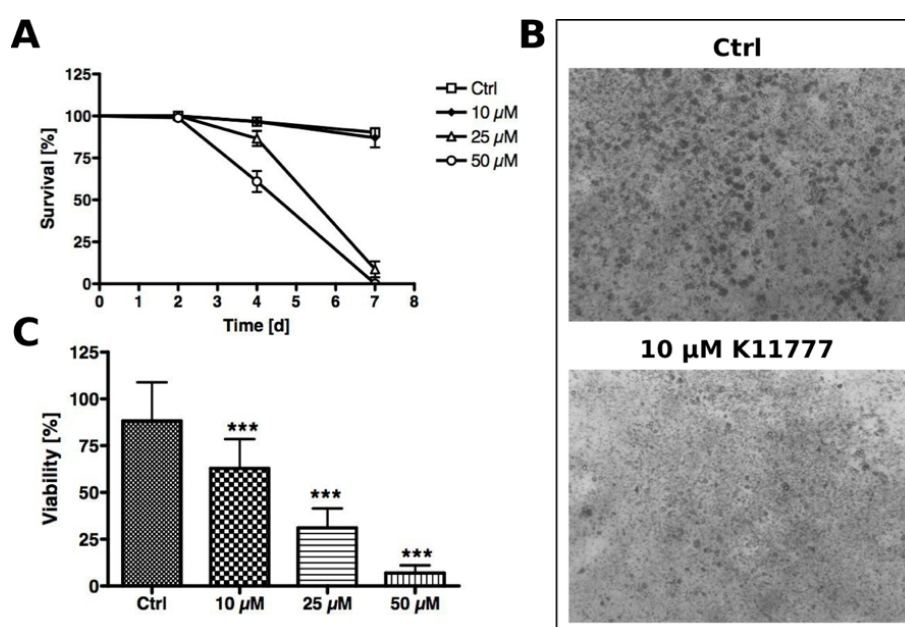


Fig. 4.36: Effects of K11777 on metacestode vesicles and primary cells. (A) Metacestode vesicles were cultivated for 7 days in the presence or absence of K11777. Disrupted vesicles were counted on day 2, 4 and 7. The control was supplemented with DMSO. p below 0.001 for 25 μM and 50 μM samples. (B) Metacestode vesicles were treated with DMSO or 10 μM K11777 for 7 days in conditioned medium, followed by primary cell isolation and cultivation in conditioned medium. The regeneration of primary cells was documented on day 7. (C) Freshly isolated primary cells were cultivated in 10 % FCS/DMEM without phenol red supplemented with K11777 in the indicated concentrations. After 2 days the Resazurin viability assay was performed. (***) p below 0.001.

4.4 Targeting Jun kinase (JNK) with the inhibitor AS601245

Jun kinase in *E. multilocularis* was previously described by Riedl [153]. However only a weak effect was observed with the JNK inhibitor II (SP600125, Biomol). The inhibitor AS601245 (JNK inhibitor V, Calbiochem) was therefore tested for an effect on *E. multilocularis* larval material. Survival of metacestode vesicles treated with 50 μM AS601245 (AS) was severely decreased (Fig. 4.37), lower concentrations however showed no effect (data not shown). To investigate if AS affects viability of parasite material at lower concentrations pre-treatment experiments were carried out. Metacestode vesicles were treated with AS for 7 days. Subsequently, primary cells were isolated and regeneration of aggregates from these cells was observed. Primary cell cultures of vesicles treated with 20 μM AS for 7 days showed no regeneration, while in samples pre-treated with 2 μM viability was only slightly impaired (Fig. 4.38). These results showed, that also no killing effect on vesicles was observed viability of the parasite was affected.

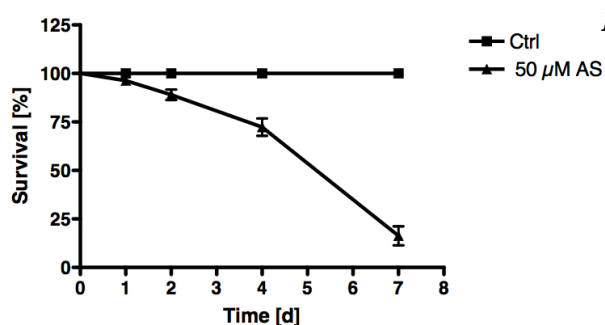


Fig. 4.37: Survival of metacestode vesicles treated with AS601245. Metacestode vesicles were incubated for 7 days in 10 % FCS/DMEM supplemented with AS. Disrupted vesicles were counted at day 2, 4 and 7. *p* below 0.001

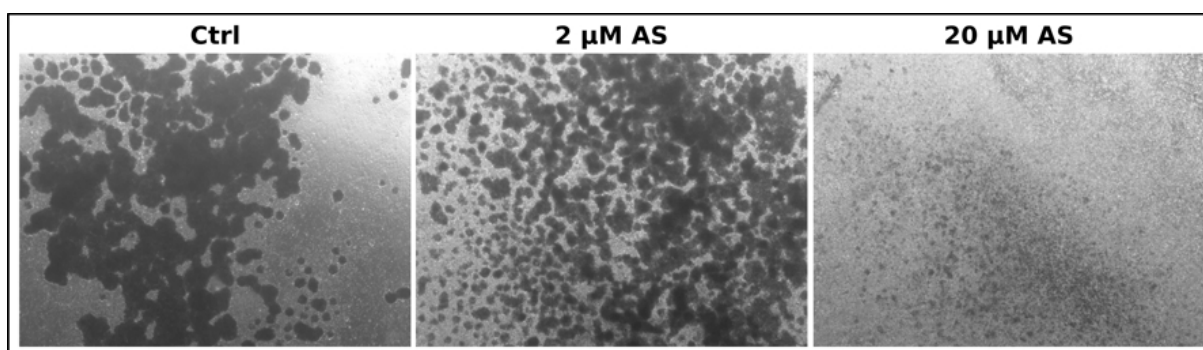


Fig. 4.38: Regeneration of primary cell aggregates from pre-treated metacestode vesicles. Axenic metacestode vesicles were incubated in conditioned medium supplemented with the indicated concentration of AS for 7 days. The control was supplemented with DMSO. Subsequently, primary cells were isolated and cultivated in conditioned medium. Aggregation was documented on day 4.

Pre-treatment experiments indicated that AS601245 could have an influence on viability of *E. multilocularis* stem cells. Therefore AS was subsequently tested on primary stem cell cultures in the Resazurin assay. The experiments revealed that a concentration of 20 μM reduced viability of primary cell cultures to 50 % and 50 μM had an even stronger effect, decreasing living parasite material to 25 % (Fig. 4.39A). 2 μM AS had no effect in this experiment, although this is probably due to a short treatment period of 2 days. Treatment of protoscoleces with 20 or 50 μM AS for up to 2 weeks revealed a time dependent effect of AS601245 on survival of protoscoleces (Fig. 4.39B). While treatment with the inhibitor showed only a slight effect after two days, survival was reduced to 50 % on day 7 and to 25 % on day 14. In these experiments the difference between 20 μM and 50 μM was not significant.

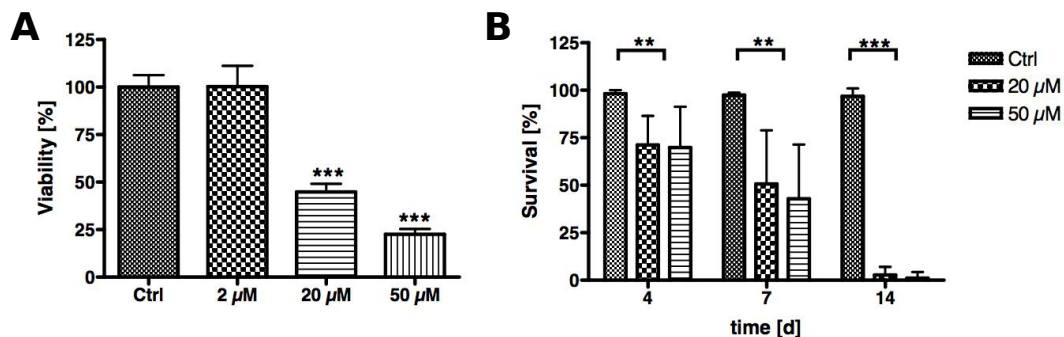


Fig. 4.39: Treatment of primary cells and protoscoleces with AS601245. (A) Freshly isolated primary cells were incubated in 10 % FCS/DMEM without phenol red supplemented with the indicated concentration of AS. After 2 days the Resazurin assay was carried out. (B) Protoscoleces were isolated from secondary infected jirds and cultivated in conditioned medium with 20 μM or 50 μM AS for the indicated time. Samples were stained with 0.03 % methylen blue and dead protoscoleces were counted. (**) p between 0.001 and 0.01, (***) for p below 0.001.

4.5 The effect of Albendazole in the new *E. multilocularis* *in vitro* cultivation systems

The current standard in AE treatment with Albendazole (ABZ) is 400 to 800 mg daily, given in two doses, which should give the optimal plasma level of 0.65- 3 μM 4 h after the morning dose [23]. In recent years much progress in *in vitro* cultivation systems have been made [43] that could also influence the effect of inhibitors *in vitro*. Therefore, it is necessary to study ABZ effect in these *in vitro* systems for a better evaluation of the putative new inhibitors against *E. multilocularis*. ABZ was used on metacestode vesicles in *in vitro* experiments (Fig. 4.40A). The chosen concentrations varied from 4 μM , which

is the therapeutic plasma concentration to 50 μM , a concentration that was used for other tested inhibitors. With 50 μM effective killing of metacestode vesicles was achieved, while a concentration of 4 μM lead to a 50 % decreased survival. 10 μM and 20 μM both reduced survival to 37 %. On primary cells, using the Resazurin health assay no effect was seen, even a high concentrations of 100 μM (Fig. 4.40B).

All together these data show, that ABZ was very efficient against metacestode vesicles, but showed no effect against primary cell cultures.

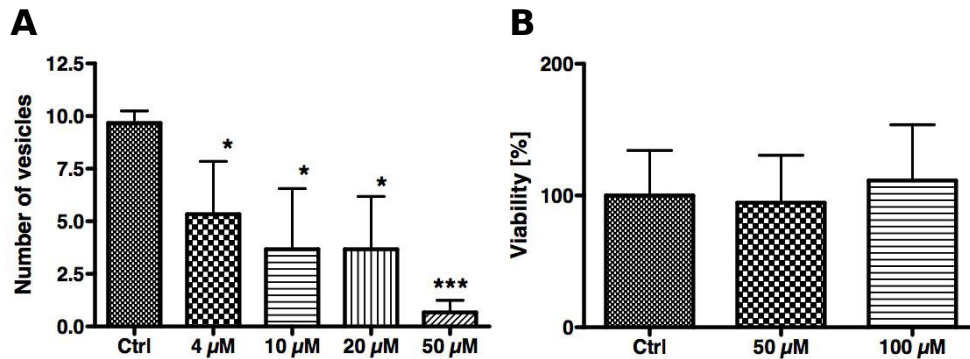


Fig. 4.40: Effect of ABZ on *E. multilocularis*. (A) Axenic metacestode vesicles were cultivated in 2 % FCS/DMEM supplemented with DMSO or ABZ. Dead vesicles were counted at day 7. (*) p below 0.05, (***) p below 0.001. (B) Primary cells were incubated in 10 % FCS/DMEM without phenol red in the presence of ABZ or DMSO. Subsequently the Resazurin Health assay was carried out.

4.6 The utilization of inhibitor combination treatment against *E. multilocularis* larvae

Treatment options against AE are currently very limited and rely mostly on benzimidazoles [20], which are mostly parasitostatic and depend on a life-long treatment of the patients [24]. For a new approach of anti-AE treatment ATP-competitive inhibitors of conserved signalling systems are considered. However, most inhibitors promote resistance development. Combination therapies are already successfully employed in *Plasmodium falciparum* [154] as well as in cancer treatment [155]. For a first step into testing the effect of combination-based therapy of AE several inhibitor combinations were tested on *E. multilocularis* *in vitro* cultures.

4.6.1 Comparison of inhibitors in single drug *in vitro* assays

To evaluate the efficacy of the employed compounds against *E. multilocularis* the effect of the inhibitors in metacystode vesicles and primary cells was compared. In metacystode vesicles survival on day 7 for the different compounds and concentrations was summarized in Tab. 4.5. In the experiments HNMPA(AM)₃ and LY294002 showed the lowest performance. Effects below 100 μM and 50 μM , respectively, were not detected. Imatinib and K11777 showed the highest effectivity in killing metacystode vesicles *in vitro*, while the effects of AS601245 were observed at higher concentrations. In metacystode vesicles Imatinib reduced survival of metacystode vesicles at 10 μM stronger than K11777. Interestingly Albendazole (ABZ) which is currently used in anti-AE therapy only shows weak effect in this cultivation system. 4 μM ABZ corresponded to the desired plasma levels in patients only reduced survival of metacystode vesicles to 53.3 %.

Tab. 4.5: Summary of inhibitor treatment on metacystode vesicles. Depicted is the effect on survival of metacystode vesicles [%] at day 7. (n.e) no effect, (n.d) not determined.

	4 μM	10 μM	20 or 25 μM	50 μM	100 μM
HNMPA(AM) ₃	n.d	n.e	n.e	n.e	20
LY294002	n.d	n.e	n.e	71.3	66
Imatinib	n.d	46.7	10	0	0
AS601245	n.d	n.e	n.e	22.5	n.d
K11777	n.d	90	10	0	n.d
Albendazole	53.3	36.7	36.7	6.7	n.d

In primary cells viability of the cultures was compared with the Resazurin health assay, which reflects the status of the cells after two days of treatment (Tab.4.6). In primary cells HNMPA(AM)₃ was more effective than in metacystode vesicles, showing an effect already at 25 μM . LY294002 was less effective compared to metacystode vesicles. ABZ showed no reduction in viability of primary cells. Highest effects were seen with Imatinib and K11777.

Tab. 4.6: Summary of inhibitor treatment on Primary cell cultures. Primary cells were incubated with the indicated amount of inhibitor for 2 days. Subsequently the Resazurin health assay was carried out and the viability [%] compared to the control was measured. (n.e) no effect, (n.d) not determined.

	10 μ M	20 or 25 μ M	50 μ M	100 μ M
HNMPA(AM) ₃	n.e	67.9	50.7	n.d
LY294002	n.e	n.e	97.2	77
Imatinib	82.7	49.4	23.2	n.d
AS601245	n.e	44.9	22.6	n.d
K11777	50.4	25.6	10.6	n.d
Albendazole	n.e	n.e	94.6	111.5

Taken together these results showed that Imatinib and K11777 both had a strong effect on metacestode vesicles and primary cells. ABZ was most effective on metacestode vesicles, but had no activity against primary cells. HNMPA(AM)₃, LY294002 and AS601245 only showed medium performance against metacestode vesicles and primary cells.

4.6.2 Combination-treatment of parasite material

The insulin signalling cascade was shown to promote parasite development and inhibitors against the insulin receptor and the PI3K were decreasing parasite survival. A combination of two inhibitors, HNMPA(AM)₃ and LY294002 was tested to study, whether this leads to a more effective shutdown of the signalling cascade (Fig. 4.41A). Additionally, Imatinib was tested in combination with HNMPA(AM)₃, to block two different signalling cascades. LY294002 had no significant effect in the Resazurin assay, while HNMPA(AM)₃ reduced viability to 59 %. Combination of HNMPA(AM)₃ and LY294002 had a synergistic effect on the cultures and reduced viability by another 17 % to 42 % in total. Combination of HNMPA(AM)₃ with Imatinib was even more effective, reducing viability to 19 % compared to the control. Taken together, these results show that targeting of two different signalling cascades is a more promising approach than combination of two inhibitors in the same pathway.

In a second experiment Imatinib was tested together with AS601245 as both inhibitors displayed activity against primary cells and metacestode vesicles (see Tab. 4.6). Imatinib and AS601245 reduced viability of primary cell to 49.4 and 44.9 %, respectively. A combination of the two compounds resulted in a survival of 8.4 % after only 2 days (Fig. 4.41B).

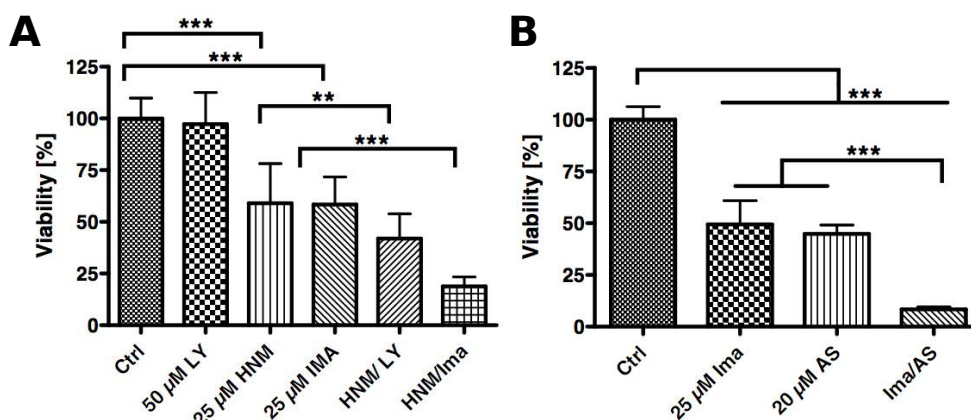


Fig. 4.41: Effect of inhibitor combinations in the Resazurin health assay. Primary cells were incubated in 10 % FCS/DMEM supplemented with the indicated inhibitors for 2 days. Subsequently the Resazurin assay was carried out. (A) HNMPA(AM)₃ was used in the concentration of 25 μ M, LY294002 with 50 μ M and Imatinib with 25 μ M. DMSO was added to the control. (B) 25 μ M Imatinib and 20 μ M AS601245 were added. The control was supplemented with DMSO. (**) *p* between 0.001 and 0.01, (***) for *p* below 0.001.

Imatinib was one of the most effective inhibitors used in the study. Therefore, Imatinib was investigated in the combination with ABZ for its potential use as a supplement in ABZ based therapy. In a first approach metacystode vesicles were treated with ABZ, Imatinib and a combination of both for 7 days. In this experiment Imatinib had a stronger effect than ABZ in killing metacystode vesicles. Combination of Imatinib and ABZ intensified the effect of Imatinib, however no significance could be achieved (Fig. 4.42A). A lower concentration of Imatinib (10 μ M) had no effect on parasite survival and also no additive effect to ABZ (data not shown).

In primary cells Imatinib reduced viability to 50 %. Combination of Imatinib and ABZ lead to a total viability of 27 %, although ABZ alone had no effect on primary cells (Fig. 4.42B) Treatment of primary cells in long term cultures 20 μ M ABZ affected regeneration negatively. Cavities were visibly smaller than in the control. 10 μ M Imatinib reduced cavity size, furthermore, the aggregates had an unhealthy, deteriorating appearance. The combination of both inhibitors blocked aggregation and regeneration efficiently (Fig. 4.42C).

Having shown that K11777 is one of the most effective inhibitors tested on primary cells and metacystode vesicles, K11777 was additionally investigated in combination with ABZ (Fig. 4.43). 10 μ M K11777 reduced survival of primary cells in the Resazurin assay to 55 %. Combination of K11777 with 50 μ M ABZ lead to an overall survival of 36 %, which indicated that ABZ and K11777 worked synergistically in these experiments.

Taken together the data show that the most effective inhibitor combination was Imatinib with AS601245. Furthermore, Imatinib and K11777 both displayed promoted effects together with ABZ.

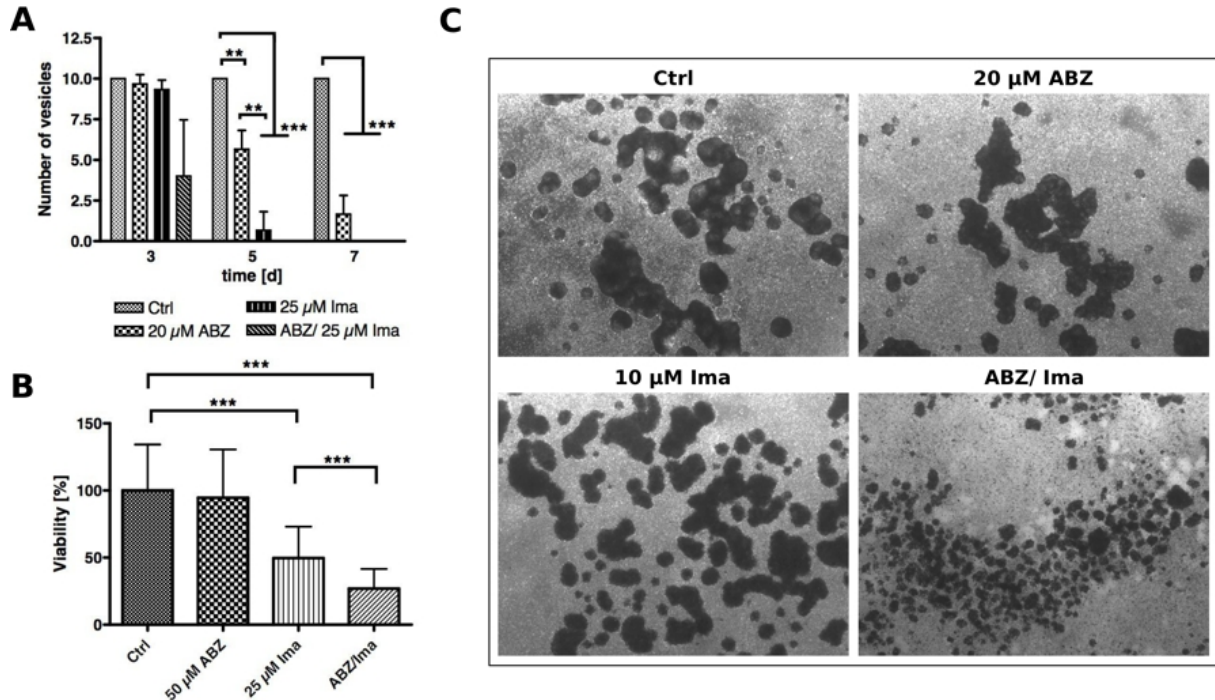


Fig. 4.42: Effect of ABZ and Imatinib combination treatment on *E. multilocularis*. (A) Metacystode vesicles were cultivated in 2 % FCS/DMEM supplemented with ABZ and Imatinib for up to 7 days. The control was supplemented with DMSO. Dead vesicles were counted after 3, 5 and 7 days. (B) Primary cells were incubated in 10 % FCS/DMEM supplemented with the indicated amounts of the inhibitors for 2 days. Subsequently the Resazurin assay was carried out. DMSO was added to the control. (C) Freshly isolated primary cells were cultivated in conditioned medium in the presence of ABZ and Imatinib or DMSO. Development of aggregates was documented at day 14. (**) p between 0.001 and 0.01, (***) for p below 0.001.

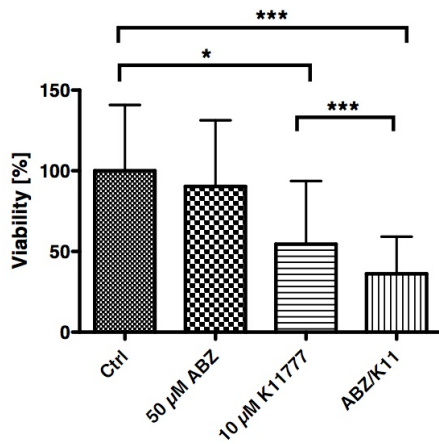


Fig. 4.43: Combination treatment of primary cells with ABZ and K11777. Primary cells were incubated in 10 % FCS/DMEM supplemented with the indicated amounts of the inhibitors for 2 days. Subsequently the Resazurin assay was carried out. DMSO was added to the control. (*) p below 0.05, (***) for p below 0.001.

4.7 The effect of the *Clostridium botulinum* C2 toxin on *E. multilocularis*

The C2 toxin is a binary bacterial toxin of the AB-type toxins, composed of two non-linked proteins that act as a binding/translocation component and an enzyme component. C2 toxin exhibits actin-ADP-ribosylation activity [156]. Furthermore, those toxins are currently investigated as possible delivery systems for eukaryotic cells [157].

C2 toxin was tested on metacestode vesicles and primary cells. Treatment of metacestode vesicles had no visible effect on the cultures (data not shown), neither inducing killing, nor increasing or decreasing growth. However in primary cell cultures high numbers of vesicles formed in samples treated with a combination of C2II and C2I components of the toxin, which were not present in the controls (Fig. 4.44B). Aggregation in these cultures was not affected (Fig. 4.44A). Staining of vesicles with HE revealed that the vesicles contained no cells (Fig. 4.44C) and are therefore no metacestode vesicles. The origin of the vesicular structures are unknown, as they also appeared in experiments with low aggregation and also in cultures of protoscoleces (data not shown). In protoscoleces cultures no effect on killing was observed.

Fahrer et al. [158] developed a carrier system system to transport C2I-fusion proteins into cells. This system was used to study cellular uptake of the C2I subunit in form of a C2I-streptavidin fusion protein. Biotin was incubated with the fusion protein to allow binding to the streptavidin part. The C2II-C2I-Biotin complex was incubated with primary cell aggregates and uptake of Biotin into the cells was documented with fluorescence microscopy. For the *Echinococcus* experiments periods of 2 to 10 h were tested. Furthermore different concentrations of C2II and C2I components were used. In none of samples an uptake of Biotin into *E. multilocularis* cells was observed (data not shown).

4 Results

Taken together the results suggest that C2 toxin binds to *Echinococcus* cells, but is not internalised. Stimulation of vesicle formation therefore must be due to a stimulation of parasite material from binding of the toxin. As the toxin was not taken up, it had no lethal effects by interacting with the parasite actin cytoskeleton. The mechanism by which vesicle formation is stimulated is still unknown, as well as the origin of the vesicles themselves.

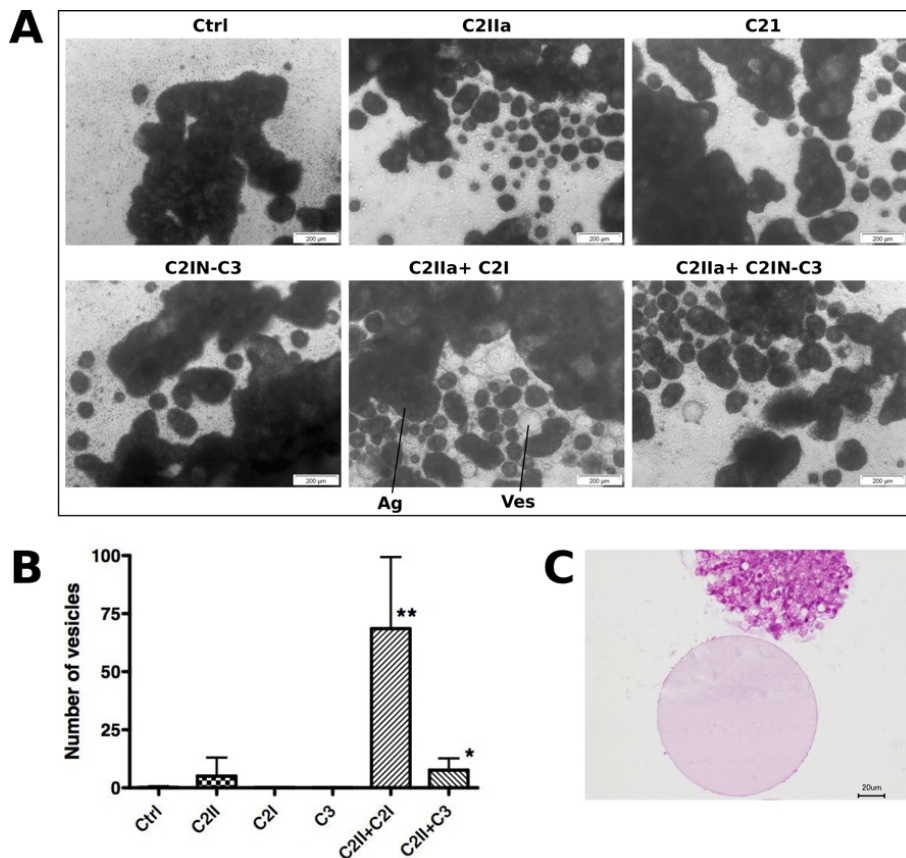


Fig. 4.44: Effect of C2 toxin on parasite material. (A) Primary cells were cultivated in conditioned medium supplemented with 200 ng/ml C2IIa and 100 ng/ml C2I or 100 ng/ml C2I-C3. Vesicles formed after 4 to 9 days. Ag: aggregate, Ves: vesicle. (B) Formation of vesicles in primary cell cultures. (**) p between 0.001 and 0.01, (***) for p below 0.001. (C) Samples were embedded in Technovit 8100 and 4 μ m sections were stained with HE. Depicted is a vesicle and part of a primary cell aggregate.

5 Discussion

As a multicellular metazoan organism the fox tapeworm *Echinococcus multilocularis* relies on signalling mechanisms for its developmental processes that have arisen early in metazoan evolution [16, 48]. These signalling systems are based on soluble factors that bind to surface or intracellular receptors and activate intracellular signalling cascades to evoke the appropriate cellular response. As these signalling cascades also mediate cell-cell communication, they could serve as potential host-parasite communication channels. By sensing host factors the parasite could regulate its development depending on the current status of the host. Evidence of this hormonal-crosstalk between host and parasite has been already obtained and further investigation are currently performed [53, 99, 159].

Although the molecules that are involved in cellular signalling are highly conserved, many significant changes were induced since the separation of Protostomia and Deuterostomia. These changes on structural and functional level therefore can be employed to find new targets for chemotherapy. The goal is to find inhibitors that target only parasite enzymes without cross-reacting with human homologues. The study of *Echinococcus* signalling systems helps to understand the factors that promote development to identify new targets for anti-AE therapy.

5.1 Insulin signalling in *E. multilocularis*

Insulin signalling is of special interest in *E. multilocularis* as the disease is first established in the liver near the portal vein, where the highest body concentrations of insulin is reached [64, 65]. Furthermore, IGF-I is highly expressed in the liver [66] and its involvement in cancer development in humans emphasises proliferative functions of this factor [62, 63]. Although in mammals mitogenic IGF-I and metabolic insulin signalling are usually separated, cross-talk between the two signalling systems as well as hybrid receptor complexes were reported [63, 160]. Additionally, interaction between human insulin and invertebrate insulin receptors was shown to be possible [52]. The presence of two host-derived members of the insulin family in the vicinity of the parasite implied that insulin could be involved in host-parasite cross-communication and organ tropism of *E. multilocularis* by sensing host derived factors with endogenous surface receptors.

Previous works on *E. multilocularis* larval material indicated that host insulin might be involved in proliferative processes, as it stimulated metacestode growth, survival and BrdU incorporation when exogenously added to *in vitro* cultivated vesicles [124,130]. Two insulin receptor homologues, EmIR1 [161] and EmIR2 [125] were identified in *E. multilocularis*. EmIR1 was shown to be expressed in metacestode vesicles and protoscoleces and immunohistological experiments revealed a high abundance of EmIR1 in glycogen storage cells of metacestode vesicles. Furthermore, Yeast two Hybrid (Y2H) experiments indicated that the ligand binding domain of EmIR1 is able to interact with pro-insulin [124]. The same work also demonstrated that in the course of host insulin stimulation the MAP kinase cascade is activated [124].

In this work we extended our knowledge on insulin signalling mechanisms in *E. multilocularis*. Several lines of evidence clearly suggest, that insulin promotes parasite development *in vitro*. First, insulin stimulated proliferation of primary cell cultures and metacestode vesicles, as it was shown by BrdU incorporation experiments. Second, insulin increased the development of new metacestode vesicles from primary cells and protoscoleces. Furthermore, aggregate and cavity size of the primary cell cultures was significantly increased. The effects of insulin on *E. multilocularis* larvae could be blocked by the insulin receptor inhibitor HNMPA(AM)₃. And third, insulin stimulated phosphorylation of EmIR2 and the PI3K/ Akt pathway proteins in response to host derived insulin. The IR inhibitor HNMPA(AM)₃ and the PI3K inhibitor LY294002 both blocked insulin induced phosphorylation, thereby giving proof of the link between insulin, the insulin receptors and the PI3K/ Akt pathway. Additionally, it was already reported that EmIR1 and the MAPK cascade are activated in response to insulin [124].

In previous experiments it was shown that insulin increases the volume of metacestode vesicles [124, 130]. However, due to a high variation between the experiments no significant result could be gained. Nevertheless, this work and previous experiments [124] clearly proved that exogenous insulin stimulated proliferation of primary cell cultures and metacestode vesicles. Additionally, in primary cells the aggregate and cavity size increased in response to insulin, which indicated a better development of the cultures compared to the control. Therefore, it can be concluded, that host insulin has mitogenic effects on *E. multilocularis* larvae. Interestingly, in the culture system for metacestode vesicles used in this work, a negative effect was observed for 100 nM insulin. A similar effect was already reported in experiments with *T. crassiceps* [103], where it was suggested that a saturation concentration of ligand could activate negative feedback mechanisms. However, the saturation concentration in *E. multilocularis* experiments clearly depended on the experimental setup, since it was observed in BrdU incorporation assays, but not in long-term cultivation experiments. Furthermore, the overall insulin concentration used by Escobedo

et al. [103] was much higher and is not directly comparable to the concentrations used in this work.

In primary cell cultures and protoscoleces parasite metacestode vesicle formation was increased when host insulin was added to the cultivation medium. These data indicate, that insulin might drive the development of larval material towards the metacestode stage. In the case of primary cell cultures, which mimic stem cell driven oncosphere-metacestode transition [45] these data might represent the primary vesicle formation from the oncosphere during the establishment of the disease. Furthermore, it was demonstrated that protoscoleces can contribute to the existing pool of vesicles [131, 132]. Protoscoleces could come into contact with the surrounding host tissue, when a vesicle is broken or dying. In that case, the de-differentiation of protoscoleces could be regulated by host insulin.

Next to mitogenic and developmental effects, host insulin also stimulated glucose uptake of metacestode vesicles, thereby acting as a metabolic regulator. Similar results have also been obtained for *S. mansoni*, *S. japonicum* and *M. vogae* [100–102], although with much higher (unphysiological) insulin concentrations. Taken together these results demonstrated that insulin regulates proliferation of *E. multilocularis* larval stages, but also promotes the development towards the metacestode stage and regulates the glucose metabolism.

Two members of the insulin receptor family were already identified that could mediate the insulin response. Extensive mining of available genome data supported the assumption that EmIR1 and EmIR2 are the only insulin receptors present in *E. multilocularis*. RT-PCR analysis showed only slight differences in the abundance of *emir1* and *emir2* cDNAs and they seemed to be expressed in all tested larval stages. The *Emir2* isoform seems to be expressed in a stage specific manner, as it was more abundant in non-activated protoscoleces and primary cell culture. *Emir2a* and *b* were found in all tested larval stages, whereas *emir2d* was only weakly expressed. These data indicated that the *emir2* isoforms could serve distinct signalling functions.

For EmIR2 a specific antibody was produced against the β subunit, complementary to the EmIR1 immunoserum [124]. The antibody recognised a band at 87 kDa that corresponds to the calculated size of the EmIR2 β chain. A smaller band was detected at 60 kDa, that could either represent solubilised immunoglobulin or a degradation product of EmIR2. Analysis of the receptor processing indicated an assembly of the receptor complex similar to other known members of the IR family [67, 69].

EmIR1 [124] and EmIR2 immunosera were used to analyse the expression of the two receptors on protein level. Interestingly, EmIR1 is not present or only weakly expressed in primary cell cultures, while EmIR2 is absent in metacestode vesicles. This finding is in

contrast to the RT-PCR data and could be explained by post-transcriptional regulation that results in a repression of the translation. Furthermore, differential expression of EmIR1 and EmIR2 in vesicles and primary cells indicated a functional difference of the receptors. EmIR1 is highly abundant in glycogen storage cells [124] and could therefore mediate the glucose uptake observed in this study. In *S. mansoni* it was demonstrated that SmIR1 is involved in glucose uptake, but not SmIR2 [102]. Interestingly, SmIR1 is the homologous receptor to EmIR2 and SmIR2 to EmIR1. Therefore, the glucose uptake in *E. multilocularis* and *S. mansoni* is not mediated by the same receptor homologue. Assuming a similar functional divergence of the two insulin receptors in *E. multilocularis* it must have developed after the separation of cestodes and trematodes.

Primary cells are characterised by a high proliferative activity and especially early cultures consist mainly of stem cells (communication Uriel Koziol). Therefore a low EmIR1 expression could be expected when this receptor is specific for mediating the glycogen synthesis in *E. multilocularis*. That EmIR2 is the only insulin receptor expressed in this culture system, suggests that it might be responsible for the observed proliferative effects. However further analysis has to be carried out to confirm this assumption.

Immunohistochemical analysis on the EmIR2 distribution in the larval stages was performed using the EmIR2 immunoserum. In primary cell aggregates stained cells were distributed evenly throughout the aggregate, but no specific cell types could be distinguished with this method. A stronger staining was observed on the cavity border, which could indicate that EmIR2 is able to sense signals from cavity fluid. In protoscoleces EmIR2 is found mainly in the scolex and the periphery. It is interesting to note that although no EmIR2 was detected in metacestode protein samples, staining of infected liver material showed a staining of metacestode vesicles. Therefore, it is likely that EmIR2 is expressed in this larval stage, although to a very low extent and thus was not detected in western blot.

In this work, it was shown that EmIR2 is a functional receptor. Stimulation with host insulin induced serine-phosphorylation in *in vitro* cultivated larvae material. However, no tyrosine phosphorylation was detected for EmIR2. A possible explanation could be the mutated YXXYY autophosphorylation motif [162, 163] of EmIR2, where only the residues Y¹⁴⁶⁰Y¹⁴⁶¹ are present. Wilden et al. [164] reported that mutation of the first tyrosine of this motif results in a 50 % decreased basal phosphorylation, without affecting the time and dose-dependent response to insulin. Due to a low sensitivity of the western blot method and low basal phosphorylation the insulin induced tyrosine phosphorylation might have been below the detection level. Therefore, serine phosphorylation was used as an indirect indicator for receptor activation since phosphorylation of various serine residues in the hu-

man insulin receptor occurred subsequently to tyrosine phosphorylation [133].

Furthermore, Y2H analysis revealed that EmIR2 recognises a broader ligand spectrum than EmIR1. In the experiments EmIR2 interacted with insulin, IGF-I and *E. multilocularis* insulin-like peptides 1 and 2, while HIR and EmIR interacted only with insulin.

Expression analysis confirmed that *emilp1* and *emilp2* transcripts were present in all larval stages, with the highest expression in activated and non-activated protoscoleces and the lowest expression in primary cells.

Taken together, these data underline the functional divergence of EmIR1 and EmIR2. EmIR2 might mediate signals from host insulin and IGF-I as well as *Echinococcus* ILPs. In the liver, all these peptides should be available. However, in protoscoleces after ingestion by the final host, only endogenous ILPs should be present. Therefore, the ILPs seem to be the main ligand for EmIR2 in protoscoleces. Stimulation of developmental processes by host insulin might suggest that the EmILPs have a similar function in promoting the development of the adult worm. However, studies on the expression of the EmILPs in the adult stage and the effect of EmILP1 and 2 *in vitro* are needed to confirm this assumption. EmIR1 was specific for pro-insulin and did not bind IGF-I or EmILP1 and EmILP2. Taking into consideration previously discussed data on EmIR1, it is likely that EmIR2 senses host insulin to regulate glucose metabolism and proliferation in metacystode stage.

Previously, the MAPK cascade was identified as mediator of insulin signals in *E. multilocularis* [124]. In the mammalian signalling system the PI3K/ Akt pathway is involved in insulin signalling as well [83, 88, 89]. Multiple components of this pathway were identified on genomic level, analysing data from the genome sequencing project. The high conservation of the molecules indicate the presence of a functional signalling cascade similar to the mammalian system. However, important differences were already detected: First, no NPXY motif was detected in EmIR2 that is important for interaction with downstream molecules. Second, no PI3K regulatory subunit was so far identified, which could notify that the PI3K activity is regulated in an alternative fashion. Third, only one Akt homologue is present in *E. multilocularis*, which has unusual N and C-terminal extension. Therefore, EmAkt is most likely involved in integrating signals from various signalling systems. These data suggest that the signalling system in *E. multilocularis* could be simpler and more basic than the mammalian counterpart.

The activation of the PI3K/Akt pathway was measured by phosphorylation of Akt substrates and Em4E-BP. Phosphorylation strongly increased after 5 min and had already disappeared after 30 min, which indicated a fast signal transmission and tight regulation of the pathway. Furthermore, inhibitors against the insulin receptors and the PI3K, HNMPA(AM)₃ and LY294002, respectively, were able to block the phosphorylation of Em4E-

BP. These results emphasise the link between insulin binding, the activation of the receptor and transmission of the insulin signals via the PI3K/Akt pathway.

In *in vitro* experiments HNMPA(AM)₃ and LY294002 killed *E. multilocularis* larval material. Additionally, HNMPA(AM)₃ reduced the vesicle formation in primary cell cultures and induced dramatic changes in the morphology of primary cell aggregates, with no living cells remaining at higher concentrations.

LY294002 was used in concentrations of 10 to 50 μM on eucaryotic cell lines [165–167]. Therefore, the effects of LY294002 in *E. multilocularis* *in vitro* cultures were observed in the upper concentration range. The low effects of this inhibitor could be contributed to a poor solubility and low bioavailability [167, 168]. Furthermore, in EmPI3K only three of the four residues that are important for the binding of the inhibitor are conserved, which could reduce the binding affinity for the *Echinococcus* protein [136]. Considering that inhibition of PI3K with rapamycin had no drastic effects on *Echinococcus* protoscoleces [169] and metacestode vesicles (data not shown), the PI3K/ Akt pathway might not be crucial for survival of *Echinococcus* larvae. Therefore, it can be concluded that the PI3K pathway might not be a promising target of anti-AE chemotherapy.

Additionally, LY294002 had only long term effects in primary cells, while HNMPA(AM)₃ was very effective in primary cells cultures. HNMPA(AM)₃ inhibits the insulin receptor directly, therefore blocking PI3K and MAPK both, which could result in the overall more drastic effects on parasite viability. Due to the high proliferative activity of primary cells, these data could indicate that the proliferative effects of insulin in *E. multilocularis* are transmitted via the MAPK cascade.

So far, no information about the binding mechanism for HNMPA(AM)₃ to the insulin receptor ATP- binding site is available. In previous studies HNMPA(AM)₃ was used in concentrations up to 100 μM [100, 170], which was within range of the experiments in this study. Taken together, these results show that inhibition of the insulin receptor leads to an effective killing of *E. multilocularis* larvae. Development of an inhibitor or antibody with high specificity for the *Echinococcus* insulin receptors might be valuable for the treatment of AE patients.

A further question raised in regard to the role of host insulin is its possible influence on organ tropism. The oncosphere is taken up by the host along with its food, which ensures high insulin concentrations in the blood stream. After passing into the blood stream the oncosphere might be targeted to the liver by high insulin concentrations, where it settles and where the mitogenic insulin effects promote the oncosphere-metacestode transition and later proliferation of larval material. *E. multilocularis* and *E. granulosus* infect primarily the liver [2], where they come into contact with high concentrations of insulin. In contrast

the *T. solium* metacestode stage develops in the muscles and the brain, although it takes the same infection route as *Echinococcus* species, passing the portal vein [171]. Escobedo et al. [103] observed that *T. crassiceps* reacted to insulin stimulation, whereas no insulin dependence was measured for *T. solium*. However, in this study *T. solium* evagination and *T. crassiceps* budding was measured. Therefore, these results were not comparable with the data obtained in the present work, which focused on the developmental effects of insulin. Thus, it can not be excluded that insulin plays a role in the development of *Taenia* species during cysticercosis.

To address the question of organ tropism and insulin dependence *in vivo* experiments are required. Streptozotocin treatment can mimic diabetes in mice and gives the possibility to study the effect of insulin on infectivity and organ preference under controlled conditions. An interesting finding that could relate to organ tropism and metastasis formation is the observed adaptation of parasite isolates to the peritoneal passage. Older isolates showed no increased proliferation upon stimulation with exogenous insulin, which was shown by BrdU incorporation experiments. That the PI3K pathway is no longer activated might indicate that insulin is not registered on the cell surface, which would result in an insulin resistance. However, growth and aggregation is not influenced in these isolates, which indicates that they rely on other stimuli for proliferation and survival. Since fresh isolates usually represent material that has recently grown in the liver of the host, loss of responsiveness in old isolates might be caused by an adaptation to peritoneal culture, where availability of insulin should be lower. In the course of a long-time chronic infection this might lead to metastasis formation in other organs like lung and brain. Furthermore, it emphasises the need for cryo-conservation techniques and regular isolate turnover as other signalling systems could be changed as well.

Next to the stimulation by exogenous insulin, insulin-like peptides might also activate the signalling. As it was observed for EmIR2 was able to bind EmILP1 and EmILP2 in Y2H experiments. Therefore, it was suggested that these peptides could have an influence on the proliferation of *E. multilocularis* larvae. In primary cells EmILP2 significantly increased BrdU incorporation, whereas EmILP1 had no effect. However, it is not clear, if this was due to a lower expression of EmILP1 or if this peptide serves a distinct function. These questions have to be answered in future experiments. A next step would be the synthesis of specific antibodies against the ILPs to enhance purification and detection. Further, it is unclear whether the ILPs might also affect the surrounding host tissue. Interestingly, on genome level two ILP homologues were identified in *Taenia solium*, which could indicate that insulin signalling also plays a role in this organism. In *Schistosoma japonicum* one low conserved insulin homologue was found [124], but no studies have been made so far to investigate the function of this peptide. Highly conserved insulin-like peptides were also identified in the cestode *Hymenolepis microstoma* and identical sequences to *emilp1* and

emilp2 are present in *E. granulosus*. Among the described organisms *E. multilocularis* is the only one, for which it was demonstrated that it can sense host insulin and endogenous insulin-like factors.

In this study now we gained a deeper understanding of the influence of insulin on *E. multilocularis* development and its use as a possible target for anti-AE chemotherapy. The PI3K cascade seems not suitable for anti-AE treatment, however the results on insulin receptor inhibition are more promising and development of suitable inhibitors against the insulin receptors might lead to effective AE chemotherapy.

5.2 Abl kinases and Imatinib

Abl kinases have arisen early in the evolution of metazoan organisms [106] and play a pivotal role in regulating essential processes like proliferation, survival, differentiation and cell adhesion [112, 172]. Due to this key position, deregulation of the Abl signalling promotes in cancer formation [172] and inhibitors that block Abl activity are available. Furthermore, the important role of Abl in cellular signalling implied these proteins as possible targets for anti-helminthic chemotherapy.

In *E. multilocularis* two homologues of Abl kinases were identified. This finding is in contrast to other invertebrates, where usually only one Abl is present [106]. However in the trematode *Schistosoma mansoni* two homologues were found as well [119]. EmAbl1 and EmAbl2 are 33 and 37 % identical to the *Schistosoma* proteins. The low homology is caused by the less conserved C-terminus of the proteins and is with 82 and 76 % much higher in the tyrosine kinase domain. Furthermore an unusual Scr-Abl hybrid kinase was found in *E. multilocularis*, which has high homologies to the *S. mansoni* TK6 [120]. EmTK6 has Abl and Src specific conserved tyrosine residues, but lacks the elongated C-terminus found in Abl kinases. Beckmann et al. [120] suggested a role for SmTK6 in the signalling in the gonads of *S. mansoni*. In complex with other signalling molecules SmTK6 might regulate cytoskeletal reorganisation, mitosis, cell growth and polarity. However *in vitro* studies on *S. mansoni* and *E. multilocularis* have to be undertaken to confirm the proposed role.

Recently, Beckmann and Grevelding [119] demonstrated that Imatinib has severe effects on the adult stage of *S. mansoni* at concentrations between 10 and 100 μ M. Imatinib blocks the function of type III kinases including Abl, c-Kit and the platelet derived growth factor receptor (PDGFR). Intensive BlastX searches on the available *E. multilocularis* genome data have revealed that c-kit and PDGFR are absent in the genome. Therefore, EmAbl1,

EmAbl2 and EmTK6 are most likely the only binding partners for Imatinib in this organism. Nagar et al. [148] identified 21 residues in the human Abl1 kinase that are involved in the binding of Imatinib. Of these 18 are present in EmAbl1, 20 in EmAbl2 and 18 in EmTK6. The high conservation of the Imatinib binding sites makes it likely that the parasite Abl kinases are inhibited by Imatinib, which was already shown for the *Schistosoma* proteins [119, 120]. However, in these experiments the inhibition of SmTK6 by Imatinib was significantly lower than for SmAbl1 and SmAbl2. Therefore, it can be expected that EmAbl1 and EmAbl2 are more responsive to Imatinib than EmTK6, which has to be investigated in future experiments.

In *in vitro* cultures Imatinib had drastic effects on survival and morphology of *E. multilocularis* larvae. The effects were clearly time- and dose dependant. Higher concentrations of Imatinib effectively killed metacystode vesicles and protoscoleces, while low concentrations had weaker effects and needed longer time periods to appear. Imatinib also significantly decreased vesicles formation in primary cells and blocked regeneration in pre-treatment experiments. These data indicate that Abl kinases are important for development of *E. multilocularis* larvae.

Although a concentration 10 μ M Imatinib had only weak effects in the survival and viability experiments, it induced morphological changes already after a treatment period of 24 h, which indicated decreased viability.

In studies of Imatinib on mammalian cell lines concentrations around 10 μ M are regularly used and no significant negative effects on the cells [173]. However in other *in vitro* studies concentrations up to 100 μ M Imatinib were used [174, 175]. In the treatment of Abl-related leukemias Imatinib is given in daily doses of 400 to 800 mg, which leads to a average plasma level of 4 to 6 μ M [176, 177]. Taken together, the concentrations used in the present work were still in the range of previous *in vitro* studies and the effect of Imatinib on *E. multilocularis* was comparable to the results obtained for *S. mansoni* [119]. Furthermore, although higher concentrations had more drastic effects, significant damage of larval material was already observed at 10 μ M Imatinib. Considering the time-dependence of Imatinib it is likely that prolonged treatment with lower doses might have a high, beneficial impact on AE-treatment. Additionally, combined treatment with Albendazole and Imatinib could improve the current ABZ based therapy and will be discussed later. Furthermore, it has to be considered that Imatinib was generated to specifically target the human Abl. Therefore it might be worthwhile to investigate Imatinib-related compounds that may exhibit higher affinities for *Echinococcus* proteins than their human homologues.

5.3 The cystein protease inhibitor K11777

A second useful approach in identification of new drug targets in parasitic helminths is the study of compounds that are efficient against other parasites. Effort has been made to establish Praziquantel for co-treatment with Albendazole, which showed good effects against cystic echinococcosis, but was less effective against alveolar echinococcosis [29,178].

A novel small molecule inhibitor K11777 that blocks cystein proteases and was shown to be effective against several parasites like *Trypanosome cruzii* and *Schistosoma mansoni*, [129,179].

In *E. multilocularis* ten genes coding for cysteine proteases were identified by extensive genome wide BlastX searches. All of these belong to the cathepsin L and B family. Previously, Sako et al. [150,152] reported two cathepsin L-like and 2 Cathepsin B like proteins that are expressed in *E. multilocularis* and partially secreted. Interestingly, for EmCLP1 two genes are present in the genome. K11777 blocks the activity of both, cathepsin B and L [180], but in *S. mansoni* cathepsin B is considered to be the main target of K11777, due to its predominant activity level [181]. The sequence of the *E. multilocularis* cathepsins was very well conserved, including the reported K11777 binding sites [151].

Analysis of the newest transcriptome data available in our lab indicated that three cathepsins are predominantly expressed, namely EmCPB1, EmCLP2 and EmW.000477200(L-like cathepsin). The overall expression of these three candidates were between 11 and 45 %, whereas the expression of the other cathepsins was under 5 % in most stages. The analysis did not show any indication, which cathepsin of *E. multilocularis* could be the target for K11777 and *in vitro* activity and inhibition assays should be performed.

In the *in vitro* cultivation systems K11777 was very effective at higher concentrations, but preliminary pre-treatment experiments proved that also lower concentrations (10 μ M) block *E. multilocularis* development. K11777 is water soluble and has a high bioavailability with low toxicity for host cells [179]. In experiments with *T. cruzii* [182] and the hookworm *Ancylostoma duodenale* [183] concentrations up to 100 μ M were used and it could be shown that a concentration below 20 μ M had no negative effects on host cells [182]. Therefore, the concentrations used for *in vitro* experiments with *E. multilocularis* are well within the range. However, more experiments are needed to study the effects of K11777 in detail.

Taken together, these data show that K11777 is a very promising candidate for anti-AE therapy, as it shows high effects in metacestode and stem cell cultures. In the future, more detailed analysis in *in vitro* cultivation systems and *in vivo* studies on infected rodents have to be performed. Furthermore, experiments with a combination of ABZ and K11777 have been carried out and are discussed below.

5.4 The JNK inhibitor AS601245

The *E. multilocularis* Jun kinase was recently characterised by Riedl [153]. In the mammalian system, JNK is involved in the regulation of apoptosis, immune response and cell cycle [184, 185]. Recently, it was shown that JNK is highly active during the blastema formation in planarians and that inhibition of JNK lead to a defect of blastema formation, most likely by blocking neoblast mitosis and motility [186]. In the *E. multilocularis* cultivation system, the JNK inhibitor SP600125 exhibited only weak effects, probably due to a low binding affinity. Therefore, AS601245, a cell permeable ATP-competitive JNK inhibitor with a lower selectivity was tested in the *in vitro* system. Strong effects on parasite material were observed with 20 and 50 μM . Primary cells in the Resazurin assay were more sensitive to the JNK inhibitor than metacestode vesicles. In total, JNK is not a likely candidate for single compound therapy, as its effects range in the medium spectrum of efficacy compared to other tested substances. However, the results in young primary cells indicated a good effect on stem cells. It could be worthwhile to consider using AS601245 for supporting anti-AE therapy based on other compounds. Therefore, AS601245 was tested in combination with Imatinib where it showed a very strong synergistic reduction of primary cell viability. Furthermore, AS601245 should be tested in combination with ABZ, as it is the current standard anti-AE therapy.

5.5 Albendazole

Albendazole (ABZ) is currently used for AE-treatment in two daily 400 mg doses, leading to a plasma concentration of 0.65 to 3 μM [23]. In previous studies ABZ or other benzimidazole derivates were used in concentrations varying from 0.1 to 36 μM . [27, 187–189]. For a better evaluation of new compounds ABZ was tested on our currently used cell culture systems. On metacestode vesicles ABZ had a significant effect, although the concentration used for human therapy killed only 50 % of the treated metacestode vesicles. Higher concentrations were comparable to other inhibitors in that system like Imatinib and K11777. Interestingly, ABZ had no effect on the viability of primary cells in the Resazurin assay. A possible explanation could lie in the expression of ABZ-resistant beta-

tubulins, which are the targets of ABZ [27]. Brehm et al. [28] described three β -tubulin isoforms and further isoforms were identified in the genome data of *E. multilocularis* [134]. EmTub-2 shows characteristic exchanges that could result in resistance to ABZ [134].

According to our newest transcriptome analysis available in our group, EmTub-2 represents 53 % of the beta-tubulin transcripts in metacestode vesicles and even 79 % in 2 days old primary cells. The presence of this isoform predominantly in primary cells could be responsible for the observed ABZ-resistance. However, Real-time PCR experiments have to be carried out for a comparative analysis of the beta-tubulin expression in *E. multilocularis* larvae.

In the case that stem cells are resistant to ABZ treatment, surviving stem cells could compensate the loss of differentiated cell during anti-AE therapy. Therefore, the lack of effect in culture systems consisting mainly of stem cells could explain the problem that ABZ acts merely parasitostatic.

5.6 Combination therapy as a new approaches for anti-AE treatment

As observed above ABZ was very effective in killing metacestode vesicles, but showed no effect in stem cell cultures. This might explain the observed regeneration of parasite tissue during AE treatment.

Imatinib and K11777 were very active against primary cells in *in vitro* experiments and showed high effects against metacestode vesicles. Using these two compounds in combination with ABZ increased the effect of single treatment. The synergistic effect of these combinations might improve current chemotherapy, however further studies in parasite cell culture systems and *in vivo* experiments in rodents should be performed. Interestingly, the most effective combination used in this study was Imatinib with the JNK inhibitor AS601245, although it exhibited only medium effects when used alone. In *in vitro* experiments with cancer cell lines AS601245 has been used in combination with other therapeutics to strengthen their effects. Due to this ability the inhibitor should be tried together with ABZ in further experiments AS601245, to investigate if it has the same enhancing effects. Inhibition of the insulin and PI3K signalling cascade with one or two inhibitors showed only medium effects. It is not clear, whether this is due to a low binding affinity of the inhibitors or that blocking of the pathway can be compensated by other signalling systems. The combination of Imatinib and HNMPA(AM)₃ was highly effective.

Taken together the data showed that the two most effective inhibitors in the *in vitro* experiments were K11777 and Imatinib, which both could improve ABZ based therapy. AS601245 does not appear to be a promising treatment option on its own, but seems to enhance the effect of other inhibitors [190]. Furthermore, inhibition of the insulin receptor could be employed as an addition to other inhibitors. Whether it will be possible to use the tested compounds for therapy directly has to be tested in *in vivo* experiments. Side effects are possible as the tested inhibitors are designed against or able to bind the respective human homologues. Therefore, another option could be the use of related compounds that show decreased affinity for the human protein. The Resazurin assay and later metacestode vesicle killing assay might be an effective and time saving testing system.

5.7 C2 toxin

The C2 toxin belongs to the group of binary toxins and induces actin-ADP ribosylation when it is taken up by the target cells [156]. C2 toxin was tested on *E. multilocularis* larvae to study its potential use as a delivery system in this organism [157]. Interestingly, C2 toxin induced massive vesicle formation in primary cell cultures and protoscoleces. However, it was shown that these vesicles do not contain cells and their origin is still unclear. Experiments to study uptake of the C2I-Biotin complex failed. Therefore, we assume that the C2I subunit of the binary toxin is not taken up into *E. multilocularis* cells. Consequently, C2 toxin cannot be used as a delivery system. The observed effects on parasite larvae are probably induced by the activation of signalling cascades.

C2 toxin was reported to bind to asparagin linked complex carbohydrates. The GlcNAc-TI gene (α -1,3-mannosyl glycoprotein 2- β -N-acetylglucosaminyltransferase), mediates the assembly of N-linked carbohydrates and its absence abolishes C2 toxin sensitivity [191]. BlastX search in the *E. multilocularis* genome revealed the presence of the GlcNAc-T1 gene (EmW_000969800; supercontig pathogen_EMU_scaffold.007780 : 3330552-3333797). However, it can not be excluded that a protein surface receptor is involved in the uptake of C2 toxin. The lack or mutation of this protein in *E. multilocularis* might explain that the toxin is not internalized by the parasite cells.

Bibliography

- [1] S. Gilbert, “Developmental biology,” *Sinauer Associates, Inc.*, no. 8th edition, 2006.
- [2] J. Eckert and P. Deplazes, “Biological, epidemiological, and clinical aspects of echinococcosis, a zoonosis of increasing concern,” *Clin Microbiol Rev*, vol. 17, pp. 107–35, Jan 2004.
- [3] A. D’Alessandro and R. L. Rausch, “New aspects of neotropical polycystic (*echinococcus vogeli*) and unicystic (*echinococcus oligarthrus*) echinococcosis,” *Clin Microbiol Rev*, vol. 21, pp. 380–401, table of contents, Apr 2008.
- [4] N. Xiao, J. Qiu, M. Nakao, T. Li, W. Yang, X. Chen, P. M. Schantz, P. S. Craig, and A. Ito, “*Echinococcus shiquicus* n. sp., a taeniid cestode from tibetan fox and plateau pika in china,” *Int J Parasitol*, vol. 35, pp. 693–701, May 2005.
- [5] R. C. Thompson and A. J. Lymbery, “*Echinococcus*: biology and strain variation,” *Int J Parasitol*, vol. 20, pp. 457–70, Jul 1990.
- [6] M. Hüttner, M. Nakao, T. Wassermann, L. Siefert, J. D. F. Boomker, A. Dinkel, Y. Sako, U. Mackenstedt, T. Romig, and A. Ito, “Genetic characterization and phylogenetic position of *echinococcus felidis* (cestoda: Taeniidae) from the african lion,” *Int J Parasitol*, vol. 38, pp. 861–8, Jun 2008.
- [7] R. C. A. Thompson and D. P. McManus, “Towards a taxonomic revision of the genus *echinococcus*,” *Trends Parasitol*, vol. 18, pp. 452–7, Oct 2002.
- [8] P. Craig, “*Echinococcus multilocularis*,” *Curr Opin Infect Dis*, vol. 16, pp. 437–44, Oct 2003.
- [9] T. Romig, A. Dinkel, and U. Mackenstedt, “The present situation of echinococcosis in europe,” *Parasitol Int*, vol. 55 Suppl, pp. S187–91, Jan 2006.
- [10] A. Schweiger, R. W. Ammann, D. Candinas, P.-A. Clavien, J. Eckert, B. Gottstein, N. Halkic, B. Muellhaupt, B. M. Prinz, J. Reichen, P. E. Tarr, P. R. Torgerson, and P. Deplazes, “Human alveolar echinococcosis after fox population increase, switzerland,” *Emerging Infect Dis*, vol. 13, pp. 878–82, Jun 2007.
- [11] P. Deplazes, D. Hegglin, S. Gloor, and T. Romig, “Wilderness in the city: the urbanization of *echinococcus multilocularis*,” *Trends Parasitol*, vol. 20, pp. 77–84, Feb 2004.

- [12] K. Martínek, L. Kolárová, E. Hapl, I. Literák, and M. Uhrin, "Echinococcus multilocularis in european wolves (canis lupus)," *Parasitol Res*, vol. 87, pp. 838–9, Oct 2001.
- [13] D. Tappe, K. Brehm, M. Frosch, A. Blankenburg, A. Schrod, F.-J. Kaup, and K. Mätz-Rensing, "Echinococcus multilocularis infection of several old world monkey species in a breeding enclosure," *Am J Trop Med Hyg*, vol. 77, pp. 504–6, Sep 2007.
- [14] B. Gottstein and A. Hemphill, "Immunopathology of echinococcosis," *Chem Immunol*, vol. 66, pp. 177–208, Jan 1997.
- [15] P. Kern, A. Ammon, M. Kron, G. Sinn, S. Sander, L. R. Petersen, W. Gaus, and P. Kern, "Risk factors for alveolar echinococcosis in humans," *Emerging Infect Dis*, vol. 10, pp. 2088–93, Dec 2004.
- [16] K. Brehm, "The role of evolutionarily conserved signalling systems in echinococcus multilocularis development and host-parasite interaction," *Medical microbiology and immunology*, Apr 2010.
- [17] K. Ingold, B. Gottstein, and A. Hemphill, "High molecular mass glycans are major structural elements associated with the laminated layer of in vitro cultivated echinococcus multilocularis metacestodes," *Int J Parasitol*, vol. 30, pp. 207–14, Feb 2000.
- [18] B. Gottstein and R. Felleisen, "Protective immune mechanisms against the metacestode of echinococcus multilocularis," *Parasitol Today (Regul Ed)*, vol. 11, pp. 320–6, Sep 1995.
- [19] B. Gottstein and A. Hemphill, "Echinococcus multilocularis: the parasite-host interplay," *Exp Parasitol*, vol. 119, pp. 447–52, Aug 2008.
- [20] P. Kern, "Clinical features and treatment of alveolar echinococcosis," *Curr Opin Infect Dis*, vol. 23, pp. 505–12, Oct 2010.
- [21] Y. Aydin, O. Barlas, C. Yolaş, I. H. Aydin, A. Ceviz, A. Aladağ, D. Oren, and D. Akdemir, "Alveolar hydatid disease of the brain. report of four cases," *J Neurosurg*, vol. 65, pp. 115–9, Jul 1986.
- [22] P. Kern, K. Bardonnnet, E. Renner, H. Auer, Z. Pawlowski, R. W. Ammann, D. A. Vuitton, P. Kern, and E. E. Registry, "European echinococcosis registry: human alveolar echinococcosis, europe, 1982-2000," *Emerging Infect Dis*, vol. 9, pp. 343–9, Mar 2003.
- [23] E. Brunetti, P. Kern, D. A. Vuitton, and W. P. for the WHO-IWGE, "Expert consensus for the diagnosis and treatment of cystic and alveolar echinococcosis in humans," *Acta Trop*, vol. 114, pp. 1–16, Apr 2010.

- [24] P. Kern, H. Wen, N. Sato, D. A. Vuitton, B. Gruener, Y. Shao, E. Delabrousse, W. Kratzer, and S. Bresson-Hadni, "Who classification of alveolar echinococcosis: principles and application," *Parasitol Int*, vol. 55 Suppl, pp. S283–7, Jan 2006.
- [25] K. Brehm, P. Kern, K. Hubert, and M. Frosch, "Echinococcosis from every angle," *Parasitol Today (Regul Ed)*, vol. 15, pp. 351–2, Sep 1999.
- [26] F. Mosimann, V. Bettschart, and R. Meuli, "Mediastinal recurrence of alveolar echinococcosis after liver transplantation," *Liver Transpl*, vol. 9, pp. 97–8, Jan 2003.
- [27] H. Jura, A. Bader, and M. Frosch, "In vitro activities of benzimidazoles against echinococcus multilocularis metacestodes," *Antimicrob Agents Chemother*, vol. 42, pp. 1052–6, May 1998.
- [28] K. Brehm, K. Kronthaler, H. Jura, and M. Frosch, "Cloning and characterization of beta-tubulin genes from echinococcus multilocularis," *Mol Biochem Parasitol*, vol. 107, pp. 297–302, Apr 2000.
- [29] A. Hemphill, M. Spicher, B. Stadelmann, J. Mueller, A. Naguleswaran, B. Gottstein, and M. Walker, "Innovative chemotherapeutical treatment options for alveolar and cystic echinococcosis," *Parasitology*, vol. 134, pp. 1657–70, Nov 2007.
- [30] A. Ito, "Serologic and molecular diagnosis of zoonotic larval cestode infections," *Parasitol Int*, vol. 51, pp. 221–35, Sep 2002.
- [31] T. H. Le, D. Blair, and D. P. McManus, "Mitochondrial genomes of parasitic flatworms," *Trends Parasitol*, vol. 18, pp. 206–13, May 2002.
- [32] J. Knapp, J. M. Bart, M. L. Glowatzki, A. Ito, S. Gerard, S. Maillard, R. Piarroux, and B. Gottstein, "Assessment of use of microsatellite polymorphism analysis for improving spatial distribution tracking of echinococcus multilocularis," *J Clin Microbiol*, vol. 45, pp. 2943–50, Sep 2007.
- [33] K. Brehm, K. Jensen, P. Frosch, and M. Frosch, "Characterization of the genomic locus expressing the erm-like protein of echinococcus multilocularis," *Mol Biochem Parasitol*, vol. 100, pp. 147–52, May 1999.
- [34] P. Borst, "Discontinuous transcription and antigenic variation in trypanosomes," *Annu Rev Biochem*, vol. 55, pp. 701–32, Jan 1986.
- [35] K. Brehm, K. Jensen, and M. Frosch, "mrna trans-splicing in the human parasitic cestode echinococcus multilocularis," *J. Biol. Chem.*, vol. 275, pp. 38311–8, Dec 2000.
- [36] K. Brehm, K. Hubert, E. Sciutto, T. Garate, and M. Frosch, "Characterization of a spliced leader gene and of trans-spliced mrnas from *Taenia solium*," *Mol Biochem Parasitol*, vol. 122, pp. 105–10, Jun 2002.

- [37] K. E. M. Hastings, "Sl trans-splicing: easy come or easy go?," *Trends Genet*, vol. 21, pp. 240–7, Apr 2005.
- [38] K. Brehm, M. Wolf, H. Beland, A. Kroner, and M. Frosch, "Analysis of differential gene expression in echinococcus multilocularis larval stages by means of spliced leader differential display," *Int J Parasitol*, vol. 33, pp. 1145–59, Sep 2003.
- [39] C. Fernández, W. F. Gregory, P. Loke, and R. M. Maizels, "Full-length-enriched cdna libraries from echinococcus granulosus contain separate populations of oligo-capped and trans-spliced transcripts and a high level of predicted signal peptide sequences," *Mol Biochem Parasitol*, vol. 122, pp. 171–80, Jul 2002.
- [40] K. Hubert, R. Zavala-Góngora, M. Frosch, and K. Brehm, "Identification and characterization of pdz-1, a n-ermad specific interaction partner of the echinococcus multilocularis erm protein elp," *Mol Biochem Parasitol*, vol. 134, pp. 149–54, Mar 2004.
- [41] A. Hemphill and B. Gottstein, "Immunology and morphology studies on the proliferation of in vitro cultivated echinococcus multilocularis metacestodes," *Parasitol Res*, vol. 81, pp. 605–14, Jan 1995.
- [42] H. Jura, A. Bader, M. Hartmann, H. Maschek, and M. Frosch, "Hepatic tissue culture model for study of host-parasite interactions in alveolar echinococcosis," *Infect Immun*, vol. 64, pp. 3484–90, Sep 1996.
- [43] M. Spiliotis, K. Brehm, M. Rupp, and K. Sohn, "Axenic in vitro cultivation of echinococcus multilocularis metacestode vesicles and the generation of primary cell cultures," *Host-pathogen Interactions: Methods and Protocols*, p. 368, Jan 2008.
- [44] M. Spiliotis, D. Tappe, L. Sesterhenn, and K. Brehm, "Long-term in vitro cultivation of echinococcus multilocularis metacestodes under axenic conditions," *Parasitol Res*, vol. 92, pp. 430–2, Mar 2004.
- [45] M. Spiliotis, S. Lechner, D. Tappe, C. Scheller, G. Krohne, and K. Brehm, "Transient transfection of echinococcus multilocularis primary cells and complete in vitro regeneration of metacestode vesicles," *Int J Parasitol*, Nov 2007.
- [46] M. Spiliotis, C. Mizukami, Y. Oku, F. Kiss, K. Brehm, and B. Gottstein, "Echinococcus multilocularis primary cells: improved isolation, small-scale cultivation and rna interference," *Molecular and biochemical parasitology*, Jul 2010.
- [47] K. Brehm, M. Spiliotis, R. Zavala-Góngora, C. Konrad, and M. Frosch, "The molecular mechanisms of larval cestode development: first steps into an unknown world," *Parasitol Int*, vol. 55 Suppl, pp. S15–21, Jan 2006.
- [48] K. Brehm and M. Spiliotis, "The influence of host hormones and cytokines on echinococcus multilocularis signalling and development," *Parasite*, vol. 15, pp. 286–90, Sep 2008.

- [49] A. Skorokhod, V. Gamulin, D. Gundacker, V. Kavsan, I. M. Müller, and W. E. Müller, "Origin of insulin receptor-like tyrosine kinases in marine sponges," *Biol Bull*, vol. 197, pp. 198–206, Oct 1999.
- [50] H. Suga, K. Katoh, and T. Miyata, "Sponge homologs of vertebrate protein tyrosine kinases and frequent domain shufflings in the early evolution of animals before the parazoan-eumetazoan split," *Gene*, vol. 280, pp. 195–201, Dec 2001.
- [51] D. M. Kingsley, "The tgf-beta superfamily: new members, new receptors, and new genetic tests of function in different organisms," *Genes Dev*, vol. 8, pp. 133–46, Jan 1994.
- [52] R. Fernandez, D. Tabarini, N. Azpiazu, M. Frasch, and J. Schlessinger, "The drosophila insulin receptor homolog: a gene essential for embryonic development encodes two receptor isoforms with different signaling potential," *EMBO J*, vol. 14, pp. 3373–84, Jul 1995.
- [53] C. Konrad, A. Kroner, M. Spiliotis, R. Zavala-Góngora, and K. Brehm, "Identification and molecular characterisation of a gene encoding a member of the insulin receptor family in echinococcus multilocularis," *Int J Parasitol*, vol. 33, pp. 301–12, Mar 2003.
- [54] M. Spiliotis, C. Konrad, V. Gelmedin, D. Tappe, S. Brückner, H.-U. Mösch, and K. Brehm, "Characterisation of emmpk1, an erk-like map kinase from echinococcus multilocularis which is activated in response to human epidermal growth factor," *Int J Parasitol*, vol. 36, pp. 1097–112, Sep 2006.
- [55] V. Gelmedin, M. Spiliotis, and K. Brehm, "Molecular characterisation of mek1/2- and mkk3/6-like mitogen-activated protein kinase kinases (mapkk) from the fox tape-worm echinococcus multilocularis," *Int J Parasitol*, Oct 2009.
- [56] V. Gelmedin, R. Caballero-Gamiz, and K. Brehm, "Characterization and inhibition of a p38-like mitogen-activated protein kinase (mapk) from echinococcus multilocularis: antiparasitic activities of p38 mapk inhibitors," *Biochem Pharmacol*, vol. 76, pp. 1068–81, Oct 2008.
- [57] R. Zavala-Góngora, A. Kroner, P. Bernthaler, P. Knaus, and K. Brehm, "A member of the transforming growth factor-beta receptor family from echinococcus multilocularis is activated by human bone morphogenetic protein 2," *Mol Biochem Parasitol*, vol. 146, pp. 265–71, Apr 2006.
- [58] K. Epping and K. Brehm, "Echinococcus multilocularis: Molecular characterization of emsmade, a novel br-smad involved in tgf- β and bmp signaling," *Experimental parasitology*, Jul 2011.

- [59] I. Claeys, G. Simonet, J. Poels, T. V. Loy, L. Vercammen, A. D. Loof, and J. V. Broeck, "Insulin-related peptides and their conserved signal transduction pathway," *Peptides*, vol. 23, pp. 807–16, Apr 2002.
- [60] P. D. Meyts, "Insulin and its receptor: structure, function and evolution," *Bioessays*, vol. 26, pp. 1351–62, Dec 2004.
- [61] T. E. Adams, V. C. Epa, T. P. Garrett, and C. W. Ward, "Structure and function of the type 1 insulin-like growth factor receptor," *Cell Mol Life Sci*, vol. 57, pp. 1050–93, Jul 2000.
- [62] T. Lopez and D. Hanahan, "Elevated levels of igf-1 receptor convey invasive and metastatic capability in a mouse model of pancreatic islet tumorigenesis," *Cancer Cell*, vol. 1, pp. 339–53, May 2002.
- [63] H. Hartog, J. Wesseling, H. M. Boezen, and W. T. A. van der Graaf, "The insulin-like growth factor 1 receptor in cancer: old focus, new future," *Eur J Cancer*, vol. 43, pp. 1895–904, Sep 2007.
- [64] S. H. Song, S. S. McIntyre, H. Shah, J. D. Veldhuis, P. C. Hayes, and P. C. Butler, "Direct measurement of pulsatile insulin secretion from the portal vein in human subjects," *J Clin Endocrinol Metab*, vol. 85, pp. 4491–9, Dec 2000.
- [65] F. Shojaee-Moradie, J. K. Powrie, E. Sundermann, M. W. Spring, A. Schüttler, P. H. Sönksen, D. Brandenburg, and R. H. Jones, "Novel hepatoselective insulin analog: studies with a covalently linked thyroxyl-insulin complex in humans," *Diabetes Care*, vol. 23, pp. 1124–9, Aug 2000.
- [66] C. Rosen and M. Pollak, "Circulating igf-i: New perspectives for a new century," *Trends Endocrinol. Metab.*, vol. 10, pp. 136–141, May 1999.
- [67] F. P. Ottensmeyer, D. R. Beniac, R. Z. Luo, and C. C. Yip, "Mechanism of transmembrane signaling: insulin binding and the insulin receptor," *Biochemistry*, vol. 39, pp. 12103–12, Oct 2000.
- [68] I. Hirayama, H. Tamemoto, H. Yokota, S. K. Kubo, J. Wang, H. Kuwano, Y. Nagamachi, T. Takeuchi, and T. Izumi, "Insulin receptor-related receptor is expressed in pancreatic beta-cells and stimulates tyrosine phosphorylation of insulin receptor substrate-1 and -2," *Diabetes*, vol. 48, pp. 1237–44, Jun 1999.
- [69] K. Christiansen, J. Trandum-Jensen, J. Carlsen, and J. Vinten, "A model for the quaternary structure of human placental insulin receptor deduced from electron microscopy," *Proc Natl Acad Sci USA*, vol. 88, pp. 249–52, Jan 1991.
- [70] S. Seino, M. Seino, S. Nishi, and G. I. Bell, "Structure of the human insulin receptor gene and characterization of its promoter," *Proc Natl Acad Sci USA*, vol. 86, pp. 114–8, Jan 1989.

- [71] D. A. Bravo, J. B. Gleason, R. I. Sanchez, R. A. Roth, and R. S. Fuller, "Accurate and efficient cleavage of the human insulin proreceptor by the human proprotein-processing protease furin. characterization and kinetic parameters using the purified, secreted soluble protease expressed by a recombinant baculovirus," *J. Biol. Chem.*, vol. 269, pp. 25830–7, Oct 1994.
- [72] S. Seino and G. I. Bell, "Alternative splicing of human insulin receptor messenger rna," *Biochem Biophys Res Commun*, vol. 159, pp. 312–6, Feb 1989.
- [73] A. Denley, J. C. Wallace, L. J. Cosgrove, and B. E. Forbes, "The insulin receptor isoform exon 11- (ir-a) in cancer and other diseases: a review," *Horm Metab Res*, vol. 35, pp. 778–85, Jan 2003.
- [74] A. Belfiore, F. Frasca, G. Pandini, L. Sciacca, and R. Vigneri, "Insulin receptor isoforms and insulin receptor/insulin-like growth factor receptor hybrids in physiology and disease," *Endocr Rev*, vol. 30, pp. 586–623, Oct 2009.
- [75] M. A. Soos, C. E. Field, and K. Siddle, "Purified hybrid insulin/insulin-like growth factor-i receptors bind insulin-like growth factor-i, but not insulin, with high affinity," *Biochem J*, vol. 290 (Pt 2), pp. 419–26, Mar 1993.
- [76] A. Denley, L. J. Cosgrove, G. W. Booker, J. C. Wallace, and B. E. Forbes, "Molecular interactions of the igf system," *Cytokine Growth Factor Rev*, vol. 16, pp. 421–39, Jan 2005.
- [77] G. Pandini, F. Frasca, R. Mineo, L. Sciacca, R. Vigneri, and A. Belfiore, "Insulin/insulin-like growth factor i hybrid receptors have different biological characteristics depending on the insulin receptor isoform involved," *J. Biol. Chem.*, vol. 277, pp. 39684–95, Oct 2002.
- [78] M. F. White and C. R. Kahn, "The insulin signaling system," *J. Biol. Chem.*, vol. 269, pp. 1–4, Jan 1994.
- [79] R. Z. Luo, D. R. Beniac, A. Fernandes, C. C. Yip, and F. P. Ottensmeyer, "Quaternary structure of the insulin-insulin receptor complex," *Science*, vol. 285, pp. 1077–80, Aug 1999.
- [80] M. F. White, S. E. Shoelson, H. Keutmann, and C. R. Kahn, "A cascade of tyrosine autophosphorylation in the beta-subunit activates the phosphotransferase of the insulin receptor," *J. Biol. Chem.*, vol. 263, pp. 2969–80, Feb 1988.
- [81] M. F. White, "The irs-signalling system: a network of docking proteins that mediate insulin action," *Mol Cell Biochem*, vol. 182, pp. 3–11, May 1998.
- [82] T. Sasaoka and M. Kobayashi, "The functional significance of shc in insulin signaling as a substrate of the insulin receptor," *Endocr J*, vol. 47, pp. 373–81, Aug 2000.

- [83] A. R. Saltiel and C. R. Kahn, "Insulin signalling and the regulation of glucose and lipid metabolism," *Nature*, vol. 414, pp. 799–806, Dec 2001.
- [84] J. Avruch, A. Khokhlatchev, J. M. Kyriakis, Z. Luo, G. Tzivion, D. Vavvas, and X. F. Zhang, "Ras activation of the raf kinase: tyrosine kinase recruitment of the map kinase cascade," *Recent Prog Horm Res*, vol. 56, pp. 127–55, Jan 2001.
- [85] K. S. Ravichandran, U. Lorenz, S. E. Shoelson, and S. J. Burakoff, "Interaction of shc with grb2 regulates association of grb2 with msos," *Mol Cell Biol*, vol. 15, pp. 593–600, Feb 1995.
- [86] T. Ueda, R. Watanabe-Fukunaga, H. Fukuyama, S. Nagata, and R. Fukunaga, "Mnk2 and mnk1 are essential for constitutive and inducible phosphorylation of eukaryotic initiation factor 4e but not for cell growth or development," *Mol Cell Biol*, vol. 24, pp. 6539–49, Aug 2004.
- [87] H. J. Schaeffer and M. J. Weber, "Mitogen-activated protein kinases: specific messages from ubiquitous messengers," *Mol Cell Biol*, vol. 19, pp. 2435–44, Apr 1999.
- [88] M. Hanada, J. Feng, and B. A. Hemmings, "Structure, regulation and function of pkb/akt—a major therapeutic target," *Biochim Biophys Acta*, vol. 1697, pp. 3–16, Mar 2004.
- [89] A. G. Bader, S. Kang, L. Zhao, and P. K. Vogt, "Oncogenic pi3k deregulates transcription and translation," *Nat Rev Cancer*, vol. 5, pp. 921–9, Dec 2005.
- [90] A. M. Valverde, M. Benito, and M. Lorenzo, "The brown adipose cell: a model for understanding the molecular mechanisms of insulin resistance," *Acta Physiol Scand*, vol. 183, pp. 59–73, Jan 2005.
- [91] S. H. Um, D. D'Alessio, and G. Thomas, "Nutrient overload, insulin resistance, and ribosomal protein s6 kinase 1, s6k1," *Cell Metab*, vol. 3, pp. 393–402, Jun 2006.
- [92] Q. Wu and M. R. Brown, "Signaling and function of insulin-like peptides in insects," *Annu Rev Entomol*, vol. 51, pp. 1–24, Jan 2006.
- [93] S. B. Pierce, M. Costa, R. Wisotzkey, S. Devadhar, S. A. Homburger, A. R. Buchman, K. C. Ferguson, J. Heller, D. M. Platt, A. A. Pasquinelli, L. X. Liu, S. K. Doberstein, and G. Ruvkun, "Regulation of daf-2 receptor signaling by human insulin and ins-1, a member of the unusually large and diverse c. elegans insulin gene family," *Genes Dev*, vol. 15, pp. 672–86, Mar 2001.
- [94] R. Fernandez-Almonacid and O. M. Rosen, "Structure and ligand specificity of the drosophila melanogaster insulin receptor," *Mol Cell Biol*, vol. 7, pp. 2718–27, Aug 1987.
- [95] M. Dlakić, "A new family of putative insulin receptor-like proteins in c. elegans," *Curr Biol*, vol. 12, pp. R155–7, Mar 2002.

- [96] P. Narbonne and R. Roy, "Regulation of germline stem cell proliferation downstream of nutrient sensing," *Cell division*, vol. 1, p. 29, Jan 2006.
- [97] R. L. Seecof and S. Dewhurst, "Insulin is a drosophila hormone and acts to enhance the differentiation of embryonic drosophila cells," *Cell Differ*, vol. 3, pp. 63–70, Jun 1974.
- [98] A. Cornils, M. Gloeck, Z. Chen, Y. Zhang, and J. Alcedo, "Specific insulin-like peptides encode sensory information to regulate distinct developmental processes," *Development*, vol. 138, pp. 1183–93, Mar 2011.
- [99] N. Khayath, J. Vicogne, A. Ahier, A. BenYounes, C. Konrad, J. Trolet, E. Viscogliosi, K. Brehm, and C. Dissous, "Diversification of the insulin receptor family in the helminth parasite schistosoma mansoni," *FEBS J.*, vol. 274, pp. 659–76, Feb 2007.
- [100] H. You, W. Zhang, M. K. Jones, G. N. Gobert, J. Mulvenna, G. Rees, M. Spanevello, D. Blair, M. Duke, K. Brehm, and D. P. McManus, "Cloning and characterisation of schistosoma japonicum insulin receptors," *PLoS ONE*, vol. 5, p. e9868, Jan 2010.
- [101] L. Canclini and A. Esteves, "In vivo response of mesocestoides vogae to human insulin," *Parasitology*, vol. 136, pp. 203–9, Feb 2009.
- [102] A. Ahier, N. Khayath, J. Vicogne, and C. Dissous, "Insulin receptors and glucose uptake in the human parasite schistosoma mansoni," *Parasite*, vol. 15, pp. 573–9, Dec 2008.
- [103] G. Escobedo, M. C. Romano, and J. Morales-Montor, "Differential in vitro effects of insulin on taenia crassiceps and taenia solium cysticerci," *J Helminthol*, vol. 83, pp. 403–12, Dec 2009.
- [104] B. M. Sefton, T. Hunter, and W. C. Raschke, "Evidence that the abelson virus protein functions in vivo as a protein kinase that phosphorylates tyrosine," *Proc Natl Acad Sci USA*, vol. 78, pp. 1552–6, Mar 1981.
- [105] Y. Ben-Neriah, G. Q. Daley, A. M. Mes-Masson, O. N. Witte, and D. Baltimore, "The chronic myelogenous leukemia-specific p210 protein is the product of the bcr/abl hybrid gene," *Science*, vol. 233, pp. 212–4, Jul 1986.
- [106] J. Colicelli, "Abl tyrosine kinases: evolution of function, regulation, and specificity," *Sci Signal*, vol. 3, p. re6, Jan 2010.
- [107] S. P. Goff, E. Gilboa, O. N. Witte, and D. Baltimore, "Structure of the abelson murine leukemia virus genome and the homologous cellular gene: studies with cloned viral dna," *Cell*, vol. 22, pp. 777–85, Dec 1980.
- [108] R. Perego, D. Ron, and G. D. Kruh, "Arg encodes a widely expressed 145 kda protein-tyrosine kinase," *Oncogene*, vol. 6, pp. 1899–902, Oct 1991.

- [109] R. A. V. Etten, P. Jackson, and D. Baltimore, "The mouse type iv c-abl gene product is a nuclear protein, and activation of transforming ability is associated with cytoplasmic localization," *Cell*, vol. 58, pp. 669–78, Aug 1989.
- [110] C. L. Sawyers, J. McLaughlin, A. Goga, M. Havlik, and O. Witte, "The nuclear tyrosine kinase c-abl negatively regulates cell growth," *Cell*, vol. 77, pp. 121–31, Apr 1994.
- [111] P. J. Welch and J. Y. Wang, "A c-terminal protein-binding domain in the retinoblastoma protein regulates nuclear c-abl tyrosine kinase in the cell cycle," *Cell*, vol. 75, pp. 779–90, Nov 1993.
- [112] P. W. Manley, S. W. Cowan-Jacob, E. Buchdunger, D. Fabbro, G. Fendrich, P. Furet, T. Meyer, and J. Zimmermann, "Imatinib: a selective tyrosine kinase inhibitor," *Eur J Cancer*, vol. 38 Suppl 5, pp. S19–27, Sep 2002.
- [113] F. B. Gertler, J. S. Doctor, and F. M. Hoffmann, "Genetic suppression of mutations in the drosophila abl proto-oncogene homolog," *Science*, vol. 248, pp. 857–60, May 1990.
- [114] M. J. Henkemeyer, F. B. Gertler, W. Goodman, and F. M. Hoffmann, "The drosophila abelson proto-oncogene homolog: identification of mutant alleles that have pleiotropic effects late in development," *Cell*, vol. 51, pp. 821–8, Dec 1987.
- [115] W. Li, Y. Li, and F.-B. Gao, "Abelson, enabled, and p120 catenin exert distinct effects on dendritic morphogenesis in drosophila," *Dev Dyn*, vol. 234, pp. 512–22, Nov 2005.
- [116] E. E. Grevenkoed, J. J. Loureiro, T. L. Jesse, and M. Peifer, "Abelson kinase regulates epithelial morphogenesis in drosophila," *J Cell Biol*, vol. 155, pp. 1185–98, Dec 2001.
- [117] M. Sheffield, T. Loveless, J. Hardin, and J. Pettitt, "C. elegans enabled exhibits novel interactions with n-wasp, abl, and cell-cell junctions," *Curr Biol*, vol. 17, pp. 1791–6, Oct 2007.
- [118] K. L. Moore and W. H. Kinsey, "Identification of an abl-related protein tyrosine kinase in the cortex of the sea urchin egg: possible role at fertilization," *Dev Biol*, vol. 164, pp. 444–55, Aug 1994.
- [119] S. Beckmann and C. G. Grevelding, "Imatinib has a fatal impact on morphology, pairing stability and survival of adult schistosoma mansoni in vitro," *Int J Parasitol*, vol. 40, pp. 521–6, Apr 2010.
- [120] S. Beckmann, S. Hahnel, K. Cailliau, M. Vanderstraete, E. Browaeys, C. Dissous, and C. G. Grevelding, "Characterization of the src/abl hybrid-kinase smtk6 of schistosoma mansoni," *J. Biol. Chem.*, Oct 2011.
- [121] S. Beckmann, C. Buro, C. Dissous, J. Hirzmann, and C. G. Grevelding, "The syk kinase smtk4 of schistosoma mansoni is involved in the regulation of spermatogenesis and oogenesis," *PLoS Pathog*, vol. 6, p. e1000769, Feb 2010.

- [122] O. Hantschel, U. Rix, and G. Superti-Furga, "Target spectrum of the bcr-abl inhibitors imatinib, nilotinib and dasatinib," *Leuk Lymphoma*, vol. 49, pp. 615–9, Apr 2008.
- [123] J. Groffen, J. R. Stephenson, N. Heisterkamp, A. de Klein, C. R. Bartram, and G. Grosveld, "Philadelphia chromosomal breakpoints are clustered within a limited region, bcr, on chromosome 22," *Cell*, vol. 36, pp. 93–9, Jan 1984.
- [124] C. Konrad, "Molecular analysis of insulin signaling mechanisms in echinococcus multilocularis and their role in the host-parasite interaction in the alveolar echinococcosis," *Dissertation zur Erlangung des naturwissenschaftlichen Doktorgrades der Bayerischen Julius-Maximilians-Universität Würzburg*, 2007.
- [125] S. Hemer, "Molekulargenetische und zellbiologische untersuchungen zum insulin-signaling in echinococcus multilocularis," *Diplomarbeit an er Bayerischen Julius-Maximilians-Universität Würzburg*, 2008.
- [126] S. Reuter, A. Buck, B. Manfras, W. Kratzer, H. M. Seitz, K. Darge, S. N. Reske, and P. Kern, "Structured treatment interruption in patients with alveolar echinococcosis," *Hepatology*, vol. 39, pp. 509–17, Feb 2004.
- [127] J. El-On, "Benzimidazole treatment of cystic echinococcosis," *Acta Trop*, vol. 85, pp. 243–52, Feb 2003.
- [128] C. Dissous, A. Ahier, and N. Khayath, "Protein tyrosine kinases as new potential targets against human schistosomiasis," *Bioessays*, vol. 29, pp. 1281–8, Dec 2007.
- [129] M.-H. Abdulla, K.-C. Lim, M. Sajid, J. H. McKerrow, and C. R. Caffrey, "Schistosomiasis mansoni: novel chemotherapy using a cysteine protease inhibitor," *PLoS Med*, vol. 4, p. e14, Jan 2007.
- [130] M. Spiliotis, "Untersuchungen zur in vitro kultivierung und charakterisierung von map-kinase-kaskade-komponenten des fuchsbandwurmes echinococcus multilocularis," *Dissertation zu Erlangung des naturwissenschaftlichen Doktorgrades der Bayerischen Julius-Maximilians Universität Würzburg*, 2006.
- [131] J. D. Smyth, A. B. Howkins, and M. Barton, "Factors controlling the differentiation of the hydatid organism, echinococcus granulosus, into cystic or strobilar stages in vitro," *Nature*, vol. 211, pp. 1374–7, Sep 1966.
- [132] S. al Nahhas, C. Gabrion, S. Walbaum, and A. F. Petavy, "In vivo cultivation of echinococcus multilocularis protoscoleces in micropore chambers," *Int J Parasitol*, vol. 21, pp. 383–6, Jun 1991.
- [133] E. P. Feener, J. M. Backer, G. L. King, P. A. Wilden, X. J. Sun, C. R. Kahn, and M. F. White, "Insulin stimulates serine and tyrosine phosphorylation in the juxtamem-

- brane region of the insulin receptor,” *J. Biol. Chem.*, vol. 268, pp. 11256–64, May 1993.
- [134] P. D. Olson, M. Zarowiecki, F. Kiss, and K. Brehm, “Cestode genomics - progress and prospects for advancing basic and applied aspects of flatworm biology,” *Parasite Immunol*, vol. 34, pp. 130–50, Jan 2012.
- [135] M. P. Wymann and L. Pirola, “Structure and function of phosphoinositide 3-kinases,” *Biochim Biophys Acta*, vol. 1436, pp. 127–50, Dec 1998.
- [136] E. H. Walker, M. E. Pacold, O. Perisic, L. Stephens, P. T. Hawkins, M. P. Wymann, and R. L. Williams, “Structural determinants of phosphoinositide 3-kinase inhibition by wortmannin, ly294002, quercetin, myricetin, and staurosporine,” *Mol Cell*, vol. 6, pp. 909–19, Oct 2000.
- [137] A. C. Gingras, B. Raught, S. P. Gygi, A. Niedzwiecka, M. Miron, S. K. Burley, R. D. Polakiewicz, A. Wyslouch-Cieszynska, R. Aebersold, and N. Sonenberg, “Hierarchical phosphorylation of the translation inhibitor 4e-bp1,” *Genes Dev*, vol. 15, pp. 2852–64, Nov 2001.
- [138] R. Saperstein, P. P. Vicario, H. V. Strout, E. Brady, E. E. Slater, W. J. Greenlee, D. L. Ondeyka, A. A. Patchett, and D. G. Hangauer, “Design of a selective insulin receptor tyrosine kinase inhibitor and its effect on glucose uptake and metabolism in intact cells,” *Biochemistry*, vol. 28, pp. 5694–701, Jun 1989.
- [139] C. J. Vlahos, W. F. Matter, K. Y. Hui, and R. F. Brown, “A specific inhibitor of phosphatidylinositol 3-kinase, 2-(4-morpholinyl)-8-phenyl-4h-1-benzopyran-4-one (ly294002),” *J. Biol. Chem.*, vol. 269, pp. 5241–8, Feb 1994.
- [140] V. Gelmedin, “Targeting flatworm signaling cascades for the development of novel anthelmintic drugs,” *Doctoral thesis for a doctoral degree at the Graduate School of Life Sciences, Julius-Maximilians-Universität Würzburg, Section Infection and Immunity*, 2008.
- [141] W. A. Bovenberg, J. G. Dauwerse, H. M. Pospiech, S. C. V. Buul-Offers, J. L. V. den Brande, and J. S. Sussenbach, “Expression of recombinant human insulin-like growth factor i in mammalian cells,” *Mol Cell Endocrinol*, vol. 74, pp. 45–59, Nov 1990.
- [142] O. Laub and W. J. Rutter, “Expression of the human insulin gene and cDNA in a heterologous mammalian system,” *J. Biol. Chem.*, vol. 258, pp. 6043–50, May 1983.
- [143] H. Bekkari, D. Sekkat, J. Straczek, K. Hess, F. Belleville-Nabet, and P. Nabet, “Expression of secreted recombinant human insulin-like growth factor-ii (igf-ii) in chinese hamster ovary cells,” *J Biotechnol*, vol. 36, pp. 75–83, Jul 1994.

- [144] P. Jackson and D. Baltimore, "N-terminal mutations activate the leukemogenic potential of the myristoylated form of c-abl," *EMBO J*, vol. 8, pp. 449–56, Feb 1989.
- [145] M. D. Resh, "Myristylation and palmitoylation of src family members: the fats of the matter," *Cell*, vol. 76, pp. 411–3, Feb 1994.
- [146] S. R. Hubbard, "Src autoinhibition: let us count the ways," *Nat Struct Biol*, vol. 6, pp. 711–4, Aug 1999.
- [147] S. Hemer and K. Brehm, "In vitro efficacy of the anti-cancer drug imatinib on echinococcus multilocularis larvae," *International Journal of Antimicrobial Agents*, 2012.
- [148] B. Nagar, W. G. Bornmann, P. Pellicena, T. Schindler, D. R. Veach, W. T. Miller, B. Clarkson, and J. Kuriyan, "Crystal structures of the kinase domain of c-abl in complex with the small molecule inhibitors pd173955 and imatinib (sti-571)," *Cancer Res*, vol. 62, pp. 4236–43, Aug 2002.
- [149] M. Sajid and J. H. McKerrow, "Cysteine proteases of parasitic organisms," *Mol Biochem Parasitol*, vol. 120, pp. 1–21, Mar 2002.
- [150] Y. Sako, H. Yamasaki, K. Nakaya, M. Nakao, and A. Ito, "Cloning and characterization of cathepsin l-like peptidases of echinococcus multilocularis metacestodes," *Mol Biochem Parasitol*, vol. 154, pp. 181–9, Aug 2007.
- [151] I. D. Kerr, J. H. Lee, C. J. Farady, R. Marion, M. Rickert, M. Sajid, K. C. Pandey, C. R. Caffrey, J. Legac, E. Hansell, J. H. McKerrow, C. S. Craik, P. J. Rosenthal, and L. S. Brinen, "Vinyl sulfones as antiparasitic agents and a structural basis for drug design," *J. Biol. Chem.*, vol. 284, pp. 25697–703, Sep 2009.
- [152] Y. Sako, K. Nakaya, and A. Ito, "Echinococcus multilocularis: identification and functional characterization of cathepsin b-like peptidases from metacestode," *Exp Parasitol*, vol. 127, pp. 693–701, Mar 2011.
- [153] S. Riedl, "Molekulare charakterisierung einer c-jun n-terminalen kinase (jnk) aus echinococcus multilocularis," *Diplomarbeit an der Fakultät für Biologie der Bayerischen Julius-Maximilians-Universität Würzburg*, 2009.
- [154] A. Bosman and K. N. Mendis, "A major transition in malaria treatment: the adoption and deployment of artemisinin-based combination therapies," *Am J Trop Med Hyg*, vol. 77, pp. 193–7, Dec 2007.
- [155] N. L. Komarova, A. A. Katouli, and D. Wodarz, "Combination of two but not three current targeted drugs can improve therapy of chronic myeloid leukemia," *PLoS ONE*, vol. 4, p. e4423, Jan 2009.

- [156] K. Aktories and H. Barth, "Clostridium botulinum c2 toxin—new insights into the cellular up-take of the actin-*adp*-ribosylating toxin," *Int J Med Microbiol*, vol. 293, pp. 557–64, Apr 2004.
- [157] J. Fahrner, R. Plunien, U. Binder, T. Langer, H. Seliger, and H. Barth, "Genetically engineered clostridial c2 toxin as a novel delivery system for living mammalian cells," *Bioconjug Chem*, vol. 21, pp. 130–9, Jan 2010.
- [158] J. Fahrner, J. Funk, M. Lillich, and H. Barth, "Internalization of biotinylated compounds into cancer cells is promoted by a molecular trojan horse based upon core streptavidin and clostridial c2 toxin," *Naunyn-Schmiedeberg's archives of pharmacology*, vol. 383, pp. 263–73, Mar 2011.
- [159] S. Förster, D. Günthel, F. Kiss, and K. Brehm, "Molecular characterisation of a serum-responsive, daf-12-like nuclear hormone receptor of the fox-tapeworm *echinococcus multilocularis*," *J Cell Biochem*, vol. 112, pp. 1630–42, Jun 2011.
- [160] J. Dupont and D. LeRoith, "Insulin and insulin-like growth factor i receptors: similarities and differences in signal transduction," *Horm Res*, vol. 55 Suppl 2, pp. 22–6, Jan 2001.
- [161] C. Konrad, "Molekulare charakterisierung und funktionsanalyse einer rezeptorkinase der insulin/igf – familie des fuchsbandwurms *echinococcus multilocularis*," *Diplomarbeit an der Fakultät für Biologie der Julius-Maximilians-Universität Würzburg*, 2002.
- [162] L. Wei, S. R. Hubbard, W. A. Hendrickson, and L. Ellis, "Expression, characterization, and crystallization of the catalytic core of the human insulin receptor protein-tyrosine kinase domain," *J. Biol. Chem.*, vol. 270, pp. 8122–30, Apr 1995.
- [163] A. Pautsch, A. Zoephel, H. Ahorn, W. Spevak, R. Hauptmann, and H. Nar, "Crystal structure of bisphosphorylated igf-1 receptor kinase: insight into domain movements upon kinase activation," *Structure*, vol. 9, pp. 955–65, Oct 2001.
- [164] P. A. Wilden, C. R. Kahn, K. Siddle, and M. F. White, "Insulin receptor kinase domain autophosphorylation regulates receptor enzymatic function," *J. Biol. Chem.*, vol. 267, pp. 16660–8, Aug 1992.
- [165] V. L. Grandage, R. E. Gale, D. C. Linch, and A. Khwaja, "Pi3-kinase/akt is constitutively active in primary acute myeloid leukaemia cells and regulates survival and chemoresistance via nf-kappab, mapkinase and p53 pathways," *Leukemia*, vol. 19, pp. 586–94, Apr 2005.
- [166] C. gen Xing, B. song Zhu, H. hui Liu, F. Lin, H. hua Yao, Z. qin Liang, and Z. hong Qin, "Ly294002 induces p53-dependent apoptosis of sgc7901 gastric cancer cells," *Acta Pharmacol Sin*, vol. 29, pp. 489–98, Apr 2008.

- [167] D. Kong and T. Yamori, "Phosphatidylinositol 3-kinase inhibitors: promising drug candidates for cancer therapy," *Cancer Sci*, vol. 99, pp. 1734–40, Sep 2008.
- [168] L. Hu, C. Zaloudek, G. B. Mills, J. Gray, and R. B. Jaffe, "In vivo and in vitro ovarian carcinoma growth inhibition by a phosphatidylinositol 3-kinase inhibitor (ly294002)," *Clin Cancer Res*, vol. 6, pp. 880–6, Mar 2000.
- [169] A. C. Cumino, P. Lamenza, and G. M. Denegri, "Identification of functional fkb protein in *Echinococcus granulosus*: its involvement in the protoscolicidal action of rapamycin derivatives and in calcium homeostasis," *Int J Parasitol*, vol. 40, pp. 651–61, May 2010.
- [170] G. M. Leclerc, G. J. Leclerc, G. Fu, and J. C. Barredo, "Akt-induced activation of akt by aicar is mediated by igf-1r dependent and independent mechanisms in acute lymphoblastic leukemia," *Journal of molecular signaling*, vol. 5, p. 15, Jan 2010.
- [171] H. H. Garcia, O. H. D. Brutto, and C. W. G. in Peru, "Neurocysticercosis: updated concepts about an old disease," *Lancet Neurol*, vol. 4, pp. 653–61, Oct 2005.
- [172] M. W. Deininger, J. M. Goldman, and J. V. Melo, "The molecular biology of chronic myeloid leukemia," *Blood*, vol. 96, pp. 3343–56, Nov 2000.
- [173] M. W. Deininger, J. M. Goldman, N. Lydon, and J. V. Melo, "The tyrosine kinase inhibitor cgp57148b selectively inhibits the growth of bcr-abl-positive cells," *Blood*, vol. 90, pp. 3691–8, Nov 1997.
- [174] A. Popow-Woźniak, A. Woźniakowska, L. Kaczmarek, M. Malicka-Błaszkiwicz, and D. Nowak, "Apoptotic effect of imatinib on human colon adenocarcinoma cells: influence on actin cytoskeleton organization and cell migration," *Eur J Pharmacol*, vol. 667, pp. 66–73, Sep 2011.
- [175] C. Tarn, Y. V. Skorobogatko, T. Taguchi, B. Eisenberg, M. von Mehren, and A. K. Godwin, "Therapeutic effect of imatinib in gastrointestinal stromal tumors: Akt signaling dependent and independent mechanisms," *Cancer Res*, vol. 66, pp. 5477–86, May 2006.
- [176] B. J. Druker, M. Talpaz, D. J. Resta, B. Peng, E. Buchdunger, J. M. Ford, N. B. Lydon, H. Kantarjian, R. Capdeville, S. Ohno-Jones, and C. L. Sawyers, "Efficacy and safety of a specific inhibitor of the bcr-abl tyrosine kinase in chronic myeloid leukemia," *N Engl J Med*, vol. 344, pp. 1031–7, Apr 2001.
- [177] A. Li-Wan-Po, P. Farndon, C. Craddock, and M. Griffiths, "Integrating pharmacogenetics and therapeutic drug monitoring: optimal dosing of imatinib as a case-example," *Eur J Clin Pharmacol*, vol. 66, pp. 369–74, Apr 2010.
- [178] A. Hemphill, B. Stadelmann, S. Scholl, J. Müller, M. Spiliotis, N. Müller, B. Gottstein, and M. Siles-Lucas, "Echinococcus metacestodes as laboratory models for the screen-

- ing of drugs against cestodes and trematodes,” *Parasitology*, vol. 137, pp. 569–87, Mar 2010.
- [179] J. C. Engel, P. S. Doyle, I. Hsieh, and J. H. McKerrow, “Cysteine protease inhibitors cure an experimental trypanosoma cruzi infection,” *J Exp Med*, vol. 188, pp. 725–34, Aug 1998.
- [180] W. Jacobsen, U. Christians, and L. Z. Benet, “In vitro evaluation of the disposition of a novel cysteine protease inhibitor,” *Drug Metab Dispos*, vol. 28, pp. 1343–51, Nov 2000.
- [181] C. R. Caffrey, J. H. McKerrow, J. P. Salter, and M. Sajid, “Blood ’n’ guts: an update on schistosome digestive peptidases,” *Trends Parasitol*, vol. 20, pp. 241–8, May 2004.
- [182] J. C. Engel, K. K. H. Ang, S. Chen, M. R. Arkin, J. H. McKerrow, and P. S. Doyle, “Image-based high-throughput drug screening targeting the intracellular stage of trypanosoma cruzi, the agent of chagas’ disease,” *Antimicrob Agents Chemother*, vol. 54, pp. 3326–34, Aug 2010.
- [183] J. J. Vermeire, L. D. Lantz, and C. R. Caffrey, “Cure of hookworm infection with a cysteine protease inhibitor,” *PLoS neglected tropical diseases*, vol. 6, no. 7, 2012.
- [184] S. Carboni, A. Hiver, C. Szyndralewicz, P. Gaillard, J.-P. Gotteland, and P.-A. Vitte, “As601245 (1,3-benzothiazol-2-yl (2-[[2-(3-pyridinyl) ethyl] amino]-4 pyrimidinyl) acetonitrile): a c-jun nh₂-terminal protein kinase inhibitor with neuroprotective properties,” *J Pharmacol Exp Ther*, vol. 310, pp. 25–32, Jul 2004.
- [185] G. J. Gutierrez, T. Tsuji, J. V. Cross, R. J. Davis, D. J. Templeton, W. Jiang, and Z. A. Ronai, “Jnk-mediated phosphorylation of cdc25c regulates cell cycle entry and g(2)/m dna damage checkpoint,” *J. Biol. Chem.*, vol. 285, pp. 14217–28, May 2010.
- [186] J. Tasaki, N. Shibata, T. Sakurai, K. Agata, and Y. Umesono, “Role of c-jun n-terminal kinase activation in blastema formation during planarian regeneration,” *Development, growth & differentiation*, Mar 2011.
- [187] S. Reuter, M. Merkle, K. Brehm, P. Kern, and B. Manfras, “Effect of amphotericin b on larval growth of echinococcus multilocularis,” *Antimicrob Agents Chemother*, vol. 47, pp. 620–5, Feb 2003.
- [188] B. Stadelmann, S. Scholl, J. Müller, and A. Hemphill, “Application of an in vitro drug screening assay based on the release of phosphoglucose isomerase to determine the structure-activity relationship of thiazolides against echinococcus multilocularis metacestodes,” *The Journal of antimicrobial chemotherapy*, Jan 2010.
- [189] M. Stettler, M. Siles-Lucas, E. Sarciron, P. Lawton, B. Gottstein, and A. Hemphill, “Echinococcus multilocularis alkaline phosphatase as a marker for metacestode

- damage induced by in vitro drug treatment with albendazole sulfoxide and albendazole sulfone,” *Antimicrob Agents Chemother*, vol. 45, pp. 2256–62, Aug 2001.
- [190] A. Cerbone, C. Toaldo, S. Pizzimenti, P. Pettazzoni, C. Dianzani, R. Minelli, E. Ciamporcero, G. Roma, M. U. Dianzani, R. Canaparo, C. Ferretti, and G. Barrera, “As601245, an anti-inflammatory jnk inhibitor, and clofibrate have a synergistic effect in inducing cell responses and in affecting the gene expression profile in caco-2 colon cancer cells,” *PPAR Res*, vol. 2012, p. 269751, Jan 2012.
- [191] M. Eckhardt, H. Barth, D. Blöcker, and K. Aktories, “Binding of clostridium botulinum c2 toxin to asparagine-linked complex and hybrid carbohydrates,” *J. Biol. Chem.*, vol. 275, pp. 2328–34, Jan 2000.

A Supplementary

A.1 Analysis of ILP homologues

Tab. A.1: Homologues of insulin and ILPs in other helminths. *Sj*: *S. japonicum*; *Hm*: *H. microstoma*; *Eg*: *E. granulosus*; *Ts*: *T. solium*

Name	Systematic Name	Location
SjIns	Sjp_0020480	supercontig SJC_S000110 : 408491-417266
HmILP1	HmN_000294900	supercontig pathogen_HYM_scaffold_33 : 367620-368253
HmILP2	HmN_000294800	supercontig pathogen_HYM_scaffold_33 : 350421-350945
EgILP1		pathogen_EMU_contig_60709 : 60405-603737
EgILP2		pathogen_EMU_contig_60709 : 589375-585827
TsILP1		contig_11296: 31221-30865
TsILP2		contig_11296 : 50023-49709

A.2 Sequences

Start-, stopcodons and putative poly-A signals are highlighted in grey.

4E-BP

Full length cDNA sequence of *em4e-bp*

```
1 GTCACCTAAA CCAGAGTAAG CAACCGCTCT GCCCACTAGA CCGCTGGCGG TCAATTTGGT ACCTCCTAGC
71 CCTCTGCAGT GTTTTGTCTT CTGCATTTCA ACTAGGCTCG TAAATCGCAT CCAATCGCGG TCCTGATGGT
141 ATCCCCTTCC GAAGATTAAA AGTTACTGAT CCTTCTCAGA TTCCTAATGA TTACAGTACA ACTCCAGGTG
211 GGAGCATATT CAGCACCACC CCAGGGGGCA CTCGAATCTT CTACGATCGT GACACAATGC TGATGTGCAA
281 AAATTCACCG ATTGCACGTT CACCACCAC CGACATGGTA TGTCGACCAG GGATCACCTG TCCGGCCACA
351 TCGCTGGCG AGTGCCGTCT TCCC GCCCG ACTGCCAAA AGCCCGCAA GAACACTCGT CAGGAACATG
421 CTAGTGTACA AAAAAGTGAC GAAGGGCCTT TCGACATTGA CTTGTCAGGG AAGAGGTGCC ACTCCAGTAT
491 GCAAACACT TGGTGAAAAA GAAAGAATAC AAAGCAAACA AGTGTAGTAG GTTTTTTCAT ACCTCGCCAC
561 CACCTTTGAT AGCCATCCAT GCGTGCAAAC CCACAAATGA AGAGACAAAC TTTGCGATGC AATCGCTGTT
631 AAAGAAGCGC CCGCTCCATT TAGCTATCCC AAAAGCACCC TTATGAATAT TTATGCCTTT TTGTGAGTTT
701 ACCTTCTCCC AAATGCCTCT ACCAGCTTGC TATGCTTGCT TTTGTGAATA TGTGTATACA TTTGAGAGGA
771 ATTGAGTTTT TATATCACTG AAAAAAAAAA AA
```

A Supplementary

Putative amino acid sequence of Em4E-BP

```
1 MASNRGPDGI PFRRLKVTDP SQIPNDYSTT PGGSIFFSTP GGTRIFYDRD TMLMCKNSPI ARSPPTDMVC
71 RPGITCPATC AGECLPAAT AQKPAKNTRQ EHASVQKSDE GPFIDIDL
```

EmAbl1

Full length cDNA sequence of *emabl1*

```
1 CCTAGAATTG AAAGGCGATG AAAGTAGGGG TTTTCTGAGT TGTGGCGAAA ATGGGTGGTA GTATTGGTAA
71 GCCGGCCTCT TCGAAGGAGG GATCTGAAAA GGTGGATTTA TCGCTGAGCT TTAATCAGCA GCCGGATGAA
141 ATTTCTACTG GTGGCGAATG TGAAAAGTCT GCTCCTGTTA AAAAACAGAT TCTTTCTGTC ACCCAGAATT
211 TCGAAACGTC TGGTCTGGTG GAGCAGTGTA TTATGATCGT TCTCTATGAT TTTTCAGCTA CATTGGACTC
281 TCAACTTACT GTTAAACGAG GTGAGATCGT CCGTCTCCTG AGCTACAGCC CAGCTGGTGA CTGGTCTGAG
351 GTCGAAGCGC CTTCCCATCT GCCCAATCGA ACACCGCGCG TGCCCTGGGC GGGAGCCGGT GGGTGGGTGC
421 GCGGTTGGGT ACCCACCAGC TACCTCACAG AGCATGTGCG TCCTCCACGG GTTGGTGGAA TTGGTAGTGG
491 TACCAATGGG TGGCGAAGGG TGGGAGATGA AGAGGAGGCT GGCGCAGCGG CAGCAACGAT GGCTTACCCT
561 TGGTACCACG GTGCCGTCTC GCGTCAGGCC GCTGAACAGC TCCTACGCAG CGGCATCACT GGCTCCTACC
631 TCGTACGCGA ATCTGAATCG GCACCTGGAC AACTCTCTGT CACTGTGCGG AATCTGGGCC GAGTCTATCA
701 CTATCGCATC AGTCGGGATT CCTGTGGATG GACTTTCATC ACAGAGACGC ATCGCTTCC CACAGTGGTA
771 CAACTGATTC ATCATCACTC ACAAGCCGCA GATGGACTTA TTTGCCCCCT ACTCTATCCG GCCGCCCGGC
841 GCGAACAGCC ATCGGTAATG CGGGGCGCTG CCACCAATAG TGGAGCAGTC GAAGGTTGTG CTGACAGTAA
911 AGCGCGTGGC GGCTACGTTG GCTTCGACGA CTGGGAGATT GACCGCTCTG AGATCATGAT GCGCAACAAA
981 CTCGGTTGGG GTCAGTATGG TGATGTCTAC GAGGCTCTCT GGAAGCGCTA CAATTCTATC GTTGTCTGTA
1051 AGACGCTGAA GCAAGACGTG GACCTGAATC TGAATGACTT TCTTGCTGAG GCCTCAATTA TGAAGAACTT
1121 CCAGCACAAG AACCTTGTTT GATTTCTCGG CGTCTGCACT CGAGAGCCGC CCTACTACAT AGTGGCGGAG
1191 TACATGCCCC ATGGAAACCT GCTGAATTAC CTGCGCCAAC GGAGTCCAGG AGAACTCACC CCACCCATTC
1261 TCCTCTACAT GGCTGTTCAA ATCGCCTCTG GCATGGCCTA TTTGGAAGCC AACAACTTTA TTCACCGCGA
1331 TCTGGCAGCC CGCAACTGTC TAGTGGGCGA TCAGTACACT ATCAAGGTGG CCGACTTCGG CTGCGCGCGC
1401 TATATGCAAC TGCATGAGGA CACCTACACC GCCCGTAATG GGGCCAAATT CCCCATCAAG TGGACTGCCC
1471 CCGAAGGACT TGCCTATTTT CGTTTCTCCT CCAAGTCTGA TGTGTGGGCA TTTGGGGTTG TTCTTTGGGA
1541 ACTGGCCACC TACGGTCTCT CTCCCTATCC TGGTGTGGAA CTGCACGGTG TCTACCAACT TCTGGAAAAG
1611 GGTTACCGCA TGCAACGTCC TCATGGCTGT CCTGAGTCCG TTTACAGCAT TATGCTGCGA TGCTGGTCTT
1681 GGGAGGCAGC AGATCGTCCA ACGTTTTTGT CAATCAAGGC GGAATTGGAG GAAATGTGGC GAACTATCGA
1751 TATGACAGAG GCTGTAGCTC AAGAGCTGGC CACTCCGCCA GCAGCCAAA CCACGGACCA CATGCAATTC
1821 ATCACTGCCA CCTTACCAC CGCCACCACC ACCATTACCA CCGCAGTCGG TGTTGGCCCT GGTATCAACG
1891 GCGGGGGAGA AGCGATGCTG TCCTCTGTCC CCGTTTCCAT GATTGTGCGT ATGCCATCAT ACCAACAGGA
1961 TGATGACGAG GCCGAGAAG ACCCTTCTC TCCCTACAA TCCACCACCT CCTGCACCTC TTCCTTCTT
2031 GCGGCTGTCT CTTCTCCAG TGCTGCTGAA ACTGATGGTC AGGATGGTGA TGATGAAGGC GAGGAGGACT
2101 TGTGTCTCAA ATCACTTGTT GATAAGGGCG CGTTGAGCTC AACAGCCAAT TGGATCACA CGCGGACCTC
2171 TGACAGTCTC TACCAGGGCG ACTACATAGT CAGTGGTGGT GGTGGTGGAG GCGGTGGCGT TGTCGGGGCG
2241 ACACCCGCCT CTGATTTACC CTTCCGACG CACAAATCTA CCACCTGCGA TAGCCAGGTC TCCGCTCCCG
2311 CCTCCCTGCC TCCTCTCCAC CATCTCCAGC AGTTCCAACA CCATCGCAAT AGAGCCAACA ATCACAGCCA
2381 TCACTACCAC CGTCATTATC AGCACCAGCT TCAGCACTCG GAAACTGGAC GAAGCATGCC TAGACGTCGA
2451 AGCGGACCTA ATCATTGGC CGGCCAGTTC GAGGAAGGTT CCCTGCGGTG TCCGATGCGA CCGAAGGAGA
2521 AGAACATAAC ACCAGCAGAG AGCGGTGTGG GTGAGTCGAT AGTCTCAGCA GACTCGCCGG GCGGGAATAG
```

A Supplementary

2591 CAACGCAATG CAACAAGAGG AGGGGGCGGT GGTAATGGCT CCACAGCGGA GTAATCACAA GGCGGCTGCA
2661 GTGGTAGCAG TAGCAGTTGA AGCGAACAAAT TGTGTGTGA CACCTACGAG GGATATGATA TCAGAAGTGG
2731 CCCCTGATGA AAGGCGTATG CGGCTCGATG TCGAGTCAGT GACACAATTC ACTACCTGC CAGCACAGGA
2801 CCGCATCACA CGGTACTTGG AGAGTCTGGG CGAGCTCGGT GACGCGTCGG AAGAGAGGAC CCCAAAGGCC
2871 AAGGGTGGTG CACATCCACC CCACCCCT CTTCTGTCCC ATTTCCCTCC CCCTCCGCA GTACCCAC
2941 CACCACAGCC CGCACAGCAT CTTCGCAACT CCCGAATGCT GCCCACTGAA CATCGACGAA ATGCCGTGGG
3011 ACGCTCTGCC TCATGTTACC AGACTGTGTC CAGCGTGCAG CTGCTGCTGC CACCCTCCAC GACCACCACC
3081 AACGGTTCGG TGGAGACGCA AGAGAGCCTT CCAACCACCT CCACTCCTAG CCCCGCGGTG GGTGAGACTA
3151 TCACACCAC CGACGATGTC TATCAGGCAC CAACTCTAGC GCAGGACAGC AGCATTGGCG GTAATGGGG
3221 TGTGAAGGCA GCGCCAACCG CGGAAGTGTG GTCTGAAGTA GAGCAAGCGG AGCTGACCGC CTGCCTGAAT
3291 ACCCTCTCGC TGGAGGCCAC TGAACTCTCC ACTGCCTGTC CTCAACTCGC CGCCGAGTTG TCTGCCCTCT
3361 CGCTGCAACT CTCGGCCTGT CGCGGGAAGG TCGAAGCGCG CTTACGTGCC TCCGCCAACG GAGTCGGTGG
3431 CACTGCAGAG GAGAATCTCT GCTTGGCAGG CGTTGCGCAA GCTTTGCGGC ACATTCAACA AGCACTCGCA
3501 GAGATGCGCG CGCGAGTGGG AGAGGCACAA ACTCCCACCC CTTCCCTGCC GGCCCCCTCT GCTACGGCCC
3571 CTGCTGCCAC AAACGCCAAT GCTACTACCG TCTCCACCTA GAATATGTAC ATATGCATGC CTCAACGCGC
3641 ATTTACCGAC GCTGACACCA ACACCAACCT CCGCTAATTC TACTACCGGT TTAGAGTCGA ATTCTTCAAC
3711 CTTCTCGCTC CTTATGCATC TCTCTCCTTT CTTCTCTTCT CAGTTTACTA CGAACGTGCG GGTGATTGCC
3781 TGCCCTGGCA GTAGCTGTAT CATGATGGTG ATGTGGATAA TATGCGTAGC GTGATTTTGA ATTTGCCGTG
3851 CGTTACTTGG TTGGACTTCC TTCCGGGTAG TATGTATGCG AAATAAACG ATCATGCCAT ATTAATAAAAA
3921 AAAAAAAAAA A

Putative amino acid sequence of EmAbl1

1 MGSIGKPAS SKEGSEKVDL SLSFNQQPDE ISTGGECEKS APVKKQILSV TQNFETSLV EQCIMIVLYD
71 FSATLDSQLT VKRGEIVRLR SYSPAGDWSE VEAPSHLPNR TPRVPWAGAG GWVRGWVPTS YLTEHVRPPR
141 VGGIGSGTNG WRRVGDDEEA GAAAATMAYP WYHGAVSRQA AEQLLRSGIT GSYLVRESES APGQLSVTVR
211 NLGRVYHYRI SRDSCGWYFI TETHRFPTVV QLIHHHSQAA DGLICPLLYP AARREQPSVM RGAATNSGAV
281 EGCADSKGGG GYVGFDDWEI DRSEIMMRNK LGWGQYGDVY EALWKRYNSI VAVKTLKQDV DLNLNDFLAE
351 ASIMKNLQHK NLVRFGLVCT REPPYYIVAE YMPHGNNLNY LRQRSPGELT PPILLYMAVQ IASGMAYLEA
421 NNFHRDLAA RNCLVGDQYT IKVADFLAR YMQLHEDTYT ARNGAKFPK WTAPGLAYF RFSSKSDVWA
491 FGVVLWELAT YGLSPYPGVE LHGVYQLEK GYRMQRPHGC PESVYSIMLR CWSWEAADRP TFLSIKAELE
561 EMWRTIDMTE AVAQELATPP AAQTTHMQF ITATSTTATT TITTAAGVGP GINGGGEAML SSVVSMIVR
631 MPSYQDDDE AAEDPSSPSQ STTSCTSSSS AAVSSSSAAE TDGQDGDDEG EEDLCLKSLV DKGALSSTAN
701 WITTRTSDSL YQGDYIVSGG GGGGGGVVRA TPASDLPFAT HKSTTCDSQV SAPASLPPLH HLQQFQHRN
771 RANNHSHHYH RHYQHQLQHS ETGRSMRRR SGNHLAGQF EEGSLRCPMR PKEKNITPAE SGVGESIVSA
841 DSPGNSNAM QQEEGAVVMA PQRSNHKAAA VVAVAVEANN CCVTPTRDMI SEVAPDERRM RLDVESVTQF
911 TTLPAQDRIT RYLESLGELG DASEERTPKA KGAHPPHPP LLSHFPPPPP VPPPQPAQH LRNSRMLPTE
981 HRRNAVGRSA SCYQTVSSVQ LLLPPSTTTT NGSVETQESL PTTSTPSPAV GETITPTDDV YQAPTLAQDS
1051 SIGGNGGVKA APTAEVSSEV EQAELTACLN TLSLEATELS TACPQLAEEL SALSLSLQLSAC RGKVEARLRA
1121 SANGVGGTAE ENLCLAGVAQ ALRHIQQALA EMRARVEEAQ TPTPSLPAPS ATAPAAATNAN ATTVST

EmAbl2

Full length cDNA sequence of *emabl2*

1 TTCGAGGTGT TTTTGTAAT ATTTTGACTC GTGTGTTGGT GTTTTATTAA CCTAGTAGTT TGGAGGCTTA

A Supplementary

71 CTTGAGTGCC ATTAGGTCTT CGTTCTGAGT GTTACTGAT GTAAATGGT AGTCAACATG CTAAACCTAA
141 AAAGGCTGCC TCAGAAAGTG TCGACCGAAA TTTCACTTTT CGAATTAATA AGGGCAAAA GTCGAAATGT
211 GGTGATGATG GAACATCCGT TTCTTCGCTG GACGTGATGT CGGTCCCTGA CGGTGATTTA ACAGTCTGT
281 ATGATTATGA CCCTCCTGTA AATGCACATG GATCTGCTAT CGTCGTAAGA AAGGGTGATT CACTGTGGTT
351 GTACGGTCGG AGCTCCACGG GCGATTGGTT GGATGTGCTT TGTCGACGCA CAGGCGAACG CGGCTGGGA
421 CCAGTATCAT GTCTCTTCGA TCCGACTTCG TCGAAACCTC TCATCGCCTC TGGCGTGCT ACTGCCTCT
491 CCGCCCCCAG TGCTCACGTC TCCTGTCCCA GTCTGATCGG CGAGCGATGG TACCACGGCG CTATTCACCG
561 GAGCTATGCA GAATATCTTC TCAATAGCGG CATAACTGGC AGTTTCCTTG TCGCGAATC CGAGAGCAGT
631 TTCGGCAAAC TCACTCTCAG CCTCCGCTCC GACGGACGCA TCTTCCACTA CCGTATCTCC ACGGATGAGA
701 ATAACCAATT CTATGTCAAT GAGGTGAGTC GTTTCGCCAC AGTTTCGGAG CTTGTGCAGC ACCATGAGAA
771 GGTGGCAGAT GGTCTGGCCT GTCCCTTACT CTACGGCGTC TCCAAGCGGG ATCAGAATAA TCACGGCGGC
841 TTTGACTCCG ACTACGACGC CTGGGAGATC GACCGCACCG ATGTCATCAT GAAACACAAA TTGGGCTCGG
911 GCCAGTACGG TGTAGTCTAC GAGGCCATCT TCAAACCCTA TGACGTTACT GTGGCTGTGA AAACGCTTAA
981 GGAGGACATA ACTCTGCGTG ATGAATTCCT TCAGGAGGCC CGGTTGATGA AGAGCCTTCG GCATCCGAAC
1051 CTTGTTTCGTC TTTTGGGCGT CTGCACTCAA GAGCCGCCCT ACTACATAAT CACGGAATTC ATGTGCAACG
1121 GCAACTTGCT TGACTACTTG CGAATCCAGC CCCGGGATGT TCTCTCCCCT CCGGTGCTTT TGCAAATGGC
1191 CATTATGTG TGCTGCGCTA TGACCTACCT GGAGGAGCAC AATTTTATCC ACCGGGACTT GCGGCGCGC
1261 AACTGCCTAG TTGGCGAGGC AATGACCGTA AAGGTTGCCG ACTTTGGGCT AGCGCGCTAC ATGGAGCGTG
1331 ACGTGACGTA CCGGGCACGG GAAGGCGCCA AGTTTCCTAT CAAATGGACA GCACCCGAGG GCCTTGCTA
1401 CAACTGCTTC TCCATCAAGT CTGACGTCTG GGCTTTCGGC GTGCTGCTGT GGGAGATCGC GACCTACGGG
1471 GCCGCGCCGT ATCCCGGTGT GGAGTTGCAG GATGTCTATG TTCTCCTCA AAGGGGCACT CGCATGGAAG
1541 CACCTCAAGG CTGTCTGAT GCTGTCTACC AACTCATGCT TGATTGTTGG AGTTGGAACT CGGAGGACAG
1611 ACCGAGCTTT AAGGAGGTGT ACACGCGTCT TGA AACCATC CGCACCTCT CAGACATCAG CGAGGCTGTG
1681 GAACATGAGC TTCAACGCCA TCGCATTAGG ATGCCGCTC CTCCACTCCC TCCTCCGTCT CCTACAACCTG
1751 TCGCTGCCTT CACCCCACGA CGAAGCAGCA GCTGCGATCG TATAGACGAG AGCAATCTAT CCCC AACCGC
1821 CGAGATGGG AGGCGTGGT ATGCAGAGTC CTTACAGTC CAGGATGCGG TCTCAGACT AGTCGATAGT
1891 GGTGGTGGCA GTGGTAGTGA CCTCCACCAA CAACAGCAAC AGTTCTCCGC CTATCCATGT TGTCAGCAGG
1961 GCTGTATGGT CCCAGGCAAC CGATTCTCCG AGGTCTTCC GTCTTCATTG CTTCCACCTC CTCCTCTGCA
2031 CACCAACGCG GACTTTGCAG TAGTAGGAGC AGAGATTGGT GGTGCAGGTT CTTTAGGCCG CAGAAAGGCT
2101 GCTCCCCCG CACCGCCGTT GCGCACGACT ACGTTACGAG CTGATGAGCC CTGTGAAAAA GTCCTGTGT
2171 CACTCCAGGT CTCGACCGAT GATCGCCAGA CCTTCTCACA GCCCGGAGAG GAGCGCTTGC CATCGCCGCC
2241 TAACGCCGTT CTCTGTGGTG TCAATTGGCC CTCATCACGA TCTCAGAGTA GCCCTCTCT CAACAGCGAT
2311 GTGGCGGTCT CAGTGACAGC TTCAGTTCCT CGCCGCACAC CGATTCCCGT GCCACCACAG CGCACAGAGT
2381 CAACACGAAG TCAGGATTCG GAGGTGGCTG AAGGTGTCCC TAAATCGAGT CCAAGATGG GCCTGCCCTC
2451 CACCACTCAA TCTCCATCCA ATGGTCTGGC AACGGCAAGT AGTGGCAGTA CCAACAGTGA ACTTCTCTCC
2521 CGCCTGAAGC GCCAACTGGA CAATTGAGG TCCACTGACA GTCCACTCG TTCGCCCGTC CCACCCGGTG
2591 CCGCCACTGT CACCGCGGAG ATGATCCAAG CCTCGAAGTC GAAGCTTAAG GCAACCACTA CCACCACTCC
2661 TGCCACCATC ACAGCCATAG AGACCCAACC CGCACCTCT GTGCCCGCAT GGAGGGAGCT GGTGGTTCAG
2731 CGGCGTCTCA AGAATGCCGA GCCGCTGCA GGTAAGCGGA TGAGCTGGAC ACCCATGTCC AACTCTGTT
2801 CTTCTCTTC CGCCCTCAA CAACAACAGC AATCATCAA CGTGGAGGTT TTTCCAGAAG TGGTGGAGGA
2871 GGAGGAAGAG GGTGGAGAAG AACGGGAAGG AGCTCTCCA GCCATCATGT CGCAGTCGGT GACGTACACA
2941 AGCAGTTCCA CCGTGATGCC CCCATCATCG TTGGTAAGTC GTTCTCTTA CGAGCATCTG CTGCGGCAGG
3011 TGACGGATCT CTGCGCTGAT CTGAATCTGG CGAAAGTAAA TCTCCGAAT GAGCACAATA GCACATTGGT
3081 GGATCGAATT GAGGGGCTGA AACAGGCCCTG CTTGGGGTAT GCAGATGAAA TGGACTGTTC AGCCACGCA
3151 AAGTTTCGAT TCAGGGATGA GTGCGCTCGA CTACAGGCTG CGGCAGATAC CCTGCGTAGT ATATGTGGTG
3221 TTGGTGCAGG AGCAGCGGTT GGCGCAGAGC TGGGAGGTCG TCGAAAGACA TATCAGGCCG TCTACACAAC
3291 GGTAGAGGCT ATTCACCAGT CTCTATTGCG TCTGACACCT GCGGTTCTT CAAGTGACGC TGTGGAAGAA

A Supplementary

3361 TCTACAGCTC CCTCAACCCG CAGTGCCTTT GTCAGCACGG GTGTCATCTC **ATAA**AGGAGT GGTCTGAATC
3431 CATCTGTATA TACTGTGTAC ATACTTCTTT TTGTCCTCTC AAATCTCTTT CGCGTTCTCC AATATAAGTA
3501 AGGAAGTCAA ACTGCTCTGG TGCAATCTTG TCTCCTCTTT CGTCCCTCTT CTGCTTCTTT TTCCCACGAG
3571 AATGCAAACG CTGCATAGGA ACGTCCCCTT TTTTGCTTCC TAAAAATCCT CAAAAGGTAC TCGCAGCTCT
3641 ACTATTACCT CAAACCAATG TGATTCGAA TTTCGGGGTG TTTTATTAAA AAAAAAAAAA AAAAAA

Putative amino acid sequence of EmAbl2

1 MGSQHAKPKK AASESVDRNF TFRINKGKKS KCGDDGTSVS SLDVMSVPDG DLTALYDYDP PVNAHGSAIV
71 VRKGDSDLWLY GRSSTGDWLD VLCCRRTGERG WVPVSCLFDP TSSKPLIASG AATASSAPSA HVSCPSLIGE
141 RWHYGHAIHRS YAEYLLNSGI TGSFLVRESE SSFGKLTLSL RSDGRIFHYR ISTDENNQFY VNEVSRFATV
211 SELVQHHEKV ADGLACPLLY GVSKRDQNNH GGFDSYDAW EIDRTDVIMK HKLGSQYGV VYEAIKPYD
281 VTVAVKTLKE DITLRDEFIQ EARLMKSLRH PNLVRLGVC TQEPPIIIT EFMCGNLLD YLRIQPRDVL
351 SPPVLLQMAI HVCCAMTYLE EHNFIHRDLA ARNCLVGEAM TVKVADFGLA RYMERDVTYR AREGAKFPIK
421 WTAPEGLVYN CFSIKSDVWA FGVLLWEIAT YGAAPYPGVE LQDVYVLLQR GTRMEAPQGC PDAVYQLMLD
491 CWSWNSED RP SFKEVYTRLE TIRTSSEISE AVEHELQRHR IRMPPLPP PSPTTVA AFT PRRSSCDRI
561 DESNLSPTAE MGRRGHAESF TVQDAVSRLV DSGGSGSDL HQQQQF SAY PCCQQGCMVP GNRSEVFP
631 SLLPPPPLHT NADFAVVGAE IGGAGSLGRR KAAPPAPLR TTTLRADEFC EKVPVSLQVS TDDRQTSQP
701 GEERLPSPN AVLCGVNWPS SRSQSSPLN SDVAVS TAS VPRRTPIPVP PQRTESTRSQ DSEVAEGVPK
771 SSPKMGLPST TQSPSNGLAT ASSGSTNSEL SSRLKRQLDN SRSTDSPTRS PVPPGAATVT AEMIQASKSK
841 LKATTTTTTPA TITAIETQPA PSVPAWRELV VQRRLKNAEP PAGKRMSWTP MSNSCSSSA LKQQQSSNV
911 EVFPEVVEEE EEGGEEREGA LPAIMSQSVT YTSSTVMPP SSLVSRSSYE HLLRQVTDLC ADLNLAKVNL
981 PNEHNSTLVD RIEGLKQACL GYADEMDCSA HAKFRFRDEC ARLQAAADTL RSICGVGAKA AVGAELGRR
1051 KTYQAVYTTV EAIHQSLRL TPAVPSSDAV EESTAPSTRS AFVSTGVIS

EmAkt

Full length cDNA sequence of *emakt*

1 GAGTGGTTCG ATTCGCGCGT TGGGGTTTTG GAAGATTGGC TTTTGTATTG CCATTTTTCT CATTACTTGG
71 GTCGAA**ATGC** AGGTGGATGA ATCATTAAAC TGTTCAACAC CTATGGGAAC TCTAACACCC ACATCTGCAC
141 CAATGGCGGT AGACCCTTTA TCTTCCTTTG TACAGTTCCA ATCCGCTTCC ATGTCCCAA TTCCCTGTAA
211 TACGCCGCAA TTTTCGAATC CCTCTACAGT TTCCTCCCTT GTTCCCGGAG CCGGCACCCC GTGTGCGGGT
281 TTAAGTCAGG AGCACTTTGT TCCCCACGCT CCCGTTTCTA TGCCCCACTT GACGGGTGGA CTGCCCGGCT
351 CCACTGACCT TCTTGGTCAT CAACAGGCTC TTGCCATCAA CCCCACCTCT CTCATGCAAT ATTTCCGAAT
421 TCGCACCTA CCTCTCACCC GGAAAGTCAT CCGCGAAGGC TGGCTCATGA AGAGGGGTGA ACACATCAA
491 ACATGGCGCC GACGATACTT CATTCTCAGA GAGGATGGTA CCTTCTATGG ATATAAAAAAT ATTCCAAGAG
561 ACAACCTAGA GCAACCTCTA AATAATTTTA CCGTTCGAGA CTGTCAGATA ATATGCCTGA ACAAGCCCAA
631 GCCCTACACA ATCCTAATGC GAGGTCTCCA GTGGACGACG GTGGTGGAGC GATTGTTTTT CGTTGAACAC
701 GAAGTCGAAC GCGATGAGTG GATCAGTGCC ATCCAAATGG TCGCCAACCG ACTTCGCTCT GAAAATGAGG
771 CACCCACAAG CGTTTTCAA GTCGATTCG CTGAAGACGT CGTCATTGAT TTTCTCAGA GGCCACCTAA
841 GCGTTACTCC ACTGATGACT TTGAGCTTTT AAAGGTGCTT GGCAAAGGAA CTTTGGCAA AGTTGTCTT
911 TGCAAAGAAA AGGAGTCCGG CTGCTTCTAC GCTATGAAA TCCTTAAGAA GACCGTTCTA ATTGAGAAA
981 AGGAGGTCCG TCACACACAG ACAGAACATC GGGTGCTGCA ACTCAATCAC CATCCCTCA TGACGCAGTT
1051 GAAGTACTCC TTCACCACAC GGGACCATAT CTTCTTCGTT ATGGAGTACT GTAATGGCGG TGAATCTTC
1121 TACCACCTCT CGCGAGAGCA TGTCTTCTCC GAGTCGCGGA CACAATTCTA CGCCGCCGAA ATCACATCTG

A Supplementary

```
1191 CTCTTGGATA CCTACATAGT CAGAACATCG TCTATAGAGA CCTGAAATTG GAGAACTTGT TGCTGGATAA
1261 GGATGGTCAT ATCAAGATAA CCGACTTCGG GCTGTGCAAG GAGGACATAG GCTTCGGCTC GACTACAAAG
1331 ACCTTCTGCG GCACGCCTGA GTACTTGGCG CCGGAGCTGC TCCTGGACAA TGATTACGGA CTCTCCGTGG
1401 ATTGGTGGAG TCTAGGCGTC GTCATGTACG AAATGATGTG CGGTCGACTG CCTTTCTACT CCAACGAACA
1471 CGAAATCCTC TTTGAACTCA TCCTCCAGGA GAGCGTAAAG GTGCCGGACA ACCTAAGTCC CGTGGCACGT
1541 GACATTCTAA TCCGCCTCCT CATGAAGGAT CCAGCCGAAC GACTTGGTGG GGGCAAGGCG GACGCCATTG
1611 AAGTCATGGT GCACCCCTTC TTCGAGTCTA TCTCCTGGGA TAAACTGATC CGCAAGGACA TCATACCGCC
1681 GTGGAAGCCG GATGTGAACG GTGACATGGA TACCAAATAC ATTCCCAGAG AGTTCAGAG GGAGAACGTG
1751 GCAGTTACGC CACCGGAGAA GAGCGTCGCT TCAGCTATCA TGGCAGCCGA CAGAGTCTCA GTCGTCAAAG
1821 TGTTCTCAGC TTCGGAGACA ATGGCTCTAT ACCTGAAGGC GCCCTTCCA ACTGACTCTC CCACTCTCTC
1891 CTCTGCAAAG GCGCAAAGTT TGACTGTTA TATCAGGGG ACTTTTGGAG GCTCCTTCCC GGTGGACGTG
1961 ATCACAGTTC GTCGCATTCA ACCAAATTCC CCTTCTCTCC GTCGTATATT CGGACATGCT TATTTTCTC
2031 CCCGCGGTCA ACTGTTTAC TCGTGCCTGC GTGTCTCATT CGTGGAAATC ATGGTCATCT CGCACTGTGT
2101 ATCTCTCTGT CTCTTCATT CGCTCTCCAT CCCTGCGACG TGGCATTCT CTGTGACCAT TGCTGACGCG
2171 GTTGTTCGCC CTCTGCTTTC TTCACTACCA CTTTGGGACG TTTAAATCTC AGTCCCAGT TGTTTTGCA
2241 ATACTGATAT TGCTAATAAA GAACATATAT ATACTGCTGT AAAAAAAAAA AAAAAAAAAA
```

Putative amino acid sequence of EmAkt

```
1 MQVDESLNCS TPMGTLTPTS APMVDPLSS FVQFQSASMS QIPCNTPQFS NPSTVSSLVP GAGTPCAGLS
71 QEHFVPHAPV SMPHLTGGLP GSTDLLGHQQ ALAINPTSLM QYFRIRTLPL TRKVIREGWL MKRGEHIKTW
141 RRRYFILRED GTFYGYKNIP RDNLEQPLNN FTVRDCQIIC LNKPKPYTIL MRGLQWTTVV ERLFFVEHEV
211 ERDEWISAIQ MVANRLRSEN EAPTSVFKVD FAEDVVIDFP QRPPKRYSTD DFELLKVLGK GTFGKVVLC
281 EKESGCFYAM KILKKTVLIE KEEVGHTQTE HRVLQLNHHF FMTQLKYSFT TRDHIFVME YCNGGELFYH
351 LSREHVFSSES RTQFYAAEIT SALGYLHSQN IVYRDLKLEN LLLDKDGHK ITDFGLCKED IGFSTTKTF
421 CGTPEYLAPE LLLDNDYGLS VDWWSLGVVM YEMMCGRLPF YSNEHEILFE LILQESVKVP DNLSPVARDI
491 LIRLLMKDPA ERLGGGKADA IEVMVHPFFE SISWDKLIRK DIIPPWKP DV NGDMDTKYIP EEFQRENAV
561 TPPEKSVASA IMAADRVSVV KVFSASETMA LYLKAPFPD SPTLSSAKAQ SLTVYIRGTF GGSFPVDVIT
631 VRRIQPNPSPS LRRIFGHAYF SPRGQLFDSC LRVSFVEIMV ISHCVSLCLF ISLSIPATWH FSCTIADAVV
701 RPLLSLPLW DV
```

EmILP1a

Full length cDNA sequence of *emilp1a*

```
1 AATTAGTCAG CAGTGAGTGG TCTGGTGGAG ACCCCGCTCA GACACCGTCG CTTGCAAAGT CCTATCTGCG
71 AAAGGGGTTT CACCTGTTCT CCTTCTTCTT CTTCACTCCT CTTCAGCCCT TTTGAGATGG ATAAACGCAA
141 CAATTTCTCC GATCCACGAC GAATCATGTG CCGCTATCAG TTGATCGTCA ACCTCAAAAT GCAGTGCCGA
211 GATAGAGGGA CGTATTCGCC CTACGAACGG GGTCCGCGTA TCAAGCGAGG TCTTCGATTG GGTGACCAG
281 CTCCGTTATA CAGTCCGTTG AAGAGTCGAG GAAGAAAGCA TGATGATTTT TGCTCCATTT ACCTTCGCTA
351 CGAGCCTTAC ACCATCGTCA CGGAATGCTG CTGTCTGGC TGTACTCGTC GGTTTTTGGA GCAGTCTGT
421 GCAAAGGC GAAACCGATGT CTCGACCTCC TCTTCCACCC TCTCGCCCTC CTCCATCACC TTCTCCTATC
491 ATCAATCTTT ATTTTGTAA AAGCCGTATT CAGCAACTAT TTTCTCCCC CCACTCCTTA ATCCATCAGG
561 CATTTGTATA GATCTCGACT GATCCCTTTG TGAAAAAGC CTTGTCGATT AATTGGCCAA ATTACTCTGC
631 ATTTAAAT GAATAAATCG ATTAAGATT GGTGTGGATT TCTACAAAAA AAAAAAAAAA AAAAAAAAAA
701 AAAAAAAAAA AAAAAAAAAA AAAAA
```

A Supplementary

Putative amino acid sequence of EmILP1a

```
1 MCERGFTCSP SSSSLLFSPF EMDKRNNFSD PRRIMCGYQL IVNLKMQCGD RGTYSPIYERG PRIKRGLRLG
71 RPAPLYSPLK SRGRKHDDFC SIYLRYPYPT IVTECCCRGC TRRFLEQFCA KG
```

EmILP1b

Full length cDNA sequence of *emilp1b*

```
1 ACTTGACCGA GGTTCCTGTC TTCGAGAAATG CATAGTCCCT TCCACCCATC CGTGGCTGAC CCACCCACCA
71 TCTTTCCCCA TTCGACGGTT ACCACCAACC CCGCTTCCCC GCATCTACTC ATTCTTGCGA TGTTAATGAC
141 CTTTTACTA GTGAATTCCT CGCCTCTGCC AAGCGATCTC GAGAGCGGTG TGAATTATGT AGACCAGAAA
211 ACAATATTTG TTCCTAGTTT TGAGATGGAT AAACGCAACA ATTTCTCCGA TCCACGACGA ATCATGTGCG
281 GCTATCAGTT GATCGTCAAC CTCAAAATGC AGTGCGGAGA TAGAGGGACG TATTCGCCCT ACGAACGGGG
351 TCCGCGTATC AAGCGAGGTC TTCGATTGGG TCGACCAGCT CCGTTATACA GTCCGTTGAA GAGTCGAGGA
421 AGAAAGCATG ATGATTTTTG CTCCATTTAC CTTGCTACG AGCCTTACAC CATCGTCACG GAATGCTGCT
491 GTCGTGGCTG TACTCGTCGG TTTTGGAGC AGTTCTGTGC AAAAGGCTGA ACCGATGTCT CGACCTCCTC
561 TTCCACCCTC TCGCCCTCCT CCATCACCTT CTCCTATCAT CAATCTTTAT TTTTGTAATA GCCGTATTCA
631 GCAACTATTT TCCTCCCCC ACTCCTTAAT CCATCAGGCA TTTGTATAGA TCTCGACTGA TCCCTTTGTG
701 TAAAAAGCCT TGTCGATTAA TTGGCCAAAT TACTCTGCAT TAAAAATGA ATAAATCGAT TAAGATTGCG
771 TGTGGATTTC TACAAAAAAA AAAAAAATAA AAAAAAATAA AAAAAAATAA AAAAAAATAA AA
```

Putative amino acid sequence of EmILP1b

```
1 MHSPFHPSVA DPPTIFPHST VTTNPASPHL LILAMLMTFS LVNSSPLPSD LESGVNYVDQ KTIFVPSFEM
71 DKRNNFSDPR RIMCGYQLIV NLKMQCGDRG TYSPIYERGPR IKRGLRLGRP APLYSPLKSR GRKHDDFC SI
141 YLRYPYPTIV TECCCRGCTR RFLEQFCAKG
```

EmILP2a

Full length cDNA sequence of *emilp2a*

```
1 GGTCAAACGT CAACGCCAAC AAGTACAGCA ATGCTCTTCCC CAAGTCATTA TATTCGCCGTA TTCCTACTAT
71 TAAACATATT TTTTCTCATT TCTGGCGGTT GTGCGGTATC ACCTCTTCAT GACTGGGAGG AGGAAGGCGA
141 CGCTCTATCA GAGGACAGTC TAAGCATGAT GAAACGAGCG AATACTGAAT ACGCAACAAC AGAAGTAGAT
211 CGTCCGCGTA TTCTTTGTGG CCAGTCGCTG ATTACACACC TAAAGGAGCA GTGTGGACAA CGCGGAACAT
281 TCTCACCTA CCACAAGCGC GCAGTTCGTG AGCTCATCAG AGTGGCTAGA GGGCTTCCTG TCAAATCCAC
351 TTGCACAAAC GATACGACGA TATCTGTGAA GTGTACTTGC GATACGAACC CGATAGTCCA CTTTCTCAAT
421 GCTGTTGTT AGGCTGTACA AGAGCCTACT TGGAGAACTT TTGCGCTGAG GCTTAAAAAG TAAAGCAGGC
491 AAGTGGAGAC ATTCCAAATC TCCAATTCTT CCGCTCCCTC CCTACCTCAC CCCACTTTTG TCAGATCTTC
561 TATCCGCGTC GTCGGAAGAT CTGGGTCCTA CATAACACGT GTAAGTTCTC CCCTTCCACT CACCCACTCA
631 CTCAGTCCGT CGCAAGGCAT TCTTTCACCT TAATGTCCTG CCCGTCTCAA TCCCCCTCTG ACTTTGTTCG
701 CGTTCCACAC CTACACACTT TTTTCATGCGA AAAGGCTCCT GTTTATAAAG AAGTCAGTGG ATATTGCAAA
771 AAAAAAATAA AAAAAAATAA AA
```


A Supplementary

Putative amino acid sequence of EmILP2a

```
1 MSSPSHYIPV FLLLNIFFLI SGGCAVSPLH DWEEEGDALS EDLSLMMKRA NTEYATTEVD RPRILCGQSL
71 IHTLKEQCGQ RGTFSFYHHR AVRELIRVAR GLPVKSTCTN DTTISVKCTC DTNPIVHFLN AVV
```

EmILP2b

Full length cDNA sequence of *emilp2b*

```
1 GGTCAAACGT CAACGCCAAC AAGTACAGCA ATGCTCTTCCC CAAGTCATTA TATTCCTGTA TTCCTACTAT
71 TAAACATATT TTTTCTCATT TCTGGCGGTT GTGCGGTATC ACCTCTTCAT GACTGGGAGG AGGAAGGCGA
141 CGCTCTATCA GAGGACAGTC TAAGCATGAT GAAACGAGCG AATACTGAAT ACGCAACAAC AGAAGTAGAT
211 CGTCCGCGTA TTCTTTGTGG CCAGTCGCTG ATTCACACCC TAAAGGAGCA GTGTGGACAA CGCGGAACAT
281 TCTCACCTTA CCACAAGCGC GCAGTTCGTG AGCTCATCAG AGTGGCTAGA GGGCTTCTTG ACATATCAGA
351 TTTTGTTGAT AGTCAAATCC ACTTGCACAA ACGATACGAC GATATCTGTG AAGTGTACTT GCGATACGAA
421 CCCGATAGTC CACTTTCTCA ATGCTGTTGT TTAGGCTGTA CAAGAGCCTA CTTGGAGAAC TTTTGCCTG
491 AGGCTTAAA AGTAAAGCAG GCAAGTGGAG ACATTCCAAA TCTCCAATC TTCCGCTCCC TCCCTACCTC
561 ACCCCACTTT TGTCAGATCT TCTATCCGCG TCGTCGGAAG ATCTGGGTCC TACATAACCAC GTGTAAGTTC
631 TCCCCTTCCA CTCACCCACT CACTCAGTCC GTCGCAAGGC ATTCTTTCAC CTTAATGTCC TGCCCGTCTC
701 AATCCCCCTC TGACTTTGTT CGCGTTCAC ACCTACACAC TTTTTCATGC GAAAAGGCTC CTGTTTATAA
771 AGAAGTCAGT GGATATTGCA AAAAAAAAAA AAAAAAAAAA AAAAAAAAAA AAA
```

Putative amino acid sequence of EmILP2b

```
1 MSSPSHYIPV FLLLNIFFLI SGGCAVSPLH DWEEEGDALS EDLSLMMKRA NTEYATTEVD RPRILCGQSL
71 IHTLKEQCGQ RGTFSFYHHR AVRELIRVAR GLPDISDFVD SQIHLHKRYD DICEVYLRYE PDSPLSQCCC
141 LGCTRAYLEN FCAEA
```

EmPI3K

Full length cDNA sequence of *empi3k*

```
1 GCCTGATTGG TCGCAGTTCA TGCCAGGTTT CCTGTCCTTA TTGCATGATG CCTAGTCCCA GTATTTATTT
71 TCGACGGGAT TTATTTACCA TATTTTTTAC TTGTTCACTG ATTATGTACA TCTCTGCGTG CCTATCCTTA
141 CCTCATTCCCT TCATTCTATG TTGAAAATTA GGTTAAAGAC ATATCAATGT CGTTATTGTA ATTTCTTGTT
211 AAAGTAGCGT AAATTCATGG GAAATTCATA TGACATTAGT GTCCTGCGTT GAAGTGTGTA TGGCTTGCTA
281 AATAGTGTGA AATTGGTGCT GGAGTATTCC ATTAATAAAT TCGCTCCTAT AGCGGGTCTC CCGTTTTCGA
351 TTTAGTTCTT CCCGCCTTTT TCTGTACCGA TTTGCGCATT AGGCGTTTAT CGCAGTCACA CAGCTCCAT
421 TTATAATGCT AATATAAGTC AATTTTGGGT AATAATGAAC AGGTGCAAAT AATAATCCAT GTTTAATTC
491 TTGTTTAGTA ATGCCAGGAT GCCTCCAACC ACATTGGAGA GTTCGGACCA CATGTTCCAA CATTGCTCGT
561 CGATGAAACA TGACTTTTTA ATGCCTAACG GTATTGTCTT AACCTTGAAG CCCGACCCGG ATATTAGTTT
631 GCGGATCTG AAGGCTCACC TCTGGGATTT GGCTTCTGCC GAACCCTTT ACGAATGTCT GGGTCTTCCA
701 AATGACTACC TCTTCCAGG TATTTATCA CCCAAGGCTG AGGAGGAGGA ATTTTACGAT GAGCAATGCA
771 AATTTGCTGG TCTTCAGCTT TTCCTTCTT TCATGCTCTT GGAAAAAGTT TCCGACGACG CTCAGATAAT
841 TGAGCAGAAG CGCAATGCCA TGATTGCCAA AATATCCACC ATATCTCAGG CTCACCTCAA GGCAGCAGAA
911 GGGGGCAACC CAGAGCTAGC TTGGGCTCGC CAGTGCCTCC TCGAGATGTC TGAAGCCAAT ATGAGGCGTC
```

A Supplementary

981 TGGAGGCAGG AGGGCCCGTT TCCATGGCGC ATTACCTCAC AGCCGCTTCA CTTCAACCGA AGCTGAATAC
1051 AGCACTGCAG CGACGTCTGC AACGCCTACC TTACCTTACC ATCTCGGCAG TTTGTGTAGA CTGCTACAGT
1121 CCGCCAACCC AGCACCTCCT CAAACTGAAT CTTCCTAAGT CAATCACTGT GCGCGCGGCG ATTAAGGAGA
1191 TCATTGATGA GCAGAGGCGA CTTGTGCAGG GTGATGTTAG TTGCCATGAT GTGGATCCAG CCCCTCAGTA
1261 CCTTCTCAAA GTGTGTTGTT CTCAAGAGTA TTTATTTGAA CAAGAGAGTG CACTGGTCCA CTACGCTTAC
1331 GTACAGGAGT GTCTTCAACG CGACGACATT CCACGCCTCA CTCCAGTCCT TCTCAAAGAT GTCCTAGAAT
1401 GCCTCGGCTT GCCAGTGCCG GAGGTGGTAA ACTGTGAGGG TTGCACACCA GCATACCCCT CCCCTGCAGT
1471 CGTCTCTAAC GCCGCTCCCC TCCCTTCTGT TATCGATCTC TACGGGGTGA AGGAAGAGGA TGAGGATGAA
1541 GGCGATGAGG CGATGGAGGC AAGCGTAGAT TTGTGGGACT TACGGGACTA CTTCTCTCTT ACTGTCCGCG
1611 CTGCTCAAAA ACTCACCACC CTGACGAAA ATCCCTCAAC GGAGCAATG GATACCGGTT TATTCTTAC
1681 AGGCTCCTCT AGTTTCAGTG ATCTCACCAC GGATGTGACG TCATCGCTGG GTGGCAGTGA GAGTAGCGGC
1751 AGTGGCGGGG GGGGAGGAGC GTCAGCCTCC ACCACCCAC TATCGGCTTC GTCGGCCTCA AGTCTTGATG
1821 CCTCATCGGG TAGTGTGGTG AACTACATTG TTCGAGTGGG ATTGGCTCAT GGTGGACAAC TGCTTGCGAA
1891 GTACCAGAAC ACACGAGGTG CAATAATCGT AATGGGTGGC AATTCGGCCC TCAATGGAA CCAATCACTT
1961 AACTTTTCGCC TAATCTACTC CAACCTGCCA CTCGCCACCA GGGTCTGTGT TGCTTACTC CAAGTAAAC
2031 GACGTCCTGG CCGAATCATG GAGTTCCCGG TAGGCTGGGC GAATATGAAC CTCTTTGATG AGAGGGGCTA
2101 CCTTGTTACG GGTGCGCGCT CTCTTCCCCT GTGGCGCAGC AGCTTACCT CACCAGAAAC TGAAACCACC
2171 CACCAACTCA ATCTCGCCGG CACTGTGGCC GAGAATCCCG ATCCCGAGTT CACTCTTG TGGAATTTCT
2241 GTCATCCTAG CAACCAAAAG GCCCGTATCC GCTTTCCTAT CTCCCGTTC ATCACCACCG TGCGCGGCGC
2311 CTCCCCTAAT ACGCCCACTG CTACCATCGT CCCTTCGCTC CATTCCAGCG ACTCCGACAT CCGTGTGATC
2381 CGTGATCTCA TACACCGGGA CCCCTTCTAC GAGTTATCAG AGCAGGACAA GGCTCTTCTC TGGCGCATCC
2451 GCGACTCATG CTGCCGTAGA CTTTACCCTG CTGAATCGTT GCCTTGCTT GTGCAGGCTG TGGCTGGGA
2521 AAGACGCGAG TTGGTGGAGG AGTTCTACCG CCTCCTTGCT GTTTGGCCAC GACCCCTACC CGTGGAAACC
2591 TGTCTCCAAC TCCTGGGTGT GGCAGGCCTT GCTGGTCCG CTGCCGCCGA AGGGACGTTT GGAGAGGGTG
2661 GTGGGGGCG TATGTGATG GCCGGGGGGC GCACGACCGG TGTAGCGGAC CCTCTGGTTC GCGATATTGC
2731 GGTGCAAGGG CTGCAGGCGA GACTTTCAA TGCAGGATCTA GCTGACTATT TGCTTCAACT GGTACAGGTG
2801 GTACGAACCG AAGCCTTCTT GGTAACCCA CTGACCTGTT TCCTTCTTCA ACGAGCCCTC GACTGTCCCA
2871 CACTGATCGG GGTTCGGTTG TGCTGGCATC TGCCTCCCA ACTAGACAAT CCGGATGCC GCCTTCGTTT
2941 TGGTCTGATT CTGGACGCC TCTGTGCGG TTTTGGACCT CGGCTCCTAC TCTTCGTCCA TGAACAAGTC
3011 AATGCACTT ATCGACTTAC GGATCTTGCC ATCTCTGTCA AGCGTATCGC AGAGGATGAG GAACAGCGAG
3081 CCCGTTCAA GTTTGGCTA CATCGCAGT AAGTTCGACG CGATCTTGTG GGCATCCTCT CCCCTTACG
3151 TTTCTCTATC AAACCTCGTC CAGTGGTAGA ACAGCAATGT ACCGTGAAAC GCTCTAAAAA GCGTCTCTT
3221 TGGATAGTCT GGGCCAATCC AGACAATCTC GGATTTCAACC ACCACAAAAT TCATCAACTC CTCTTCAAGC
3291 ACGGTGATGA TCTGCGGCAG GATATGCTCA CTCTCCAGAT CCTCAAAGTG ATGGATCACA TCTGGAAGGA
3361 CGAGGGACTC AATCTCGATC TCACCACCTA CGACTGCCTT GCCACAGGCG ACGAGATGGG CCTGATTGAG
3431 GTGGTGC GCA ACTCTCAGAC CATCATGTCC ATTCAGGGAC AGCGAGTGCG CTCTGCAATG CAGATTGACT
3501 CCTCCCAACT ACATAAGTGG TTTTTCGAGA AGAAGGCTCC TCCACTGGG TCGGAGGAGG CCTATGAGTC
3571 GGCCATCCGG CGGTTACGCA ACAGCTGCGC AGGCTACTGT GTGGCTACCT TTGTGTTAGG TATTCGCGAC
3641 CGGCACAATG ACAACATTAT GGTGGATGAT TCGGGTCGTC TATTTTATAT TGATTTTGGC CACATCTTAA
3711 ATAACAAGAA GAAGAAGTTT GGCATCACGA GAGAACGTGT GCCGTTCTGT CTGACAAGTG ACTTTGCCTG
3781 TGTGATCGCT CGAGGGGAAG AGAAGCCCTA CCGAAGCAAG GGGTTCATGG ATTTTACACG GCTGTGCGAG
3851 GATGCCTACC GCATTCTGCG ACGGCATTCC AACCTTCTCC TCACCCTTCT CGCCATGATG GTACCCTCCG
3921 GTCTGCCCCG ACTCACTTGC GCCAGCGATC TGGAATACGT GCGCAAGACC CTGGCTGTGG AGCTGCGTGA
3991 CGAGGAGGAG GCGCTAAACT ACTTCAACGC CAAGTTTAAAT GAGGCCTACA ATGGTGC GTG GACTACGAAA
4061 ATCGATTGGT TCGCCCACTG GGTCCGCCGA TCGATCAACAG AGTACCGACA GAGAGACCTG CACTTTTATT
4131 TACTCTATAT GTGATAATAC

A Supplementary

Putative amino acid sequence of EmPI3K

```
1  MPPTTLESSD  HMFQHCSSMK  HDFLMPNGIV  LTLKPDPDIS  LADLKAHLWD  LASAEPLYEC  LGPPNDYLFQ
71  GISSPKAEEE  EFYDEQCKFA  GLQLFLPFMR  LEKVSDDAQI  IEQKRNAMIA  KISTISQ AHL  KAAEGGNPEL
141 AWARQC LLEM  SEANMRRLEA  GGPVSMAYHL  TAASLQPKLN  TALQRR LQRL  PYLTISAVCV  DCYSPPTQHL
211 LKLNLPKSIT  VAAAIKEIID  EQRRLVQGDV  SCHDVPDAPQ  YLLKVCCSQE  YLFEQESALV  HYAYVQECLQ
281 RDDIPRLTPV  LLKDVLECLG  LPVPEVNCE  GCTPAYPSPA  VVSNAAPLPS  VIDLYGVKEE  DEDEGDEAME
351 ASVDLWDLRD  YFSLTVRAAQ  KLTTLTQNPS  TEQLDTGLFF  TGSSSFSDLT  TDVTSSLGGS  ESSGSGGGGG
421 ASASTTPLSA  SSASSLDASS  GSVVNYIVRV  GLAHGGQLLA  KYQNRGAI I  VMGGNSALQW  NQSLNFR LIY
491 SNLPLATRVC  VVLLQVKRRP  GRIMEFPVGW  ANMNLFDER G  YLVTGRRSLP  LWRSSFTSPE  TETHQLNLA
561 GTVAENPDPE  FTLVLNFC HP  SNQKARIRFP  ISRFITTVRG  ASPNTP TATI  VPSLHSSDS D  IRVIRDLIHR
631 DPFYELSEQD  KALLWRIRDS  CCRRLYPAES  LPWLQAVAW  ERRELVEE FY  RLLAVWPRPL  PVETCLQLLG
701 VAGLAGSAAA  EGTFGEGGGG  SYVMAGGRTT  GVADPLVRDI  AVQGLQARLS  NADLADYLLQ  LVQVVRTEAF
771 LVNPLTCFLL  QRALDCPTLI  GVRLCWHLRS  QLDNPDARLR  FGLILDALCR  FGGPRLLLFV  HEQVNALHRL
841 TDLAISVKRI  AEDEEQRARF  KFELHRSEVR  RDLEGILSPL  RFSIKLGPVV  EQQCTVKRSK  KRPLWIVWAN
911 PDNLGFHHHK  IHQLLFKHGD  DLRQDMLTLQ  ILKVM DHIWK  DEGLNLDLTT  YDCLATGDEM  GLIEVVRNSQ
981 TIMSIQQQRV  RSAMQIDSSQ  LHKWFLQKKA  PPLGSEEAYE  SAIRRF TNSC  AGYCVATFVL  GIRDRHNDNI
1051 MVDDSGRLFH  IDFGHILNNK  KKKFGITRER  VPFVLTSDFA  CVIARGE EKP  YRSKGFMDFT  RLCEDAYRIL
1121 RRHSNLLLLTL  LAMMVPSGLP  ELTCASDLEY  VRKTLAVELR  DEEEALNYFN  AKFN EAYNGA  WTTKIDWFAH
1191 WVRR
```

EmTK6

Full length cDNA sequence of *emtk6*

```
1  CCCAGCCATT  CATGCTTTCA  TGAACTCAA A  GTTGCACA A  GGGGAATTGT  TTTACTTGCC  ACGACCACAA
71  AGAAAATCTT  CAGTGCCATG  GAGACAATGG  CATGACGCCG  ATGGGTGCAA  ATTCCCAAGG  GGGTGGCCAG
141 GGACTAGGGC  AAGCCCCATT  CGGTCGT CAC  TATGGTCTT  CAGGTGACGC  TGCATCGGTC  GGTGCCAATC
211 AGTCCGCCAT  TGTGCCTGCT  TCGCGTGGTG  CACATCAACC  CTCCCAACAG  TACTCCGTGA  ATCTTTACGG
281 CATGCAGAAT  GGACCACAAC  AGAGTGCATC  CTACGCCTAC  AGTCTCGCCC  AACCTCCCGC  GACTCTTGAC
351 CAGCAGCTGG  CAGAGCAGTC  ACCTCGAGTT  GTCCGTGTTC  ACGCTTTATA  CACTTACGTT  GCGCAAAACG
421 CTGATGATCT  GAGCTTCCAG  AAGGGTGATG  TCATGCTAGT  CGAGTCGGGC  TTATCCGAAG  CCTGGTGGTT
491 GGCGCGTCAC  TTGAGGACCG  GGCAACAGGG  CTACATACCC  AGTAACTATG  TGA CTGTAGA  AAATGGTCTC
561 TCTACACAAA  TGGAAGCCTG  GTATGACATT  ACACGTAAAG  ATGCCGAGAG  AATGCTTTTG  ATGCCGGGT
631 TGCCTCAAGG  GACTTACATT  TTACGCCCTT  GTTCCGATTC  CCGAAGTTAT  GCTCTCTCCA  TCCGGTTCGA
701 AATTGAGAGG  AATATGTATG  CAATAAAGCA  CTACAAGATC  CGAACTCGCG  ATAACGGTGC  CGGCTTCTAC
771 ATCACCAATC  GAACCAACTT  TGCTTCTGTC  GCCGATCTCA  TCTCTACTA  TCAGTCCACT  AGCGATGGGC
841 TGTGCTGTCT  CCTATCGCAG  CCGTGTCCGC  GGAAGTATAC  CCCGCCGGTG  CAGTTCCTGT  ACATCGAGGC
911 AAATCGGCGG  AGCCTGGAAT  TCATCTGCGA  GCTAGGCAAC  GGCAGCTTCG  GCATGGTTTA  CCGGGCTCGG
981 TGGAACAAGA  CCTTCGACGT  GCGGGTGAAG  AAGCGCCTCG  CTACCACGGA  CCGCGCACTT  TTCATTGAGG
1051 AAGCGAAAGT  GATGCACAAA  TTGCATCACC  GCCGATCGCT  TCGCCTCCTC  GGTGTCTGCA  CCGAGCCGGC
1121 TGATGAGCCT  GTTTTCATCA  TCACAGAGTT  GCTAGAGAAG  GGTGCTCTGC  GCAACTTCTT  CAGCAGCGAA
1191 GAGGGCCGCC  AACTCTTCCT  CAGTGACCTT  ATCGATATGA  TTGCTCAGAT  TGCCGAAGGA  ATGGCATAAC
1261 TGGAGGAGAT  GAATTCGTC  CACCGAGACC  TTCGAGCCGC  CAACATCCTT  GTGGATCGCG  ACAACTCCGT
1331 CAAGGTAGCT  GATTTCCGAC  TTGCAAAAAT  GCTTGATTCG  GATGTTCAA A  ATGATGGCGT  CATTAAATTC
1401 CCCATCAAGT  GGACCGCGCC  AGAGGCGGGT  CTTCCCGACC  ACCATTCAG  TATAAAGTCG  GACGTCTGGT
```

A Supplementary

1471 CCTTCGGTGT GTCATGTAC GAAATCGTCA CTTACGGTGG CACTCCCTAC CCCCCTTCA CTAATCGGGA
1541 GACGGTACAG CAGGTAGAGC GCGGCTATCG AATGCCAAAT CCGAATACAC CGACACAGCC GTGTCCGGAC
1611 GACCTCTACG ACATCATGAT GCAGTGTGG TCAGCACGAC CCGAGGATCG ACCTACCTTC CACAACCTCT
1681 ACGACATCTT TGAGAACTGG GCCGTCCAGA CGGAGGGTCA GTACATCTCG GATGGAGCGC AAAACACTTC
1751 ATCAGTCAC CGCAGCCGCC GCCACCTCTA CAAAGACCGC GTGTGATTGT CGTTTATCCA TCCACCCGAT
1821 CTCTCCGCGC TGCATTTGAC TTCATCAATT CAATCCACCC TATCCCCTTT CCCTCTCTC AACTGACTCC
1891 TTCATGTCGA TTTTTTGACG CCTTGGCTTT CTCTTCTCTC GTGTTCTTTT GCTAAGATTA ACACCGTCCC
1961 AATAAGACTC GTGGCTTGCA ATGGCTGCAG GGAACGGGAA TTCGTTTTTC GAAAGTGGAA TCTGGCAGTG
2031 GTTTTAGATG TCAAGTCTG GCGGGGAAG CTCGACGAAG ATGGGCTCAG GGGCTTACAT GGCATCCCCG
2101 TTTGTTGAGT CTCACCTTAT TCTGTTTTTC TTTTTTTTTC GTCCTGGTTT GTCTTCATTC TATTTTGCTG
2171 GAATTAATAA AAAAAAAAAA AAAA

Putative amino acid sequence of EmTK6

1 MGNCFTCHDH KENLQCHGDN GMTMPGANSQ GGGQGLGQAP FGRHYGPSGD AASVGANQSA IVPASRGAHQ
71 PSQQYSVNLY GMQNGPQQSA SYAYSQAQPP ATLDQQLAEQ SPRVVRVHAL YTYVAQNADD LSFQKGDVML
141 VESGLSEAWW LARHLRTGQQ GYIPSNYVTV ENGLSTQMEA WYDITRKDAE RMLLMPGLPQ GTYILRPCSD
211 SRSYALSIRF EIERNMYAIK HYKIRTRDNG AGFYITNRTN FASVADLISH YQSTSDGLCC RLSQPCPRKY
281 TPPVQFRDIE ANRRSLEFIC ELNGSFGMV YRARWNKTFD VAVKKRLATT DRALFIEEAK VMHKLHHRRI
351 VRLGVCTEP ADEPVFIITE LLEKALRNF LSSEGRQLF LSDLIDMIAQ IAEGMAYLEE MNFVHRDLRA
421 ANILVDRDNS VKVADFGLAK MLDSDVQNDG VIKFPIKWTA PEAALPDHFF SIKSDVWSFG VLMYEIVTYG
491 GTPYPRFTNR ETVQQVERGY RMPNPNTPTQ PCPDDLYDIM MQCWSARPED RPTFHNLYDI FENWAVQTEG
561 QYISDGAQNT

B List of Abbreviations

4E-BP	Eukaryotic translation initiation factor 4E binding protein
aa	Amino acids
ABZ	Albendazole
AD	Gal4 activation domain
AE	Alveolar Echinococcosis
AS	AS601245
BD	Gal4 binding domain
bp	Base pairs
<i>C. elegans</i>	<i>Caenorhabditis elegans</i>
CML	chronic myelogenous leukemia
Ctrl	Control
<i>D. melanogaster</i>	<i>Drosophila melanogaster</i>
EmIR	<i>Echinococcus multilocularis</i> insulin-like receptor
HE haematoxylin/ eosin staining	
<i>E. multilocularis</i>	<i>Echinococcus multilocularis</i>
<i>H. microstoma</i>	<i>Hymenolepis microstoma</i>
HMN	HNMPA(AM) ₃
IGF	Insulin like growth factor
Ins	Insulin
ILP	Insulin-like peptide
K11	K11777
LBD	Ligand binding domain
LY	Ly294002
Mc	Metacystode vesicles
MAP	Mitogen-activated protein
MAPK	mitogen activated protein kinase
<i>M. vogae</i>	<i>Mesocestoides vogae</i>
Na ₃ VO ₄	Sodium orthovanadate
nt	Nucleotides
ORF	Open reading frame
Pc	Primary cells
PI3K	Phosphoinositide-3-kinase
PDGFR	Platelet-derived growth factor receptor
PS+	Activated protoscoleces
Ps-	Nonactivated protoscoleces
<i>S. japonicum</i>	<i>Schistosoma japonicum</i>
<i>S. mansoni</i>	<i>Schistosoma mansoni</i>
<i>T. crassiceps</i>	<i>Taenia crassiceps</i>
<i>T. solium</i>	<i>Taenia solium</i>
Y2H	Yeast two hybrid

C Publications

Publications:

Hemer and Brehm. In vitro efficacy of the anti-cancer drug imatinib on *Echinococcus multilocularis* larvae; International Journal of Antimicrobial Agents (2012)

Conference Contributions:

March 2012, DGP Jahrestagung 2012 Heidelberg, Germany

Talk: Effects of host insulin on *Echinococcus multilocularis* development.

Sarah Hemer, Christian Konrad, Markus Spiliotis, Verena Gelmedin,
Klaus Brehm

October 2011, 6th International Symposium of the Graduate School of Life Sciences Wuerzburg, Germany
Poster: The role of insulin signalling in *Echinococcus multilocularis* development

Sarah Hemer, Christian Konrad, Markus Spiliotis, Verena Gelmedin,
Klaus Brehm

March 2011, 5th Short course for Young Parasitologists, Hamburg, Germany

Molecular characterization of evolutionary conserved signaling systems of *Echinococcus multilocularis* and their utilization for the development of novel drugs against Echinococcosis

Sarah Hemer, Christian Konrad, Markus Spiliotis, Verena Gelmedin,
Klaus Brehm

March 2010, DGP Jahrestagung 2010, Duesseldorf, Germany

Poster: Targeting Echinococcus signalling cascades for developing novel anti-infectives

Sarah Hemer, Verena Gelmedin, Christian Konrad, Sabine Lorenz,
Klaus Brehm

June 2009, 19th International Symposium on Flatworm Biology, Hasselt, Belgium

Poster: The role of insulin signalling in *Echinococcus multilocularis* development

Sarah Hemer, Christian Konrad, Markus Spiliotis, Verena Gelmedin,
Klaus Brehm